ANALYSIS AND CONTROL OF

STRIP ROLLING MILLS

by

PETER DAVID SPOONER

A Thesis submitted for the

degree of Doctor of Philosophy

Department of Computing and Control

Imperial College of Science and Technology

University of London

May 1975

ABSTRACT

Most control schemes developed for rolling mills have been concerned only with the control of centre line thickness and ignore transverse thickness variations and the important product quality factor of flatness or 'shape'. Control of these last factors has awaited the development of an instrument and of a basic analytic understanding. In this thesis a detailed analysis is developed of the transverse properties of the strip and the roll gap; the control requirements for the production of flat strip are then investigated.

The shape model is complex, requires an iterative method of solution, and is unsuitable for use 'on-line'. A simplified model is therefore developed which lacks the detail of the full model but nevertheless gives valuable insight into the shape mechanism. Explicit forms for the sensitivities of shape to important parameters are then developed.

The problems of scheduling a tandem mill are discussed and the simplified model is used to explain the important interaction between shape and reduction at a rolling stand. The scheduling problem is formulated as an optimisation problem for which solutions are obtained using conjugate gradient and projection techniques.

Open and closed loop shape control schemes are developed for the output of a tandem or single stand mill. The schemes are designed to eliminate interaction with strip thickness. Expressions for the various loop gains are developed from the simple shape model.

ACKNOWLEDGMENTS

I wish to thank my supervisor Dr. G.F. Bryant for his guidance and encouragement throughout this research and for reading the manuscript of the thesis and making many valuable suggestions.

I should also like to acknowledge the patience and understanding shown by my wife Margaret during the course of the work.

CONTENTS

INTRODUCTION

Rolling is one of the most important processes in the metal industry. In 1973, 92°/o of the aluminium, copper, and steel produced in the world was rolled, a total of 728 million tonnes of metal[1]. Since the beginning of the century the cold rolling process has progressed from small manually operated mills which took a large number of reductions to produce very unflat strip of inconsistent thickness, to highly productive computerised multistand, or tandem, mills.

A tandem cold rolling mill consists of up to six sets of independently driven pairs of "work rolls" each pair being stiffened by larger diameter 'backup rolls'. The assembly of two work rolls and two backup rolls in a support frame is called a 'four high mill stand'. In figure 1 two stands are illustrated showing the major components of interest.

The cold tandem mill receives coils of strip at room temperature which have been previously hot rolled and pickled in acid to remove the scale. Each coil may consist of two or more hot rolled coils welded together before pickling. The basic function of the mill is to reduce the thickness of the incoming strip by a factor of 50 - 90°/o, to ensure that the strip at the exit is the desired constant thickness, and furthermore to ensure that the strip lies flat when rested on a flat surface, exhibiting neither convexity nor wavy edges. This last strip property is called 'shape'. Final product dimensions are typically in the ranges: width 600 - 1600 mm, thickness 0.2 - 2.0 mm.

Strip reduction results from the high compressive stresses experienced by the strip as it passes through the roll gap. The required forces are applied by electro-mechanical screws or hydraulic actuators mounted in the support frame (figure 1), assisted by the significant tensions which are maintained in the strip between stands.

In the small roll gap region, typically 5 to 25 mm long, the strip is deformed plastically and considerable friction forces exist as slipping takes place between the rolls and the strip. This 'roll gap process' has been the subject of much impressive research[2]. The roll separating forces are high and a considerable amount of heat is generated in the roll gap; when rolling steel sheet of say 1250 mm width, forces of 1000 tonnes are typical. These forces cause significant squashing and bending of the rolls and stretch the support frame. At top speed the output strip may travel at up to 1800 metres/minute and, as a result of friction in the roll gap, 4 - 5 MW of heat might be generated in the mill; lubrication in the roll gaps and coolant of the rolls are therefore essential. In normal sheet steel rolling an oil water emulsion is often used which serves the dual purpose of reducing friction and removing heat. When rolling the thinner 'tinplate' sheet steel lubricant and coolant are normally applied separately. For non-ferrous sheet, particularly aluminium, high frictions occur and compounded oils are used.

The transverse profile of the roll gap is determined by the squashing and bending of the rolls, the camber ground onto the rolls, the thermal camber produced by non uniform roll heating, and roll wear. If this profile does not match the profile of the incoming strip, the reduction is non uniform across the strip width and a non uniform transverse distribution of stresses is set up which directly affects the flatness of the strip. It is convenient to define strip shape in terms of the stress distribution in the strip when it is constrained to lie flat.

Many mills are now being equipped with computers for the automatic control of exit thickness which is generally monitored by radiation gauges or contact micrometers. Under steady state rolling conditions it is common practice to measure all roll forces, interstand tensions, strip thickness, screw positions, and stand roll speeds. Signals from

the sensors are used by the computer to calculate roll gap settings, interstand tensions,and roll velocities required to control strip thickness within narrow limits. However most computer systems control thickness along only a single track somewhere across the width where the thickness sensor is located. Thickness variations across the width are normally ignored by present automatic thickness control schemes.

While the advances in production rolling over several decades have been remarkable, the major remaining problem today is that of consistently producing strip that is flat. To the author's knowledge there is still only one operational automatic flatness control scheme reported in the literature[3], and this is still in the development phase. The situation is the result of a lack of advance in two directions. Firstly until recently there has been no instrument available capable of measuring strip flatness on line; secondly there has been no complete detailed analysis or understanding of the factors affecting flatness in the rolling operation. One of the main aims of this thesis is to provide the necessary analysis and insight into this phenomena.

Shape is the second largest single cause for the rejection of cold rolled steel strip accounting for 1.5$^{0}/_{0}$ of the total product and a similar figure applies in the aluminium industry. It should be mentioned that not all material rejected for bad shape after rolling is necessarily scrap, the shape can sometimes be corrected by further processing in "tension levellers" but this obviously adds significantly to the production costs. There is therefore considerable economic pressure for the development of an automatic flatness or shape control scheme.

Strip flatness is a function of the transverse properties of the strip and the roll gap. If a strip is to be flat after rolling, the reduction in thickness experienced as it passes through a roll gap must be constant across the strip width. The reduction operation in metal

rolling is one of plane strain, hence any transverse variation in reduction must be accompanied by a transverse variation in elongation. If a strip is constrained, either internally or by some external means, to be flat when it has experienced a transverse variation in reduction, a non uniform transverse internal stress distribution must result. If however any such constraints are exceeded, an elongation variation can exist only in a strip with varying degrees of flatness across the width. (For example, a strip which is buckled at the edges and flat at the centre is longer at the edges than the centre). The internal stress distribution caused by a transverse variation in the reduction is termed the "Shape" of the strip: a strip with uniform stress distribution is said to have "perfect shape". If the strip remains flat with a non uniform residual stress distribution the shape is said to be "Latent"; if the strip exhibits buckles the term "manifest shape" applies.

Over the last decade a variety of shape measuring instruments have been developed of which at least three are now commercially available. (the Loevy Robertson "Videmon", the ASEA "Stressometer", and the IHI instrument). Only two of these, the Videmon and the Stressometer, are capable of measuring latent shape and so are the most promising for inclusion in a shape control scheme.

There is no complete theoretical analysis of the shape phenomena recorded in the literature. In an early paper Saxl[4] developed a model for gauge profile. The modelling of the roll bending was complete but it assumed symmetry about the strip centre line. The expression for the flattening of the work rolls against the strip was based on the work of Hertz which assumes strip and rolls of infinite width. The change in flattening near the edge is therefore ignored although Saxl does discuss the effect and suggest an heuristic solution. The major omission in this work is the effect of the transverse reduction variation

on stress. The analyses of Harguchi et al[5] and of Wilmotte et al[6] are similar in detail to that described above. The roll bending again assumes symmetry and the flattening assumes infinite strip and roll width. Unlike Saxl, these authors ignore the errors in flattening near the strip edge resulting from this derivation. The problem of the internal stress distribution is again not considered. In the case of Wilmotte this omission is justified since he is concerned only with hot rolling. The analysis of Sabatini[7] is believed to be the first to include an expression for the transverse stress distribution. The derivation is based on dividing the strip into longitudinal elements and relating elongation variations to stress via Youngs modulus. The interaction between the strips due to shear, and the effect of transverse slip variations are ignored. The remainder of the model is similar to those already described. The work of O'Connor and Weinstein[8] is similar to that of Sabatini although the work roll flattening expression is in more detail and does not assume infinite width strip and rolls. The model derived by Edwards and Spooner[9] differs from that of Sabatini mainly in that it recognises the importance of including the effect of the transverse variations in slip at the exit of a stand, on the stress distribution. The derivation of an expression for the stress equations is however theoretically weak and ignores the change in the stress distribution along the strip explained by St Venants principle.

One assumption common to all the analyses discussed is that of symmetry about the strip centre line. Asymmetric shape distributions are not uncommon in practice, particularly in the Aluminium industry where for certain products the strip is slit in half longitudinally part way through a sequence of rolling operations. All of the models discussed also assume a fixed centre line thickness for the strip. The effect of parameter variations on shape can be investigated but

any interaction with thickness is ignored. A model including these effects will be required in order to study designs of combined gauge and shape control schemes.

In chapter 1 of this thesis a complete model of the shape phenomenon is derived. Unlike earlier models, symmetry is not assumed and the effects of the interaction between thickness and shape are included. An expression is derived for the transverse stress distribution which includes the effects of transverse slip variations and of longitudinal changes in the distribution. The flattening of the work rolls against the strip is analysed without the assumption of infinite strip and roll width. The resulting expressions for both the stress distribution and the roll flattening are believed to be original.

The extreme complexity of the model renders it unsuitable for use on-line and also makes it difficult to gain a simple physical understanding of some of the major effects. For this reason a simple approximate algebraic expression for shape has been developed in chapter 2. Much of the detail of the full model is lost, as the approach adopted is to model only one important component of the shape distribution. The model also assumes symmetry and a constant centre-line thickness. The final expression is however differentiable and expressions can therefore be obtained for the sensitivity of shape to important parameters.

The method and concept of developing a simple model for the important component of the shape distribution is original. The model is of central importance in that it provides control theoretic insight into, and quantitative design information on, shape behaviour. In chapters 3 and 4 of the thesis the model is used to explain the complex interactions between shape and roll force at a rolling stand and to overcome the schedule dependency of some gains in a control system.

When rolling strip in a tandem mill, the shape of the final product is important, but also the shape at the intermediate stands must be within certain tolerances to ensure acceptable mill operating conditions. For reasons of economy and because of the mechanical layout of rolling mills, shape instruments cannot be installed after every stand. The required shape must therefore be obtained by calculating the correct "schedule" for the product using the shape model and on line measurements of certain strip and mill parameters.* This problem is studied in chapter 3.

The literature on scheduling is relatively sparse. In an early paper, Oliver and Bowers[10] obtained schedules by constraining the stand roll force distribution. More recently, Suzuki et al[11] introduced similar constraints and also considered constraints on rolling powers. Shape however has been largely ignored in the scheduling studies to date mainly because adequate analysis of the shape phenomena was not available. In chapter 3 the interaction between shape, thermal crown and roll force, which is important from the point of view of scheduling, is explained with the aid of a "scheduling diagram" which is developed from the simple shape model. The diagram does not offer a complete solution to the scheduling problem as it does not include the complex interactions of shape and thickness between stands,and unfortunately an iterative procedure is required. The solution is obtained by formulating the problem in state variable terms as a constrained two point boundary value problem which is solved using conjugate gradient and projection techniques.

* The term "schedule" refers to the distribution of the reduction between the stands, the values of interstand tension, roll ground crowns and roll bending jack forces.

The understanding of the physical mechanisms at a rolling stand gained from the scheduling diagram enables the best form of cost function to be derived and also greatly assists in interpreting the results of the optimisation routine into practical engineering results.

Finally the problem of on line shape control is discussed in chapter 4. The behaviour of all available controls is analysed particularly in relation to their effect on final strip thickness, as a basic requirement of any shape control scheme must be that it does not interact with strip thickness. Both open and closed loop forms of control are discussed and the circuits derived for both are believed to be original. Most of the gains in these circuits will be dependent on the dimensions of the strip being rolled. The problem of these "schedule dependencies" is solved by using the expressions for the sensitivities derived from the simple shape model in chapter 2.

CHAPTER 1

ANALYSIS OF SHAPE

The residual stresses introduced into a strip as it is reduced in thickness through a stand of a rolling mill are determined by the variation between the entry and exit thickness profiles. If the strip is reduced plastically by varying amounts across the width the elongation must also vary. If the strip remains flat variations in length are inhibited and transversely varying residual stresses result.

Immediately after leaving the roll gap the strip thickness undergoes an elastic recovery which is dependent upon the stress and the thickness distributions. The elastic recovery will therefore, in general, vary across the strip width and the thickness profile will change. In order to calculate the actual thickness profile between stands therefore the elastic recovery must be added to the roll gap profile. The work of Ford et al[12] has shown that this recovery is related to thickness and stress by the expression,

$$h_e = \frac{h_2(1 - \nu^2)(K_2 - \sigma_2)}{E}$$

where h_e = elastic recovery in thickness

h_2 = exit thickness from the plastic zone

ν = Poissons ratio

σ_2 = exit stress

K_2 = yield stress

E = Youngs modulus of elasticity

A block diagram of the basic structure of the shape model is shown in figure 2. The exit thickness profile (ignoring elastic recovery) is determined from the sum of the deformation of the section of the work rolls in contact with the strip, calculated in block 4, the total

deflection of the work rolls due to bending and shearing, block 5, and the initial roll profile. As we shall show, the internal stress distribution in the strip is determined from the ratio of the entry and exit strip profiles and the entry strip shape; this is calculated in block 1. The force developed in the roll gap at any point across the strip is a function of entry and exit thickness and stress at that point. The exit thickness profile however, which determines the stresses, is itself a function of the roll force, via roll deformation. The stresses produced in the strip by conditions in the roll gap, feed back on the roll force and modify the roll gap conditions. The model is therefore iterative. The bending and shearing deflection of the work rolls is determined by the forces developed in the strip and by the forces applied by the backup roll (block 6). These forces are determined by the relative profiles of the adjacent surfaces of the work and backup rolls. The effects of forces applied to the rolls by bending jacks, used on some mills to modify the roll bending, are also included in these calculations (blocks 5 and 7).

To simplify the model derivation the roll length is discretised and values of the exit thickness and entry and exit stresses are calculated at the centre of each section. The forces between the strip and the work rolls and between the work and backup rolls are approximated by a series of point loads acting at the centre of each section.

Each section of the model discussed above will now be analysed in detail.

1.1 Work Roll Deflection

Figure 3a shows the forces acting on the work roll. The loading will be considered as a series of equivalent point loads $p(x) - q(x)$ acting at discrete intervals along the roll. The change in roll diameter at the roll neck will be ignored as this will only affect

the deflection of the roll in the necks and the stresses in the roll barrel in the vicinity of the necks, neither of which will influence the strip thickness produced. The length to depth ratio of the roll will generally be in the region of three for most mills and the deflection due to shear will therefore be significant and must be included. The expressions for deflection due to bending and shearing will be derived separately.

1.1.1 Deflection due to bending

An expression for the deflection due to bending will be derived using Macaulays Method[13]. Consider the beam shown in figure 3b. The bending moment at any point x along the beam can be written as*:

$$E.I.\frac{d^2y}{dx^2} = -J_1x + q_1'\left[x - a - \frac{\delta x}{2}\right] + q_2'\left[x - a - \frac{3\delta x}{2}\right] \ \ldots$$

$$+ q_n'\left[x - a - (2n-1)\frac{\delta x}{2}\right] \qquad 1.1.1$$

where J_1 = roll bending jack force at one end of the roll

E = Youngs modulus of elasticity

I = moment of inertia

y = deflection (positive downwards)

x = distance along the roll

q = resultant force on work roll $(q(x) - \rho(x))$

* N.B. By Macaulay's method if the contents of any of the square bracket becomes negative it is ignored.

By integrating 1.1.1 twice, expressions for the slope and the deflection of the beam are obtained.

$$\text{Slope} = \frac{dy}{dx} = \frac{1}{EI}\left\{-\frac{J_1 x^2}{2} + \frac{q_1'}{2}\left[x - a - \frac{\delta x}{2}\right]^2 + \frac{q_2'}{2}\left[x - a - \frac{3\delta x}{2}\right]^2 + \cdots\right.$$

$$\left. + \frac{q_n'}{2}\left[x - a - (2n-1)\frac{\delta x}{2}\right]^2 + R\right\} \qquad 1.1.2$$

$$\text{Deflection} = y = \frac{1}{EI}\left\{-\frac{J_1 x^3}{6} + \frac{q_1'}{6}\left[x - a - \frac{\delta x}{2}\right]^3 + \frac{q_2'}{6}\left[x - a - \frac{3\delta x}{2}\right]^3 + \cdots\right.$$

$$\left. + \frac{q_n'}{6}\left[x - a - (2n-1)\frac{\delta x}{2}\right]^3 + Rx + S\right\} \qquad 1.1.3$$

To evaluate the constants of integration (R and S) we assume that the deflection is specified at two points along the roll, say

$$y(x_1) = D_1$$
$$y(x_2) = D_2$$

Then

$$D_1 = \frac{1}{EI}\left\{-\frac{J_1 x_1^3}{6} + QM_1 + Rx_1 + S\right\} \qquad 1.1.4$$

$$D_2 = \frac{1}{EI}\left\{-\frac{J_1 x_2^3}{6} + QM_2 + Rx_2 + S\right\} \qquad 1.1.5$$

where $QM_i = \frac{q_1'}{6}\left[x_i - a - \frac{\delta x}{2}\right]^3 + \cdots + \frac{q_n'}{6}\left[x_i - a - (2n-1)\frac{\delta x}{2}\right]^3$

Solving for R and S gives,

$$R = \frac{1}{(x_1 - x_2)}\left\{EI(D_1 - D_2) + \frac{J_1}{6}(x_1^3 - x_2^3) - QM_1 + QM_2\right\} \qquad 1.1.6$$

$$S = EID_1 + \frac{J_1 x_1^3}{6} - QM_1 - Ax_1 \qquad 1.1.7$$

1.1.2 Deflection due to shearing

The deflection due to shearing at any point along a beam is given by[14]

$$y(x) = \frac{4}{3AG}\int_0^x V(x)\,dx \qquad 1.1.8$$

where A = cross section area

G = modulus of rigidity

V = shear force

The variation of shear force along the roll is shown diagramatically in figure 4.

The area under the curve up to any point x is given by:

$$\int_0^x V(x) = J_1 x - q_1'\left[x - a - \frac{\delta x}{2}\right] - q_2'\left[x - a - \frac{3\delta x}{2}\right] - \ldots$$

$$- q_n'\left[x - a - (2n - 1)\frac{\delta x}{2}\right] \qquad 1.1.9$$

If the contents of any square bracket is negative it is ignored. The deflection due to shearing at any point along the beam is determined by substituting equation 1.1.9 into 1.1.8.

1.2 Backup Roll Deflection

The deflection of the backup roll is caused by forces from the work rolls, the screws, and any roll bending jacks. The general form of the loading is shown in figure 5. The same assumptions and procedures used in the previous section to find the deflection of the work roll are used here to find the deflection due to bending and shearing of the backup roll.

1.2.1 Deflection due to bending

For a beam loaded as in figure 6 the expression for the bending moment is

$$\frac{d^2y}{dx^2} = \frac{1}{EI}\left\{- R_1 x + J_1[x - a] + q_1\left[x - z - \frac{\delta x}{2}\right] + q_2\left[x - z - \frac{3\delta x}{2}\right] + \cdots \right.$$

$$\left. + q_n\left[x - z - (2n - 1)\frac{\delta x}{2}\right] + J_2[x - L + a]\right\} \qquad 1.2.1$$

By integration the following expressions for slope and deflection are obtained

$$\text{Slope} = \frac{dy}{dx} = \frac{1}{EI}\left\{- \frac{R_1 x^2}{2} + \frac{J_1}{2}[x - a]^2 + \frac{q_1}{2}\left[x - z - \frac{\delta x}{2}\right]^2 + \frac{q_2}{2}\left[x - z - \frac{\delta x}{2}\right]^2 \cdots \right.$$

$$\left. + \frac{q_n}{2}\left[x - z - (2n - 1)\frac{\delta x}{2}\right]^2 + \frac{J_2}{2}[x - L + a]^2 + A \right\} \qquad 1.2.2$$

$$\text{Deflection} = y = \frac{1}{EI}\left\{- \frac{R_1 x^3}{6} + \frac{J_1}{6}[x - a]^3 + \frac{q_1}{6}\left[x - z - \frac{\delta x}{2}\right]^3 + \frac{q_2}{6}\left[x - z - \frac{\delta x}{2}\right]^3 \cdots \right.$$

$$\left. + \frac{q_n}{6}\left[x - z - (2n - 1)\frac{\delta x}{2}\right]^3 + \frac{J_2}{2}[x - L + a]^3 + Ax + B \right\}$$

$$1.2.3$$

The deflection at each end of the roll relative to some fixed datum is determined by the screw positions, ie

$$y(0) = S_1$$

$$y(L) = S_2$$

The constants of integration, A and B, can therefore be evaluated:

$$A = \frac{1}{L}\left\{EI(S_2 - S_1) + \frac{R_1 L^3}{6} - J_1\frac{(L-a)^3}{6} - q_1\frac{(L - z - {}^{\delta x}/_2)^3}{6} \cdots \right.$$

$$\left. - q_n\frac{(L - z - (2n-1)\,{}^{\delta x}/_2)^3}{6} - J_2\frac{a^3}{6}\right\} \qquad 1.2.4$$

$$B = EIS_1 \qquad 1.2.5$$

The reaction R_1 can be found by taking moments about $x = L$, then

$$R_1 = \frac{1}{L}\left\{J_1(L-a) + J_2 a + q_1(L - z - {}^{\delta x}/_2) + q_2(L - z - 3{}^{\delta x}/_2) \ldots . \right.$$

$$\left. + q_n(L - z - (2n-1)\,{}^{\delta x}/_2)\right\} \qquad 1.2.6$$

1.2.2 Deflection due to shearing

Figure 7 shows the distribution of shear force along the roll.

The shear force at any point x can be expressed by:

$$\int_0^x V(x)dx = - R_1 x + J_1[x-a] + q_1\left[x - z - \frac{\delta x}{2}\right] + q_2[x - z - 3{}^{\delta x}/_2] \cdots$$

$$+ q_n[x - z - (2n-1)\,{}^{\delta x}/_2] + J_2[x - L + a] \qquad 1.2.7$$

N.B. If the contents of any square bracket is negative it is ignored.

The deflection due to shearing is obtained by substituting equation 1.2.7 into equation 1.1.8.

1.3 Pressure Distribution between the Work and Backup Rolls

The pressure developed in the contact region between the work and the backup rolls can be determined by considering the elastic deformation between the rolls. It is assumed that at any point along the rolls, the work roll and the backup roll will each be deformed by equal amounts and the pressure is proportional to that deformation. As discussed in the introduction to this analysis, the roll is considered divided into a number of equal sections, the aim of this section is to derive an expression for a set of equivalent point loads acting on the work and the backup rolls at the centre of each section.

Referring to figure 8 it can be seen that the deformation of the rolls at the centre of the i^{th} section is,

$$\Delta_i = DB_i - DW_i \qquad 1.3.1$$

where DB_i is the distance from some datum to the bottom surface of the backup roll at section i ignoring deformation against the work roll

and DW_i is the similar distance to the top surface of the work roll

An alternative expression for the interference can be obtained from Hertz's theory for the deformation between two elastic cylinders with parallel axes[15]

$$\Delta = \frac{2(1-\nu^2)}{E} \frac{q}{\pi} \left[\frac{2}{3} + \ln \frac{2D_1}{b} + \ln \frac{2D_2}{b} \right] \qquad 1.3.2$$

$$b = 1.6\sqrt{q\,\frac{D_1\,D_2}{(D_1 + D_2)}\,\frac{2(1-\nu^2)}{E}} \qquad 1.3.3$$

where q = force per unit length

E = Youngs modulus of elasticity

D_i = diameter of cylinder i

ν = Poissons ratio

This expression assumes that the force q is constant along the length of the cylinders. The number of sections required across the roll is, for reasons which will become clear later, greater than 100. The effect of assuming the force to be a constant across each of these narrow sections is therefore small. The pressure acting between the rolls over each section can be found by combining equations 1.3.1, 1.3.2 and 1.3.3. Unfortunately it is not possible to obtain an explicit expression for q and an iterative procedure would be required to find a solution. However it has been found that the term,

$$\frac{2}{3} + \ln\frac{2D_1}{b} + \ln\frac{2D_2}{b}$$

is not very sensitive to likely variations in q. For example if q varies from 1.0 to 0.3 tonnes/mm, the above factor will change by less than $10^0/o$. The calculation can be simplified therefore by replacing q in the expression for b by a constant $\bar{q}$. $\bar{q}$ is the average value of q and can be found by dividing the total force required to reduce the strip, which is known, by the roll length.

The final expression for the force at the i^{th} section along the roll, q_i is

$$q_i = \frac{(DB_i - DW_i)}{\frac{2(1-\nu^2)}{E\pi}\left[\frac{2}{3} + \ln\frac{2D_1}{b} + \ln\frac{2D_2}{b}\right]} \qquad 1.3.4$$

$$\text{where } b = 1.6\sqrt{\bar{q}\,\frac{D_1 D_2}{D_1 + D_2}\left[\frac{2(1-\nu^2)}{E}\right]}$$

The value calculated for q must satisfy the equilibrium equation for the work roll:

$$\Sigma(p_i\ dx) + J_1 = \Sigma(q_i\ dx) \qquad 1.3.5$$

where dx is the width of each section

p_i and q_i are the values of p and q for section i

J_1 and J_2 are the jack forces acting on the roll

In the complete calculation of the force distribution q_i, the distance between the roll axis is altered by changing DW_i until the q_i calculated by equation 1.3.4 satisfies the equilibrium equation 1.3.5.

This method of calculating the pressure distribution by considering individual sections across the roll ignores the presence of shear stresses in the roll caused by the variation in deformation. The geometry of the two contacting roll surfaces dictates that the rate of change of pressure and profile will be slow. Hence it is easily shown that the shear forces on each individual section of the roll are of opposite sign and tend to cancel. The effect of shear forces can therefore be neglected.

1.4 Pressure Distribution between the Work Rolls and the Strip

The force developed between the strip and the work roll will vary across the strip because it is dependent upon entry and exit thicknesses and stresses. As with the inter roll pressure, the pressure from the strip will be approximated by a series of point loads at discrete intervals along the roll.

Since the roll force equation will have to be evaluated a number of times across the roll it is essential that a simple expression is used. In [16] a simple explicit model is derived for cold rolling which would be suitable for this application. In the shape model however a linearised roll force model has been found to yield sufficient accuracy and is used to reduce computing time. The coefficients in the linear model, which are schedule dependent, are obtained by differentiation of the model in [16] for the nominal rolling schedule values.

The linearised formula gives sufficient accuracy for the following reasons. Firstly the maximum likely transverse variation in entry and exit thicknesses is less than $5^{o}/o$ which is well within the range of the accuracy of the linear model. The stresses however can vary by more than $100^{o}/o$ if the shape is bad. The sensitivity of roll force to entry or exit stress is fairly non linear (although not as non linear as with thickness[17]). However the effect of equal changes in entry and exit stress is very nearly linear. This can be understood by the following heuristic explanation. Considering the diagram of the pressure variation through the roll gap, figure 9. The total pressure developed is represented by the area under the graph. It can be seen that the effect on total pressure of equal changes to entry and exit stress is linear since, to a first order, the friction hill area is unchanged. Results from the full shape model have shown that the stress distributions on either side of the roll gap do tend to be

similar. This effect is brought about by the complex interactions of slip and gauge in the transverse stress equations developed in section 1.6.

All the roll force models derived in the literature are based on the assumption that compression takes place in plane strain. At the extreme edges of the strip this is untrue since there is no strip present to restrain the sideways movement although there is still a friction force. Because of this the true roll force close to the strip edges will be less than that predicted by the classical roll gap equation. To investigate this error we require to know the relationship between the yield stress in simple compression (the limiting case represents the condition at the extreme edge) and the yield stress under plane strain.

Von Mises criterion states[18] that yielding begins under any conditions when the distortion energy equals the distortion energy at yield in simple compression.

$$\text{Distortion energy, } U_d = \frac{1}{2G} \cdot \frac{1}{6}\left[(\sigma_1 - \sigma_2)^2 + (\sigma_2 - \sigma_3)^2 + (\sigma_3 - \sigma_1)^2\right] \qquad 1.4.1$$

where σ_1, σ_2, σ_3 are the three normal stresses

G is the modulus of rigidity

Now in simple compression two of the stresses are zero. Therefore

$$U_d = \frac{\sigma_1^2}{6\ G} \qquad 1.4.2$$

and σ_1 must be equal to the yield stress K, hence

$$K = \sqrt{6\ G\ U_d} \qquad 1.4.3$$

The relationship between the stresses in the case of plane strain can be found from the Levy-Mises equation[18] which states

$$\frac{d\varepsilon_1}{(\sigma_1 - \bar{\sigma})} = \frac{d\varepsilon_2}{(\sigma_2 - \bar{\sigma})} = \frac{d\varepsilon_3}{(\sigma_3 - \bar{\sigma})} = K$$

where ε = strain

and $\bar{\sigma}$ is the mean stresses = $\dfrac{\sigma_1 + \sigma_2 + \sigma_3}{3}$

For plane strain $d\varepsilon_3 = 0$

therefore $$\sigma_3 = \bar{\sigma} = \frac{(\sigma_1 + \sigma_2 + \sigma_3)}{3}$$

or $$\sigma_3 = \left[\frac{\sigma_1 + \sigma_2}{2}\right] \qquad 1.4.4$$

Substituting this condition into the equation for distortion energy gives,

$$U_d = \frac{1}{2G} \cdot \frac{1}{6}\left[\frac{3}{2}(\sigma_1 - \sigma_2)^2\right] \qquad 1.4.5$$

By Von Mises criterion equations 1.4.3 and 1.4.5 can be equated

$$\frac{1}{2G} \cdot \frac{1}{6}\left[\frac{3}{2}(\sigma_1 - \sigma_2)^2\right] = \frac{K^2}{6G} \qquad 1.4.6$$

or $$K = \frac{\sqrt{3}}{2}(\sigma_1 - \sigma_2)$$

Therefore the yield stress in simple compression equals $\dfrac{\sqrt{3}}{2}$ times the yield stress in plane strain.

If the elastic recovery regions and the effect of strip tensions are ignored, the roll force is approximately a linear function of yield stress. Therefore $\sqrt{3}/2$ is an upper limit to the possible reduction in roll force caused by spread, ie the effect on roll force will be less than $14^{o}/o$.

An estimate for the portion of the strip width affected by spread can be obtained from measurements of width change taken during the rolling of strip through four stands of a tandem mill. For four approximately equal reductions of $20^{o}/o$, the increase in width is typically less than 1 mm. That is a $20^{o}/o$ reduction causes a width change of less than 0.25 mm, assuming the spread is equal on all stands. It is reasonable to assume that the degree of sideways spread is a maximum at the extreme edge of the strip. As a limiting case we will assume that at this point the material is reduced by simple compression and therefore the fractional change in width is equal to half the fractional reduction,

$$\frac{\delta w}{w} = 0.5\ R$$

Away from the strip edge the amount of spread will decrease until at some distance X from the edge the reduction process will be plane strain. The distance X affected by spread will clearly depend on the way in which the spread decays. Assume that the spread decays according to some function f(x), where x is the distance from the strip edge, such that,

$$f(0) = 1$$

$$f(X) = 0$$

Then the increase in width can be expressed by

$$\frac{\Delta w}{w} = 2 \int_0^X 0.5\ R\ f(x)\ dx \qquad 1.4.7$$

The exact form of $f(x)$ is unknown but it is expected that it will decay rather rapidly initially and therefore the major effect of spread on roll force will be limited to a very small region at the edge. As a limiting case let us assume that there is a region close to each edge of the strip where the reduction process is simple compression and, for the remainder of the width, plane strain applies. Then,

$$f(x) = 1 \qquad 0 < x \leqslant X$$

$$f(x) = 0 \qquad x > X$$

$$\text{and} \quad \Delta w = R \int_0^X dx$$

Using the measurements quoted of a 0.25 mm increase in width with a 20°/o reduction, the distance affected by the spread is,

$$X = \frac{\Delta w}{R} = \frac{.25}{.2} = 1.25 \text{ mm}$$

In practice the decay will be gradual and therefore the region will be wider but the error in the roll force will decrease. For a linear decay,

$$f(x) = 1 - \frac{x}{X} \qquad 0 < x \leqslant X$$

$$f(x) = 0 \qquad x > X$$

the region affected will be 2.5 mm but the roll force error will be less than 7°/o at 1.25 mm.

These approximate results indicate that the effect of spread on roll force is small. It can be shown that, assuming typical strip and mill dimensions, the effect of this roll force error on the bending and shearing deflection of the work roll across the strip width is less than 0.25°/o.

1.5 Work Roll Flattening

The final transverse profile of the roll gap is significantly affected by the variation in the indentation of the roll by the strip across the width. In the literature most authors have modelled this term approximately using the Hertzian expression for flattening between cylinders and flat plates. The Hertzian expressions are correct only for cylinders subjected to a uniform pressure. The method adopted was the same as that used for the inter roll pressure distribution, the expression was applied to each section of the roll where the pressure was assumed to be constant at the average value. Over most of the strip width this method gives adequate results as the variation in roll force is slow, however large errors result in the region of the strip edges where the roll force drops suddenly to zero. The influence of the unloaded roll on the roll deformation near the strip edges is not modelled and a sudden change in deformation is predicted as shown in figure 10a. A more accurate form of the deformation is clearly that shown in figure 10b.

It is proposed to develop here a more accurate model for the flattening in the form of an influence function for the deformation of the roll caused by a pressure distributed over a small area. To obtain the total deformation the influence functions will be summed across the complete strip width. Three assumptions will be made in developing the model: (a) The problem can be approximated by a band of pressure applied on the surface of a semi-infinite solid because of the relative sizes of the arc of contact between the strip and roll, and the roll diameter. (In cold rolling the arc of contact is typically 25 mm for a roll diameter 550 mm, the angle subtended by the arc is therefore approximately 1.5 degrees.) In figure 11 the roll is represented by the semi-infinite solid,

$$-\infty < x < \infty + \quad , -\infty < y < \infty + \quad , -\infty < z < 0$$

with pressure applied at,

$$z = 0 \ , \ -a < y < +a \ , \ -b < x < +b$$

(b) The band of pressure will be assumed constant in the direction of rolling. This is reasonable since the primary aim is to model the transverse variation in thickness profile of the strip leaving the stand and this will be determined by a single point on the roll circumference. (c) The variation in roll force across the strip width can be approximated by a number of equal sections over which the roll force is a constant, see figure 12. The problem then reduces to that of developing an influence function for the displacement on the surface of an infinite solid, into the solid, caused by a uniform pressure applied over a small rectangular area. The total flattening along the roll can be determined by summing the effects of each section of the strip width.

The required function can be derived from the expression for the displacement dW due to a pressure p per unit area applied at a point x_1, y_1 in the plane $z = 0$[19]. This equation, which is derived in appendix 2, is,

$$dW = \frac{(1 - \nu)}{2 \pi G} \cdot \frac{p \, dx_1 \, dy_1}{R} \qquad 1.5.1$$

where R is the distance between the point at which the force is applied (x_1, y_1) and the point at which the displacement is measured (x, y)

$$R^2 = (x - x_1)^2 + (y - y_1)^2$$

The displacement caused by a pressure p per unit area applied over an area $-a < y < a$, $-b < x < b$ on the surface $z = 0$ can be obtained by integrating 1.5.1

$$W(x, y) = \frac{(1 - \nu)}{2 \pi G} \int_{-a}^{a} \int_{-b}^{b} \frac{p \, dx_1 \, dy_1}{[(x - x_1)^2 + (y - y_1)^2]^{1/2}} \qquad 1.5.2$$

Let $A = y - y_1$ and integrate with respect to x_1 only:

$$I = \int_{-b}^{b} \frac{d\,x_1}{[(x - x_1)^2 + A^2]^{1/2}}$$

Let $X = x - x_1$

$dX = -d\,x_1$

when $x_1 = b \qquad X = x - b$

$x_1 = -b \qquad X = x + b$

$$I = \int_{x-b}^{x+b} \frac{dX}{[X^2 + A^2]^{1/2}} = \left\{ \ln\left[X + (X^2 + A^2)^{1/2}\right] \right\}_{x-b}^{x+b}$$

$$I = \ln\left[(x + b) + \left((x + b)^2 + A^2\right)^{1/2}\right] - \ln\left[(x - b) + \left((x - b)^2 + A^2\right)^{1/2}\right]$$

Therefore:

$$W = \frac{p(1 - \nu)}{2\,\pi\,G} \int_{-a}^{a} \left\{ \ln\left[(x + b) + \left((x + b)^2 + (y - y_1)^2\right)^{1/2}\right] - \ln\left[(x - b) + \left((x - b)^2 + (y - y_1)^2\right)^{1/2}\right] \right\} dy_1$$

Let $A = (x + b) \qquad B = (x - b)$

$Y = y - y_1$

$dY = -dy_1$

when $y_1 = a \qquad Y = y - a$

$y_1 = -a \qquad Y = y + a$

$$W = \frac{p(1 - \nu)}{2\,\pi\,G} \int_{y-a}^{y+a} \left\{ \ln\left[A + (A^2 + Y^2)^{1/2}\right] - \ln\left[B + (B^2 + Y^2)^{1/2}\right] \right\} dY$$

$$W = \frac{p(1-\nu)}{2\pi G}\left[I_1 - I_2\right]$$

The integral of the form I_1 and I_2 is solved in appendix 3 giving the result:

$$\int_p^q \ln\left[A + (A^2 + Y^2)^{1/2}\right]dy = \left\{\left[Y \ln\left(A + (A^2 + Y^2)^{1/2}\right)\right]_p^q - A\left[\tan z \doteq \ln(\sec z + \tan z)\right]_{\tan^{-1}\left(\frac{p}{A}\right)}^{\tan^{-1}\left(\frac{q}{A}\right)}\right\}$$

Inserting the limits, I_1 becomes,

$$I_1 = y\left\{\ln\left[\frac{\left[A + (A^2 + (y+a)^2)^{1/2}\right]}{\left[A + (A^2 + (y-a)^2)^{1/2}\right]}\right]\right\}$$

$$+ a\left\{\ln\left[\left(A + (A^2 + (y+a)^2)^{1/2}\right)\left(A + (A^2 + (y-a)^2)^{1/2}\right)\right]\right\}$$

$$- (y+a) + A \ln\left[\frac{\left[(x+b)^2 + (y+a)^2\right]^{1/2}}{(x+b)} + \left(\frac{y+a}{x+b}\right)\right]$$

$$+ (y-a) - A \ln\left[\frac{\left[(x+B)^2 + (y-a)^2\right]^{1/2}}{(x+b)} + \frac{(y-a)}{(x+b)}\right]$$

For the purposes of shape modelling we are interested in the displacement of the roll surface along a line y = constant. For convenience let y = 0. Then,

$$I_1 = 2a \ln\left[(x + b) + ((x + b)^2 + a^2)^{1/2}\right]$$

$$- 2a + (x + b) \ln\left\{\frac{[(x + b)^2 + a^2]^{1/2} + a}{[(x + b)^2 + a^2]^{1/2} - a}\right\}$$

Similarly I_2 can be shown to be:

$$I_2 = 2a \ln\left[(x - b) + ((x - b)^2 + a^2)^{1/2}\right]$$

$$- 2a + (x - b) \ln\left\{\frac{[(x - b)^2 + a^2]^{1/2} + a}{[(x - b)^2 + a^2]^{1/2} - a}\right\}$$

Finally

$$W(x, 0) = \frac{p(1 - \nu)}{2 \pi G} \left\{ 2a \ln\left[\frac{(x + b) + ((x + b)^2 + a^2)^{1/2}}{(x - b) + ((x - b)^2 + a^2)^{1/2}}\right]\right.$$

$$+ (x + b) \ln\left[\frac{((x + b)^2 + a^2)^{1/2} + a}{((x + b)^2 + a^2)^{1/2} - a}\right]$$

$$\left. - (x - b) \ln\left[\frac{((x - b)^2 + a^2)^{1/2} + a}{((x - b)^2 + a^2)^{1/2} - a}\right]\right. \qquad 1.5.3$$

It will be assumed therefore that equation 1.5.3 represents the influence function for the indentation of the roll surface caused by a uniform pressure acting over a roll length 2b and an arc length 2a. To compute the total indentation caused by contact with the strip, the strip will be divided into a number of narrow sections over each of which the pressure can be approximated by a constant. The indentation of the roll by each of these will then be computed using equation 1.5.3. Since we are dealing with an elastic media the effects are linear and the total indentation is obtained by summation.

The form of the indentation given by equation 1.5.3 for the case of a uniform roll force acting across the complete strip width is shown in figure 13. Near the strip edge there is a rapid decrease in the amount of deformation and this would result in a decrease in the strip thickness at this point. The result of such a profile would, of course, be to set up very large compressive stresses near the strip edges due to the increased elongation. In practice this indentation profile is highly modified by "feedback". The profile shown in figure 13 is the result of a uniform pressure distribution across the strip, however the increased reduction and high compressive stresses,which will result near the strip edges,will both cause an increased rolling pressure in this area. The increased rolling pressure will increase the amount of indentation and the net result will be to reduce considerably the variation in flattening near to the strip edges.

The effect of this feedback is included by iteration in the final shape model.

1.6 Transverse Distribution of Stress

When metal strip is reduced in thickness by rolling through one or more stands, a transverse variation in the longitudinal stresses is set up in the strip. This variation in stress in the strip at any point between the stands is caused by (a) any transverse variation in the reduction and hence elongation at previous stands and (b) transverse variations in the slip and hence the strip velocity at the exit of the previous stand or at the entry to the next stand. The existence of these stresses is important for two reasons. Firstly during rolling the stresses in the strip at the entry and exit of a stand affect the roll gap profile and hence the reduction and slip variations. Secondly the portion of the stresses which remain in the strip after rolling are the strip shape and determine its ability to be flat.

In the derivation of expressions for the transverse stress distributions which follow, it will be assumed that the strip remains flat and buckling does not occur. This is justifiable when considering strip during rolling since it is held under a tension which, except in certain extreme cases, will be sufficient to prevent buckling. (Buckling cannot occur unless compressive stresses are present.) After rolling, when the strip is free from constraints, the mean level of the stress will be zero. The level of compressive stress which the strip can sustain without buckling is very low, and in many cases therefore, particularly with thin wide strip, buckling will occur after rolling. Except for cases of very bad shape however the amplitude of the buckled wave will be low and often indiscernible to the eye.

1.6.1 The effect of reduction variations

The transverse variation in reduction (and hence the elongation) of an element midway between stands is determined by the conditions which existed at the last roll gap when that element was rolled. Consider an infinite length of strip that has been rolled under steady state conditions such that the reduction at the edges is greater than that at the centre. Because the strip is deformed plastically in the roll gap, any transverse variation in reduction will give rise to an equal variation in elongation. If any transverse element of the strip is considered therefore in isolation from the adjacent elements, the edges will be longer than the centre. It is clearly impossible for every transverse element of the strip to maintain the same variation in length (assuming the strip remains flat) and hence the elongation variation is inhibited and a stress variation results.

Consider the strip shown in figure 14, the stress at any point y across the strip can be expressed by the sum of two components. The first component is the difference between the strain at that point and the mean strain,

$$E\left\{\frac{1}{2b}\int_{-b}^{b}\varepsilon(z)dz - \varepsilon(y)\right\}$$

The second component, which is only non-zero in the case of asymmetric stress distributions, is the resultant bending stress[13],

$$\sigma_B = \frac{My}{I}$$

where M is the bending moment

and I the moment of inertia

For a rectangular strip thickness t width 2b,

$$I = \frac{2\,t\,b^3}{3}$$

Therefore

$$\sigma_B(y) = \frac{3\,y}{2\,t\,b^3} \int_{-b}^{b} E\,\varepsilon(z).t.z\,dz = \frac{3\,E\,y}{2\,b^3} \int_{-b}^{b} \varepsilon\,(z).z.dz$$

Hence the expression for the stress at any point across the strip is,

$$\sigma_x(y) = -E\left\{\varepsilon(y) - \frac{1}{2b} \int_{-b}^{b} \varepsilon(z)dz - \frac{3y}{2\,b^3} \int_{-b}^{b} \varepsilon\,(z).z.dz\right\} \qquad 1.6.1$$

or in discrete form,

$$\sigma_i = -E\left\{\varepsilon_i - \bar{\varepsilon} - \frac{3\,i\,\delta y}{2\,b^3} \sum_{j=1}^{K} \varepsilon_j.j\,\delta y\right\} \qquad 1.6.2$$

where δy is the width of a discrete section

and K is the number of sections

$$\bar{\varepsilon} = \frac{1}{2b} \sum_{i=1}^{K} \varepsilon_i\,\delta y$$

(N.B. The last term in equations 1.6.1 and 1.6.2 will only have a value when the stress distribution is asymmetric.)

The strain ε can be expressed in terms of thickness at each point across the strip before and after the previous rolling stand. Consider an element of strip of thickness H and length L before reduction and thickness h and length l after reduction. By continuity of volume,

$$HL = h\,l$$

Therefore $\frac{H}{h} = \frac{l}{L}$

and the strain $\varepsilon = 1 - \frac{l}{L} = 1 - \frac{h}{H} = \frac{l}{L} - 1 = \frac{H}{h} - 1$ 1.6.3

Substituting equation 1.6.3 into 1.6.2 gives

$$\sigma_{xi} = + E\left\{\frac{\bar{H}}{\bar{h}} - \frac{H_i}{h_i} - \frac{3i\ \delta y}{2b^3} \sum_{j=1}^{K} \left(1 - \frac{H_j}{h_j}\right) j\ \delta y\right\} \qquad 1.6.4$$

In the symmetric case this reduces to

$$\sigma_i = E\left\{\frac{\bar{H}}{\bar{h}} - \frac{H_i}{h_i}\right\} \qquad 1.6.5$$

The above expressions give the internal stress distribution caused by variations in reduction across an infinitely long strip where transverse variations in elongation are inhibited. Near the ends of a finite length of strip a degree of elongation variation is possible and, if the ends have no external constraints, then the end stresses must go to zero. In a strip of finite length therefore there must be a region near to each end where any stresses decay to zero. This is illustrated in figure 15 where the difference in stress from strip centre to edge is plotted against the length for a strip of length L. The length of these regions of stress decay is bounded according to St. Venants principle which will be discussed in detail later.

1.6.2 The effect of slip variations

Consider a piece of strip between stands during rolling. The ends of the strip, at the exit of stand i and the entry to stand i + 1 are not free. If the exit and entry velocities are constant across

the strip it is equivalent to maintaining the conditions of uniform elongation which apply across an infinitely long strip. In this case therefore the transverse stress distribution will remain constant at all points between the stands, see figure 16.

In practice the entry and exit velocities, which are a function of slip, vary across the width. This variation in velocity is equivalent to enforcing a strain variation on the free ends of strip whose length is equal to the interstand length. St Venants principle states that the stress variation caused by end tractions will decay to zero over a short length, and hence the final variation of the transverse stress distribution along the strip between stands will be of the form shown in figure 16.

The strip exit velocity at a stand is given by,

$$v(y) = \omega R(1 + f(y))$$

where ω = roll speed

R = roll radius

$f(y)$ = slip

The strain imposed at a point y across the strip is

$$\varepsilon(y) = 1 - \frac{\text{length of strip produced in time } \delta t}{\text{average length produced in time } \delta t}$$

$$= 1 - \frac{\omega R(1 + f(y))\ \delta t}{\omega R(1 + \bar{f})\ \delta t}$$

$$= \frac{\bar{f} - f(y)}{1 + \bar{f}}$$

Therefore the stresses imposed on the strip as it leaves a stand are,

$$\sigma^{o}(y) = E\left\{\frac{\bar{f} - f(y)}{1 + \bar{f}}\right\}$$

or in discrete form,

$$\sigma_i^{o} = E\left\{\frac{\bar{f} - f_i}{1 + \bar{f}}\right\} \qquad 1.6.6$$

The strip velocity at the entry to a stand is

$$V(y) = \frac{h(y)}{H(y)}\,\omega R(1 + f(y))$$

It follows therefore that the stress imposed on the strip as it enters a stand is, in discrete form,

$$\sigma_i^{i} = E\left\{\frac{h_i}{\bar{h}}\,\frac{\bar{H}}{H_i}\,\frac{(1 + f_i)}{(1 + \bar{f})} - 1\right\} \qquad 1.6.7$$

1.6.3 The complete stress equations

Expressions for the stress distributions at a stand entry and exit, and at a point midway between stands (the shape), can be obtained by combining equations 1.6.4 with 1.6.7 and 1.6.6 respectively.

From equation 1.6.4 the shape distribution vector residual in a strip away from any stand is

$$\Omega_i = + E\left\{\frac{\bar{H}}{\bar{h}} - \frac{H_i}{h_i} - \frac{3i\,\delta y}{2b^3}\sum_{j=1}^{K}\left(1 - \frac{H_j}{h_j}\right) j\,\delta y\right\} \qquad 1.6.8$$

The total stress distribution at the entry to a stand is a result of the residual shape produced by the previous stand (equation 1.6.8) and the slip variations at the entry to the current stand (equation 1.6.7).

The stress distribution is

$$\sigma_i = E\left\{\frac{h_i\ \bar{H}\ (1 + f_i)}{\bar{h}\ H_i\ (1 + \bar{f})} - 1\right\} + \Omega' \qquad 1.6.9$$

where Ω' is the residual shape produced at the previous stand. Similarly the stress distribution at the stand exit is obtained by combining equations 1.6.8 and 1.6.6

$$\sigma_i = E\left\{\frac{\bar{f} - f_i}{1 + \bar{f}}\right\} + \Omega_i \qquad 1.6.10$$

The shape distribution vector given by equation 1.6.8 is the transverse stress distribution which will remain in the strip after rolling (except close to free ends). This is therefore the shape of the final product.

1.6.4 The rate of change of stress distribution adjacent to a stand

There is one outstanding aspect of the stress behaviour derived so far; over what length of strip either side of a stand is the stress distribution affected by the stresses due to slip variations. (The same region will apply to the decay of stresses at the free ends of a strip). Saint Venants principle states that the effect of self equilibrating end loads on the stress distribution in a body are confined to short regions close to the ends. As a "rule of thumb", the length of these regions is normally taken to be approximately equal to the width of the material: That is if we are interested in a point at a distance greater than one strip width from the ends, the end effect can be ignored.

The various aspects of this end problem can be approximated by the behaviour of a simple structural model[20] as shown in appendix 4. A graph of the decay of the effect of a self equilibrating end load

with distance from the end of a plate is shown in figure 17. The effects can be considered negligible for a distance greater than the plate width.

Referring these results to the determination of stresses in a rolled strip two observations can be made: (1) The effect on the transverse stress distribution of variations in slip at the entry or exit of a stand becomes negligible at a distance greater than one strip width from the stand. (2) After rolling when a length of strip is laid with its ends free, the transverse stress variation will decay to zero at the ends.

1.7 The Shape Algorithm

At the beginning of this section the complete shape algorithm was described with the aid of the block diagram of figure 2. In subsections 1.1 to 1.6 the contents of the separate blocks were analysed in detail and expressions derived for the various functions. The shape model has been solved numerically on a digital computer and a flow diagram of the calculation is shown in figure 18.

In the following description the numbers in square brackets refer to the blocks in figure 18. At the start of the calculation all data relevant to the particular mill and strip being considered is read in [1] and values of the dependent mill constants are calculated [2]. All the arrays used in the calculation are initialised, linear coefficients of the roll force are calculated, and the influence function for the work roll flattening, derived in 1.5, is calculated [3]. A useful feature of the computer calculation is the ability to parameterise the calculated stress and thickness distributions to some prespecified form. A matrix used in this parameter estimation is initialised in [4]. In order to start the shape calculation proper it is necessary to estimate the variation in the output strip thickness,

this will have been setup in [3]. Using the known entry thickness variation and the estimated exit thickness variation, the entry and exit stress distributions and the shape are calculated from the expressions developed in 1.6 [5]. In [6] the roll force variation is calculated from entry and exit stresses and thicknesses using a linearised roll force expression as discussed in section 1.4. The inter roll pressure distribution and the roll deflections are inter-dependent as shown by the expression for the pressure distribution derived in 1.3; the calculation of these quantities therefore forms an inner iterative loop. The inter roll pressure distribution is calculated in [7] using the last calculated values of roll deflection. (The first time through the calculation the deflections are taken as zero). New values of backup roll [8] and work roll [9] deflection are calculated and the last values are updated by a portion of the difference between the past and present values [10]. The inter roll pressure distribution is recalculated using the new deflections. This loop is cycled three times. Using the distribution of roll force calculated in [6], and the influence function calculated in [3], the work roll flattening vector is calculated [11]. Finally in [12] the stand exit thickness profile is calculated from the calculated bending and flattening of the work roll. The thickness distribution used to start the calculation is updated by a portion of the difference between it and the value calculated in [12] and the calculation restarted at [5].

After the second iteration the shape calculated during one cycle is compared [13] with that calculated during the previous iteration. When the difference is within some specified tolerance, the calculation is stopped. The stress and thickness parameters are estimated [14] and all relevant information printed out [15].

In order that the rapid changes in the stresses, shape and exit thickness in the region of the strip edges are accurately modelled, it was found necessary to divide the roll into 140 equal sections.

1.8 Model Verification

In figure 19 the shape distributions calculated by the model are plotted together with shape measured at the output of a mill using a Videmon shape instrument. (Shape instruments are discussed in more detail in section 5.2). The instrument measures the average stress over sections of the strip width. In this case the shape was symmetric so only half the width has been plotted. The results are shown for three different roll bending jack forces 3, 30 and 54 tonnes, and the calculated results compare well with the instrument readings. It is particularly interesting to note the sudden large decrease in stress at the strip edge due to the roll flattening effect, the instrument readings only show a very slight tendency of decrease in stress since only the average stress over the rotor width, which was 67 mm, is recorded. This is an obvious drawback with this type of instrument.

1.9 Example of program output

In the following pages a typical output from the shape program is shown for two cases. All the relevant data concerning the mill and the strip is included in the print out.

The difference between the two cases is the entry thickness profile. In the first case the entry thickness is uniform and in the second the thickness decreases rapidly close to the edges. This latter profile is typical of the actual input to some known mills. It can be seen that the effect of this input profile is to reduce the edge effects from the shape produced. This will be discussed more in later sections.

INDUSTRIAL AUTOMATION GROUP , IMPERIAL COLLEGE

STRIP SHAPE ANALYSIS

AUTHOR P.D.SPOONER

SEPTEMBER 1974

PLANT AND PRODUCT DATA FOR STAND

	MILL PARAMETERS			SCHEDULE PARAMETERS	
WORK ROLLS	FACE LENGTH (MM)	1950.0000		MEAN ANNEALED THICKNESS (MM)	2.3600
	RADIUS (MM)	292.0000		MEAN ENTRY THICKNESS (MM)	1.2120
	GROUND CROWN (MM ON RAD)	-.1250		MEAN EXIT THICKNESS (MM)	1.1000
	THERMAL CROWN (MM ON RAD)	0		MEAN ENTRY TENSION (TONNE/MM/MM)	.0100
BACKUP ROLLS	FACE LENGTH (MM)	1950.0000		MEAN EXIT TENSION (TONNE/MM/MM)	.0100
	RADIUS (MM)	535.0000		STRIP WIDTH (MM)	1114.0000
	GROUND CROWN (MM ON RAD)	0		FRONT SCREW POSITION (MM)	.5910
	THERMAL CROWN (MM ON RAD)	0		BACK SCREW POSITION (MM)	.5910
JACK FORCE	WORK ROLL (TONNE)	25.00	25.00		
	BACKUP ROLL (TONNE)	0	0		
	WORK/BACKUP ROLL (TONNE)	54.20	54.20		
DISTANCE BETWEEN JACKS (MM)		2650.0000			
DISTANCE BETWEEN SCREWS (MM)		2510.0000			

GAUGE AND STRESS PROFILE PARAMETERS

THE GAUGE AND STRESS PROFILES ARE PARAMETERISED BY THE EXPRESSION,

$$A + B(X-0.5)_{N} + C(X-0.5)^{**2}_{W}$$

A = THE MEAN VALUE
B = THE TOTAL SKEW
C = THE PARABOLIC DIFFERENCE,CENTRE TO EDGE

THE PARAMETERS ARE FITTED BY A LEAST SQUARES CRITERION.

	A	B	C
ENTRY GAUGE,MM	1.21200	-.00000	-.00060
ENTRY STRESS,TONNE/MM/M	.01038	.00000	.00325
SHAPE,TONNE/MM/MM	.00039	.00000	.00332

PARAMETER DISTRIBUTIONS

SECTION NUMBER	DISTANCE ACROSS ROLL FACE (MM)	STRIP THICKNESS DISTRIBUTION (MM) ENTRY	EXIT	RESIDUAL STRESS DISTRIBUTION (TONNE/MM/MM) ENTRY	EXIT	ROLL FORCE P (TONNE/MM)	CONTACT PRESSURE,Q (TONNE/MM)	WORK ROLL FLATTENING (MM)	TOTAL WORK ROLL PROFILE (MM)	WORK ROLL DEFLECTION (MM)	BACKUP ROLL DEFLECTION (MM)	SHAPE (T/MM/MM)
1	3.17	0	0	0	0	0	.0906	.0142	-.1246	1562.3549	635.3932	0
3	11.91	0	0	0	0	0	.1252	.0152	-.1177	1562.3511	635.3909	0
5	20.65	0	0	0	0	0	.1489	.0163	-.1108	1562.3469	635.3884	0
7	34.19	0	0	0	0	0	.1740	.0175	-.1041	1562.3427	635.3859	0
9	45.35	0	0	0	0	0	.1987	.0190	-.0977	1562.3385	635.3834	0
11	56.47	0	0	0	0	0	.2229	.0207	-.0914	1562.3343	635.3810	0
13	67.61	0	0	0	0	0	.2466	.0229	-.0854	1562.3301	635.3787	0
15	78.75	0	0	0	0	0	.2699	.0258	-.0796	1562.3259	635.3764	0
17	89.89	0	0	0	0	0	.2928	.0302	-.0739	1562.3216	635.3741	0
19	101.03	0	0	0	0	0	.3153	.0388	-.0685	1562.3174	635.3719	0
21	112.17	1.2120	1.0991	-.00554	-.00562	.9571	.3573	.1041	-.0633	1562.3131	635.3698	-.01687
23	123.31	1.2120	1.0998	.00725	.00710	.7095	.3584	.1014	-.0583	1562.3090	635.3677	-.00297
25	134.45	1.2120	1.0999	.00316	.00311	.6624	.3784	.1024	-.0535	1562.3052	635.3657	-.00091
27	145.59	1.2120	1.1000	.01002	.01002	.6452	.3975	.1034	-.0489	1562.3015	635.3638	.00062
29	156.73	1.2120	1.1000	.01048	.01051	.6360	.4156	.1045	-.0445	1562.2980	635.3619	.00052
31	167.87	1.2120	1.1000	.01074	.01078	.6309	.4328	.1051	-.0403	1562.2947	635.3601	.00080
33	179.01	1.2120	1.1000	.01088	.01093	.6280	.4490	.1060	-.0363	1562.2915	635.3584	.00095
35	190.15	1.2120	1.1000	.01095	.01100	.6267	.4643	.1068	-.0325	1562.2886	635.3568	.00102
37	201.29	1.2120	1.1000	.01096	.01102	.6263	.4788	.1075	-.0290	1562.2858	635.3552	.00104
39	212.43	1.2120	1.1000	.01095	.01101	.6266	.4923	.1082	-.0256	1562.2831	635.3538	.00103
41	223.57	1.2120	1.1000	.01092	.01097	.6272	.5050	.1089	-.0225	1562.2807	635.3524	.00099
43	234.71	1.2120	1.1000	.01087	.01092	.6282	.5168	.1096	-.0196	1562.2784	635.3511	.00094
45	245.85	1.2120	1.1000	.01081	.01086	.6294	.5277	.1102	-.0168	1562.2762	635.3498	.00087
47	256.99	1.2120	1.1000	.01074	.01079	.6307	.5378	.1107	-.0143	1562.2743	635.3487	.00080
49	268.13	1.2120	1.1000	.01068	.01072	.6320	.5470	.1113	-.0119	1562.2725	635.3476	.00073
51	279.27	1.2120	1.1000	.01061	.01065	.6333	.5554	.1117	-.0098	1562.2708	635.3467	.00066
53	290.41	1.2120	1.1000	.01055	.01058	.6346	.5630	.1122	-.0079	1562.2694	635.3458	.00059
55	301.55	1.2120	1.1000	.01049	.01052	.6358	.5697	.1126	-.0062	1562.2680	635.3450	.00053
57	312.69	1.2120	1.1000	.01043	.01046	.6369	.5756	.1129	-.0047	1562.2669	635.3443	.00047
59	323.83	1.2120	1.1000	.01038	.01041	.6379	.5807	.1132	-.0034	1562.2659	635.3437	.00042
61	334.97	1.2120	1.1000	.01034	.01036	.6388	.5849	.1134	-.0023	1562.2651	635.3432	.00037
63	346.11	1.2120	1.1000	.01031	.01033	.6395	.5884	.1136	-.0015	1562.2644	635.3429	.00033
65	357.25	1.2120	1.1000	.01028	.01030	.6400	.5910	.1138	-.0008	1562.2639	635.3425	.00030
67	368.39	1.2120	1.1000	.01026	.01029	.6404	.5928	.1139	-.0003	1562.2635	635.3423	.00028
69	379.53	1.2120	1.1000	.01025	.01027	.6406	.5938	.1140	-.0001	1562.2633	635.3422	.00027
71	390.67	1.2120	1.1000	.01025	.01026	.6406	.5940	.1140	.0001	1562.2633	635.3422	.00027
73	401.81	1.2120	1.1000	.01025	.01027	.6405	.5934	.1139	.0002	1562.2634	635.3422	.00027
75	412.95	1.2120	1.1000	.01027	.01029	.6402	.5920	.1139	.0005	1562.2637	635.3424	.00029
77	424.09	1.2120	1.1000	.01029	.01031	.6398	.5898	.1137	.0011	1562.2641	635.3427	.00032
79	435.23	1.2120	1.1000	.01032	.01034	.6391	.5867	.1136	.0019	1562.2647	635.3430	.00035
81	446.37	1.2120	1.1000	.01036	.01038	.6383	.5829	.1133	.0028	1562.2655	635.3435	.00039
83	457.51	1.2120	1.1000	.01041	.01043	.6374	.5782	.1131	.0040	1562.2664	635.3440	.00044
85	468.65	1.2120	1.1000	.01048	.01049	.6364	.5727	.1127	.0054	1562.2675	635.3447	.00050
87	479.79	1.2120	1.1000	.01055	.01056	.6352	.5664	.1124	.0070	1562.2687	635.3454	.00056
89	490.93	1.2120	1.1000	.01063	.01064	.6340	.5593	.1120	.0088	1562.2701	635.3462	.00063
91	502.07	1.2120	1.1000	.01065	.01069	.6327	.5513	.1115	.0109	1562.2716	635.3471	.00070
93	513.21	1.2120	1.1000	.01071	.01075	.6313	.5425	.1110	.0131	1562.2734	635.3481	.00077
95	524.35	1.2120	1.1000	.01078	.01082	.6300	.5329	.1105	.0155	1562.2752	635.3492	.00084
97	535.49	1.2120	1.1000	.01084	.01089	.6288	.5224	.1099	.0181	1562.2773	635.3504	.00091
99	546.63	1.2120	1.1000	.01089	.01095	.6277	.5110	.1093	.0210	1562.2795	635.3517	.00097
101	557.77	1.2120	1.1000	.01094	.01099	.6269	.4988	.1086	.0240	1562.2819	635.3531	.00101
103	568.91	1.2120	1.1000	.01096	.01102	.6264	.4857	.1079	.0273	1562.2844	635.3545	.00104
105	580.05	1.2120	1.1000	.01096	.01102	.6264	.4717	.1072	.0307	1562.2871	635.3560	.00104
107	591.19	1.2120	1.1000	.01092	.01097	.6272	.4568	.1064	.0344	1562.2900	635.3576	.00099
109	602.33	1.2120	1.1000	.01082	.01087	.6292	.4410	.1056	.0385	1562.2931	635.3593	.00088
111	613.47	1.2120	1.1000	.01065	.01066	.6331	.4243	.1047	.0424	1562.2963	635.3610	.00068
113	624.61	1.2120	1.1000	.01028	.01030	.6399	.4067	.1038	.0467	1562.2997	635.3629	.00031
115	635.75	1.2120	1.0999	.00965	.00965	.6524	.3881	.1028	.0511	1562.3033	635.3648	-.00057
117	646.89	1.2120	1.0999	.00842	.00854	.6771	.3685	.1020	.0558	1562.3071	635.3667	-.00170
119	658.03	1.2120	1.0997	.00511	.00481	.7434	.3480	.1010	.0608	1562.3111	635.3688	-.00524
121	669.17	0	0	0	0	0	.3263	.0997	.0659	1562.3152	635.3709	0
123	680.31	0	0	0	0	0	.3041	.0985	.0712	1562.3195	635.3730	0
125	691.45	0	0	0	0	0	.2814	.0977	.0767	1562.3237	635.3752	0
127	702.59	0	0	0	0	0	.2583	.0242	.0824	1562.3280	635.3775	0
129	713.73	0	0	0	0	0	.2348	.0217	.0884	1562.3322	635.3799	0
131	724.87	0	0	0	0	0	.2109	.0198	.0945	1562.3364	635.3822	0
133	736.01	0	0	0	0	0	.1864	.0182	.1009	1562.3406	635.3847	0
135	747.15	0	0	0	0	0	.1615	.0169	.1074	1562.3448	635.3871	0
137	758.29	0	0	0	0	0	.1361	.0157	.1142	1562.3490	635.3897	0
139	769.43	0	0	0	0	0	.1102	.0147	.1212	1562.3533	635.3922	0

INDUSTRIAL AUTOMATION GROUP , IMPERIAL COLLEGE

STRIP SHAPE ANALYSIS

AUTHOR P.D.SPOONER

SEPTEMBER 1974

PLANT AND PRODUCT DATA FOR STAND

	MILL PARAMETERS			SCHEDULE PARAMETERS	
WORK ROLLS	FACE LENGTH (MM)	1550.0000		MEAN ANNEALED THICKNESS (MM)	2.3600
	RADIUS (MM)	292.0000		MEAN ENTRY THICKNESS (MM)	1.2120
	GROUND CROWN (MM ON RAD)	-.1250		MEAN EXIT THICKNESS (MM)	1.1000
	THERMAL CROWN (MM ON RAD)	0		MEAN ENTRY TENSION (TONNE/MM/MM)	.0100
BACKUP ROLLS	FACE LENGTH (MM)	1550.0000		MEAN EXIT TENSION (TONNE/MM/MM)	.0100
	RADIUS (MM)	635.0000		STRIP WIDTH (MM)	1114.0000
	GROUND CROWN (MM ON RAD)	0		FRONT SCREW POSITION (MM)	.5929
	THERMAL CROWN (MM ON RAD)	0		BACK SCREW POSITION (MM)	.5929
JACK FORCE	WORK ROLL (TONNE)	25.00 25.00			
	BACKUP ROLL (TONNE)	0 0			
	WORK/BACKUP ROLL (TONNE)	54.20 54.20			
DISTANCE BETWEEN JACKS (MM)		2250.0000			
DISTANCE BETWEEN SCREWS (MM)		2510.0000			

GAUGE AND STRESS PROFILE PARAMETERS

THE GAUGE AND STRESS PROFILES ARE PARAMETERISED BY THE EXPRESSION,

$$A + \frac{B}{W}(x-0.5) + \frac{C}{W}(x-0.5)^{**}2$$

A = THE MEAN VALUE
B = THE TOTAL SKEW
C = THE PARABOLIC DIFFERENCE,CENTRE TO EDGE

THE PARAMETERS ARE FITTED BY A LEAST SQUARES CRITERION.

	A	B	C
ENTRY GAUGE,MM	1.21314	.00000	-.03042
ENTRY STRESS,TONNE/MM/M	.00906	-.00000	.00199
SHAPE,TONNE/MM/MM	-.00095	-.00000	.00198

PARAMETER DISTRIBUTIONS

SECTION NUMBER	DISTANCE ACROSS ROLL FACE (MM)	STRIP THICKNESS DISTRIBUTION (MM) ENTRY	STRIP THICKNESS DISTRIBUTION (MM) EXIT	RESIDUAL STRESS DISTRIBUTION (TONNE/MM/MM) ENTRY	RESIDUAL STRESS DISTRIBUTION (TONNE/MM/MM) EXIT	ROLL FORCE P (TONNE/MM)	CONTACT PRESSURE,P (TONNE/MM)	WORK ROLL FLATTENING (MM)	TOTAL WORK ROLL PROFILE (MM)	WORK ROLL DEFLECTION (MM)	BACKUP ROLL DEFLECTION (MM)	SHAPE (I/MM/MM)
1	3.17	0	0	0	0	0	.0893	.0140	-.1248	1562.3602	635.3953	0
3	11.91	0	0	0	0	0	.1142	.0149	-.1177	1562.3563	635.3930	0
5	20.65	0	0	0	0	0	.1403	.0160	-.1108	1562.3520	635.3905	0
7	34.19	0	0	0	0	0	.1658	.0171	-.1041	1562.3476	635.3880	0
9	45.83	0	0	0	0	0	.1909	.0185	-.0977	1562.3433	635.3855	0
11	56.47	0	0	0	0	0	.2155	.0201	-.0914	1562.3389	635.3831	0
13	67.61	0	0	0	0	0	.2397	.0220	-.0854	1562.3346	635.3807	0
15	78.75	0	0	0	0	0	.2634	.0245	-.0796	1562.3302	635.3784	0
17	89.89	0	0	0	0	0	.2866	.0282	-.0739	1562.3258	635.3762	0
19	101.03	0	0	0	0	0	.3095	.0349	-.0685	1562.3214	635.3740	0
21	112.17	1.1428	1.0385	.01302	.01338	.5049	.3319	.0753	-.0633	1562.3170	635.3718	.00335
23	123.31	1.1622	1.0565	.01539	.01580	.5479	.3536	.0897	-.0583	1562.3128	635.3698	.00586
25	134.46	1.1767	1.0693	.01346	.01373	.5828	.3744	.0929	-.0535	1562.3086	635.3678	.00377
27	145.59	1.1874	1.0789	.01193	.01209	.6107	.3942	.0984	-.0489	1562.3047	635.3658	.00211
29	156.73	1.1951	1.0859	.01085	.01093	.6303	.4132	.1025	-.0445	1562.3009	635.3640	.00094
31	167.87	1.2006	1.0907	.01014	.01016	.6432	.4312	.1056	-.0403	1562.2973	635.3622	.00026
33	179.01	1.2045	1.0944	.00968	.00968	.6512	.4482	.1079	-.0363	1562.2939	635.3604	-.00033
35	190.15	1.2072	1.0968	.00946	.00939	.6559	.4643	.1096	-.0325	1562.2906	635.3588	-.00062
37	201.29	1.2090	1.0984	.00928	.00923	.6584	.4795	.1110	-.0290	1562.2876	635.3572	-.00078
39	212.43	1.2101	1.0995	.00921	.00919	.6595	.4937	.1120	-.0256	1562.2847	635.3557	-.00086
41	223.57	1.2109	1.1002	.00919	.00912	.6598	.5070	.1128	-.0225	1562.2820	635.3543	-.00089
43	234.71	1.2114	1.1006	.00919	.00912	.6596	.5194	.1135	-.0195	1562.2795	635.3530	-.00089
45	245.85	1.2117	1.1009	.00920	.00913	.6593	.5309	.1140	-.0168	1562.2772	635.3518	-.00087
47	256.99	1.2118	1.1010	.00922	.00915	.6590	.5415	.1145	-.0143	1562.2751	635.3506	-.00086
49	268.13	1.2119	1.1011	.00923	.00916	.6587	.5512	.1149	-.0119	1562.2731	635.3496	-.00084
51	279.27	1.2120	1.1011	.00923	.00917	.6586	.5600	.1153	-.0098	1562.2714	635.3486	-.00084
53	290.41	1.2120	1.1012	.00924	.00917	.6585	.5679	.1156	-.0079	1562.2698	635.3478	-.00083
55	301.55	1.2120	1.1012	.00924	.00917	.6585	.5749	.1159	-.0062	1562.2683	635.3470	-.00084
57	312.69	1.2120	1.1012	.00923	.00916	.6586	.5811	.1161	-.0047	1562.2671	635.3463	-.00084
59	323.83	1.2120	1.1012	.00922	.00916	.6588	.5864	.1163	-.0034	1562.2660	635.3457	-.00085
61	334.97	1.2120	1.1012	.00922	.00915	.6589	.5909	.1165	-.0023	1562.2651	635.3452	-.00086
63	346.11	1.2120	1.1012	.00921	.00914	.6591	.5945	.1167	-.0015	1562.2644	635.3448	-.00087
65	357.25	1.2120	1.1012	.00920	.00913	.6592	.5973	.1168	-.0008	1562.2638	635.3445	-.00087
67	368.39	1.2120	1.1012	.00920	.00913	.6593	.5992	.1168	-.0003	1562.2634	635.3442	-.00088
69	379.53	1.2120	1.1012	.00919	.00913	.6594	.6002	.1169	-.0001	1562.2632	635.3441	-.00088
71	390.67	1.2120	1.1012	.00919	.00912	.6594	.6005	.1169	.0000	1562.2632	635.3441	-.00088
73	401.81	1.2120	1.1012	.00920	.00913	.6593	.5998	.1169	-.0002	1562.2633	635.3442	-.00088
75	412.95	1.2120	1.1012	.00920	.00913	.6593	.5983	.1168	-.0005	1562.2636	635.3443	-.00088
77	424.09	1.2120	1.1012	.00921	.00914	.6591	.5960	.1167	-.0011	1562.2641	635.3446	-.00087
79	435.23	1.2120	1.1012	.00921	.00914	.6590	.5928	.1166	-.0019	1562.2647	635.3450	-.00086
81	446.37	1.2120	1.1012	.00922	.00915	.6588	.5888	.1164	-.0028	1562.2655	635.3454	-.00085
83	457.51	1.2120	1.1012	.00923	.00916	.6587	.5839	.1162	-.0040	1562.2665	635.3460	-.00084
85	468.65	1.2120	1.1012	.00923	.00917	.6586	.5781	.1160	-.0054	1562.2677	635.3466	-.00084
87	479.79	1.2120	1.1012	.00924	.00917	.6585	.5715	.1157	-.0070	1562.2690	635.3473	-.00083
89	490.93	1.2120	1.1011	.00924	.00917	.6585	.5640	.1154	-.0088	1562.2705	635.3482	-.00083
91	502.07	1.2119	1.1011	.00923	.00916	.6586	.5557	.1151	-.0109	1562.2722	635.3491	-.00084
93	513.21	1.2119	1.1011	.00922	.00915	.6588	.5464	.1147	-.0131	1562.2741	635.3501	-.00085
95	524.35	1.2118	1.1009	.00921	.00914	.6591	.5363	.1143	-.0155	1562.2761	635.3512	-.00087
97	535.49	1.2115	1.1007	.00919	.00913	.6595	.5253	.1138	-.0181	1562.2784	635.3524	-.00088
99	546.63	1.2112	1.1004	.00919	.00912	.6597	.5133	.1132	-.0210	1562.2808	635.3537	-.00089
101	557.77	1.2106	1.0999	.00920	.00913	.6597	.5005	.1124	-.0240	1562.2834	635.3550	-.00088
103	568.91	1.2096	1.0990	.00924	.00918	.6591	.4867	.1115	-.0273	1562.2861	635.3565	-.00083
105	580.05	1.2081	1.0977	.00934	.00929	.6574	.4720	.1104	-.0307	1562.2891	635.3580	-.00072
107	591.19	1.2060	1.0957	.00954	.00951	.6539	.4564	.1088	-.0344	1562.2922	635.3596	-.00050
109	602.33	1.2027	1.0928	.00989	.00989	.6477	.4398	.1068	-.0383	1562.2956	635.3613	-.00011
111	613.47	1.1981	1.0886	.01046	.01051	.6375	.4223	.1042	-.0424	1562.2991	635.3630	.00051
113	624.61	1.1916	1.0827	.01134	.01145	.6215	.4038	.1006	-.0467	1562.3028	635.3649	.00146
115	635.75	1.1825	1.0745	.01262	.01284	.5981	.3844	.0959	-.0511	1562.3066	635.3668	.00286
117	646.89	1.1700	1.0633	.01439	.01473	.5660	.3641	.0896	-.0558	1562.3107	635.3688	.00477
119	658.03	1.1532	1.0481	.01623	.01672	.5334	.3429	.0813	-.0608	1562.3149	635.3708	.00678
121	669.17	0	0	0	0	0	.3208	.0433	-.0659	1562.3192	635.3729	0
123	680.31	0	0	0	0	0	.2981	.0308	-.0712	1562.3236	635.3751	0
125	691.45	0	0	0	0	0	.2751	.0262	-.0767	1562.3280	635.3773	0
127	702.59	0	0	0	0	0	.2516	.0232	-.0824	1562.3324	635.3796	0
129	713.73	0	0	0	0	0	.2277	.0210	-.0884	1562.3367	635.3819	0
131	724.87	0	0	0	0	0	.2033	.0192	-.0945	1562.3411	635.3843	0
133	736.01	0	0	0	0	0	.1784	.0178	-.1009	1562.3454	635.3867	0
135	747.15	0	0	0	0	0	.1531	.0165	-.1074	1562.3498	635.3892	0
137	758.29	0	0	0	0	0	.1273	.0154	-.1142	1562.3541	635.3917	0
139	769.43	0	0	0	0	0	.1009	.0145	-.1212	1562.3585	635.3943	0

CHAPTER 2

MODEL SIMPLIFICATION

A complete understanding of the shape phenomenon is required in order to design three important areas in a full automation scheme for a tandem rolling mill.

(1) The nominal rolling schedule. This defines the proportion of the required reduction to be carried out at each stand and the level of the interstand tensions. It is designed off line from considerations of power constraints, shape, which must be held within certain practical limits, and gauge. This topic will be discussed in more detail in chapter 3.

(2) The on line modification of these nominal schedules to accommodate variations in the incoming product.

(3) On line control of strip shape.

The complete analysis of strip shape developed in chapter 1, together with the digital computer simulation which has been written, are essential for gaining a detailed understanding of the phenomenon. This program is not suitable however for use on line in schedule adaption algorithms or shape control schemes, and it will make the off line scheduling calculation unnecessarily large. Also because of the iterative nature of the shape model the form of the dependency of shape on key parameters is not obvious. Furthermore, various sensitivities of shape are required for on line control purposes as discussed above. These sensitivities would have to be obtained numerically for the complete range of likely conditions, and then the results summarised by some simple law. Apart from the enormous computing effort required for such an operation there is always the risk that, on line, a set of conditions will arise which was not covered and extrapolation could yield the wrong result. Also the structural form of the parameter

dependencies is in practice very difficult to guess from sets of computed sensitivities. For these reasons it is desirable to develop a simplified, non-iterative, model which can be differentiated to yield the required sensitivities.

2.1 Parameterisation

All of the variables in the full shape analysis are vectors defining those quantities at several points across the strip and roll width. The basic concept adopted in the simplification here is to parameterise the stress distribution (shape) with a "suitable" parameter, and to write an algorithm to calculate this parameter direct without recourse to calculating the distributions. The definition of a "suitable" parameter depends on the application. A parameter which provides a fit to the exact distribution which is 'best', according to some prescribed criteria, is not necessarily the best to give the information for, say, feedback shape control. For example the shape distribution can, in general, be of any form, however it is characterised by two effects. Firstly the deflection of the rolls due to bending and shearing; this tends to be predominantly parabolic. Secondly the flattening of the work rolls. This again tends to be parabolic over the centre portion of the strip, say 75^{o}/o of the strip width, but with a sudden decrease near the strip edges caused by the flattening of the rolls decaying to zero outside the strip. The magnitude of this "edge effect" present on the final product depends upon the incoming strip profile and the thermal camber on the rolls. These edge effects are not controllable through schedule changes and roll bending; the only means of control is the coolant spray distribution. A parabolic parameter has been chosen therefore as this will give all the information necessary for scheduling, adaption, and shape control with the exception of data required for coolant spray control of shape.

It seems likely that no single parameter is sufficient for the requirements of spray control. This is discussed in more detail in Chapter 4.

2.2 Simplified Model Structure

The aim is to model only the parabolic component of strip shape and only symmetric distributions will therefore be considered. Since only the shape and not the thickness is of interest, it will be assumed that the specified centre line thickness is always attained by automatic screw position adjustment. It is then only necessary to calculate deformations relative to the strip centre line.

The shape produced from a stand is determined by the relative profiles of the incoming strip and the roll gap; the incoming shape also has a small effect. The roll gap profile is the result of the work roll bending and shearing deflection, the work roll flattening and the camber of the work rolls. In the model derivation it will be assumed that the distribution of load acting on the work roll, from the backup roll and from the strip, can be approximated by the sum of uniform distributions and parabolic distributions. The bending and shearing deflection and the work roll flattening will be calculated for each type of load and the roll gap profile determined by summing the results. It is further assumed that the parabolic components of deflection and flattening can be approximated by the difference in the values at the strip centre and strip edge in both cases.

A block diagram for the simple model, shown in figure 20, should be compared with that of the full model in figure 2. Expressions for the parabolic components of the stress distribution, the work roll deflection and the work roll flattening will now be derived.

2.3 Work Roll Deflection

The forces acting on the work roll can be divided into three as shown in figure 21: Uniform distributed loads from the backup roll q / unit length, and the strip p / unit length (figure 21a); parabolic distributions from the backup roll ρ_B and the strip ρ_s (figure 21b); and the roll bending jack force J (figure 21c). The deflection of the roll at the strip edge relative to the centre will be derived for each of these loadings acting separately, the total deflection will be obtained by superposition.

2.3.1 Deflection due to uniform load distribution

The simple shape model assumes symmetry and a specified strip centre line thickness. The work roll can therefore be represented by a cantilever with the fixed end at the strip centre line where the slope and deflection will be zero. The cantilever subjected to the uniform loading from the strip and from the backup roll is shown in figure 22a; the general expressions for the bending moment at any point x along such a beam is

$$M = EI \frac{d^2y}{dx^2} = \frac{qx^2}{2} - p \frac{[x - F + w]^2}{2} \qquad 2.3.1$$

By integration the slope and deflection at any point can be obtained

$$\text{Slope} = EI \frac{dy}{dx} = \frac{qx^3}{6} - p \frac{[x - F + w]^3}{6} + A \qquad 2.3.2$$

$$\text{Deflection} = EIy = \frac{qx^4}{24} - p \frac{[x - F + w]^4}{24} + Ax + B \qquad 2.3.3$$

The deflection and slope are zero at the support, ie

$$y\Big|_{x = F} = 0 \quad \text{and} \quad \frac{dy}{dx}\Big|_{x = F} = 0$$

Therefore,

$$A = \frac{pw^3}{6} - \frac{qF^3}{6} \qquad 2.3.4$$

$$B = \frac{pw^3}{24}[w - 4F] + \frac{qF^4}{8} \qquad 2.3.5$$

The expression for the deflection due to bending at any point is obtained by substituting equations 2.3.4 and 2.3.5 into 2.3.3.

$$\text{Deflection } y = \frac{1}{EI}\left\{\frac{qx^4}{24} - p\frac{[x - F + w]^4}{24} + \frac{pw^3x}{6} - \frac{qF^3x}{6}\right.$$

$$\left. + \frac{pw^3}{24}[w - 4F] + \frac{qF^4}{8}\right\} \qquad 2.3.6$$

The deflection at the strip edge relative to the strip centre line is to be taken as an estimate of the parabolic component. This is obtained by setting $x = (F - w)$ in equation 2.3.6 to obtain

$$y\Big|_{x = (F - w)} = \frac{1}{EI}\left\{\frac{q}{24}\left[6F^2w^2 - 4Fw^3 + w^4\right] - \frac{pw^4}{8}\right\} \qquad 2.3.7$$

The deflection due to shearing is given by

$$y_S = \frac{4}{3AG}\int S\,dx \qquad 2.3.8$$

where S is the shear force.

A diagram of the shear force along the beam is given in figure 22b. The deflection at the strip edge relative to the centre line is therefore,

$$y_S = \frac{4}{3AG}\left[q\left(Fw - \frac{w^2}{2}\right) - \frac{pw^2}{2}\right] \qquad 2.3.9$$

2.3.2 Deflection due to parabolic load distribution

The load distributions on the work roll, from the backup roll and from the strip, are not, in general, uniform. The expression for the deflection calculated in 2.3.1 must be corrected therefore for the variation in the loads. It is assumed that the variations in the load can be approximated by parabolas. The required deflection can be obtained by considering a cantilever subjected to parabolic load distributions as shown in figure 22c. The loading on the beam at $(F - w) < x < F$ is

$$\rho_B\left[1 - \left(\frac{x}{F}\right)^2\right] - \rho_S\left[1 - \left(\frac{x}{w}\right)^2\right] \qquad 0 < x < w \qquad 2.3.10$$

The shear force and bending moment can be obtained by integration with the boundary conditions,

Shear force at $x = 0$ is $\frac{2\rho_B F}{3} - \frac{2\rho_S w}{3}$

and bending moment at $x = 0$ is $-\frac{\rho_B F^2}{4} + \frac{\rho_S w^2}{4}$

Then,

$$S = \int w\,dx = \rho_B\left[x - \frac{x^3}{3F^2} - \frac{2F}{3}\right] - \rho_S\left[x - \frac{x^3}{3w^2} - \frac{2w}{3}\right] \qquad 2.3.11$$

$$M = EI\frac{d^2y}{dx^2} = \int S\,dx = \rho_B\left[\frac{F^2}{4} + \frac{x^2}{2} - \frac{x^4}{12F^2} - \frac{2Fx}{3}\right] + \rho_S\left[\frac{2wx}{3} - \frac{x^2}{2} + \frac{x^4}{12w^2} - \frac{w^2}{4}\right]$$

2.3.12

By integrating twice and using the boundary conditions

$$y\Big|_{x=0} = 0 \quad \text{and} \quad \frac{dy}{dx}\Big|_{x=0} = 0$$

the bending deflection can be shown to be,

$$y = \frac{\rho_B}{EI}\left[\frac{F^2x^2}{8} + \frac{x^4}{24} - \frac{Fx^3}{9} - \frac{x^6}{360F^2}\right] + \rho_S\left[\frac{Wx^3}{9} - \frac{x^4}{24} + \frac{x^6}{360w^2} - \frac{w^2x^2}{8}\right] \qquad 2.3.13$$

The bending deflection at the strip edge relative to the centre line is obtained by inserting $x = (F - w)$. Then,

$$y = \frac{\rho_B w^2}{360EI}\left[45F^2 + 15w^2 - \frac{w^4}{F^2} - 40\,FW\right] - \frac{19\rho_S w^4}{360EI} \qquad 2.3.14$$

The deflection due to shearing can be obtained by combining equations 2.3.8 and 2.3.11.

$$\text{Deflection due to shearing } y_S = \frac{4\rho_B}{3AG}\left[\frac{F^2}{4} + \frac{x^2}{2} - \frac{x^4}{12F^2} - \frac{2Fx}{3}\right]$$

$$+ \frac{4\rho_S}{3AG}\left[\frac{2wx}{3} - \frac{x^2}{2} + \frac{x^4}{12w^2} - \frac{w^2}{4}\right] \qquad 2.3.15$$

The deflection at the strip edge relative to the centre line is

$$y_S = y\Big|_{x=F} - y\Big|_{x=(F-w)}$$

$$y_S = \frac{4\rho_B}{3AG}\left[\frac{w^4}{12F^2} + \frac{2Fw}{3} - \frac{w^2}{2}\right] - \frac{\rho_S w^2}{3AG} \qquad 2.3.16$$

2.3.3 Deflection due to roll bending jack forces

The deflection caused by the roll bending jack forces can be derived by considering a cantilever subjected to an end load as in figure 22d.

$$\text{The bending moment } M = EI \frac{d^2y}{dx^2} = - Jx \qquad 2.3.17$$

By integration with the boundary conditions,

$$y_B\Big|_{x = L} = 0 \qquad \frac{dy}{dx}\Big|_{x = L} = 0$$

the deflection at the strip edge ($x = w$) can be shown to be

$$y_B = \frac{Jw^2}{6EI} (w - 3L_J) \qquad 2.3.18$$

The deflection due to shear at the strip edge is

$$y_S = \frac{4Jw}{3AG} \qquad 2.3.19$$

2.3.4 Total work roll deflection

The total deflection of the work roll is given by summing equations 2.3.7, 2.3.9, 2.3.14, 2.3.16, 2.3.18, and 2.3.19. Then,

$$y_w = p\left[\frac{-w^4}{8EI} - \frac{2w^2}{3AG}\right] + q\left[\frac{F^2w^2}{4EI} - \frac{Fw^3}{6EI} + \frac{w^4}{24EI} + \frac{4Fw}{3AG} - \frac{2w^2}{3AG}\right]$$

$$+ \rho_B\left[\frac{w^2F^2}{8EI} - \frac{w^3F}{9EI} + \frac{w^4}{24EI} - \frac{w^6}{360F^2EI} + \frac{8Fw}{9AG} - \frac{2w^2}{3AG} + \frac{w^4}{9F^2AG}\right]$$

$$- \rho_S\left[\frac{19w^4}{360EI} + \frac{w^2}{3AG}\right] + J\left[\frac{w^3}{6EI} - \frac{3L_Jw^2}{6EI} - \frac{4w}{3AG}\right]$$

which is clearly of the form,

$$y_w = K_8p + K_9q + K_{10}\rho_B + K_{11}\rho_S + K_{12}J \qquad 2.3.20$$

2.4 Work Roll / Backup Roll Pressure Distribution

The work roll / backup roll pressure distribution consists in general of a uniform load acting across the roll length plus a varying distribution equal to zero at the roll ends. (In certain extreme cases with very large roll crowns it is possible that the work and backup rolls may not be in contact over the whole roll width, this condition is very rare in practice and will not be considered here.) The variation in pressure (assumed parabolic) can be determined by considering the elastic deformation between the rolls as in the full model. It is assumed that the pressure is proportional to the deformation which can be obtained by comparing the relative profiles

of the adjacent surfaces of the two rolls. Expressions must be derived therefore for the profiles of the top face of the top work roll and the bottom face of the top backup roll. The stiffness of the material can be calculated from the Hertzian expression for the deformation between two elastic cylinders given in section 1.3.

2.4.1 Profile of top face of the work roll

An expression is required for the difference in deflection, due to bending and shearing, between the centre and end of the roll and not to the strip edge as in section 2.3.

The bending deflection due to the uniform load distribution is given by equation 2.3.6 with x = 0,

$$y_B = \frac{p\,w^3}{24EI}\,[w - 4F] + \frac{q\,F^4}{8EI} \qquad 2.4.1$$

Similarly the deflection due to shearing can be obtained from 2.3.8

$$y_S = \frac{4}{3AG}\left[\frac{qF^2}{2} - \frac{pw^2}{2}\right] \qquad 2.4.2$$

The bending and shearing deflections caused by the parabolic loads can be shown to be,

$$y_B = \frac{19\,\rho_B F^4}{360EI} + \frac{\rho_S w^3}{EI}\left[\frac{w}{72} - \frac{F}{15}\right] \qquad 2.4.3$$

$$y_S = \frac{\rho_B F^2}{3AG} - \frac{\rho_S w^2}{3AG} \qquad 2.4.4$$

Similarly the deflection due to roll bending jack force can be shown to be:

$$\text{for bending , } \quad y_B = -\frac{J\,L_J^3}{3EI} \qquad 2.4.5$$

$$\text{for shearing, } \quad y_S = -\frac{4J.L_J}{3AG} \qquad 2.4.6$$

The required deflection of the work roll is given by summing equations 2.4.1 to 2.4.6. Then,

$$y = p\left[\frac{w^4}{24EI} - \frac{w^3F}{6EI} - \frac{2w^2}{3AG}\right] + q\left[\frac{F^4}{8EI} + \frac{2F^2}{3AG}\right]$$

$$+ \rho_B\left[\frac{19F^4}{360EI} + \frac{F^2}{3AG}\right] + \rho_S\left[\frac{w^3F}{15EI} - \frac{w^4}{72EI} + \frac{w^2}{3AG}\right]$$

$$- J\left[\frac{L_J^3}{3EI} + \frac{4L_J}{3AG}\right] \qquad 2.4.7$$

or

$$y = K_3p + K_4q + K_5\rho_B + K_6\rho_S + K_7J \qquad 2.4.8$$

Finally, for the profile of the top face of the work roll, the work roll crown must be included. Therefore

$$y_w = K_3p + K_4q + K_5\rho_B + K_6\rho_S + K_7J + C_w \qquad 2.4.9$$

2.4.2 Profile of the bottom face of the backup roll

The deflection of the ends of the backup roll barrel relative to the roll centre can be determined by considering a simply supported beam subjected to a uniform load q / unit length and a parabolic load distribution equal to ρ_B / unit length at the roll centre, figure 23. The supports represent the screws and the loading is assumed to extend over the complete length of the roll barrel, 2F. The deflection at the barrel end relative to the roll centre due to the uniform load can be shown to be:

$$\text{bending deflection } y_B = \frac{qF}{24EI}(12LF^2 - 7F^3) \qquad 2.4.10$$

$$\text{shearing deflection } y_S = \frac{2qF}{3AG}[2L - F] \qquad 2.4.11$$

and that due to parabolic loading,

$$\text{bending deflection } y_B = \frac{\rho_B F^3}{3EI}\left[L - \frac{59F}{120}\right] \qquad 2.4.12$$

$$\text{shearing deflection } y_S = \frac{\rho_B F}{3AG}\left[\frac{8L}{3} - F\right] \qquad 2.4.13$$

where 2F = roll barrel length

2L = distance between screws

The total deflection of the backup roll is obtained by combining equations 2.4.10 to 2.4.13

$$y = q\left[\frac{LF^3}{2EI} - \frac{7F^4}{24EI} + \frac{4FL}{3AG} - \frac{2F^2}{3AG}\right]$$

$$+ \rho_B\left[\frac{LF^3}{3EI} - \frac{59F^4}{360EI} + \frac{8LF}{9AG} - \frac{F^2}{3AG}\right] \qquad 2.4.14$$

or $y = K_1 q + K_2 \rho_B$

The profile of the bottom face of the top backup roll is therefore

$$y_{BU} = K_1 q + K_2 \rho_B - C_B \qquad 2.4.15$$

where C_B is the crown on the backup roll.

2.4.3 Roll stiffness

An expression was derived in section 1.3 for the relationship between the pressure q between the work and backup rolls at any point across the rolls and the deformation Δ of the rolls, equation 1.3.4.

$$q_i = \frac{\Delta}{\frac{2(1-\nu^2)}{E\pi}\left[2/3 + \ln\left(\frac{2D_1}{b}\right) + \ln\left(\frac{2D_2}{b}\right)\right]}$$

$$\text{where } b = 1.6\sqrt{\bar{q}\,\frac{D_1 D_2}{(D_1 + D_2)}\,\frac{2(1-\nu^2)}{E}}$$

Hence the roll stiffness $K_{13} = \frac{q}{\Delta} = \frac{1}{\frac{2(1-\nu^2)}{E\pi}\left[2/3 + \ln\frac{2D_1}{b} + \ln\frac{2D_2}{b}\right]}$ 2.4.16

Fortunately K_{13} is not very sensitive to $\bar{q}$. For typical roll diameters, D_1 = 584 mm and D_2 = 1270 mm, K_{13} varies from 3.14 to 2.65 as $\bar{q}$ goes from 0.8 tonnes/mm to 0.1 tonnes/mm; it is unlikely that values of $\bar{q}$ outside this range will be developed in practice. The stiffness K_{13} is therefore assumed constant for constant roll diameters and is calculated from equation 2.4.15 with $\bar{q}$ equal to 0.5 tonnes/mm.

2.4.4 Parabolic component of pressure distribution ρ_B

The parabolic component of the work/backup roll pressure distribution is determined from the difference in the profiles of the adjacent work and backup roll faces and the roll stiffness.

$$\rho_B = K_{13}[y_w - y_{BU}] \qquad 2.4.17$$

substituting for y_w and y_{BU} with equations 2.4.9 and 2.4.15 respectively,

$$\rho_B = \frac{K_{13}}{(1 - K_5 + K_2)}\left[K_3 p + (K_4 - K_1)q + K_6\rho_S + K_7 J + C_w + C_B\right] \qquad 2.4.18$$

2.4.5 Uniform component of pressure distribution q

The level of the uniform pressure between the rolls can be determined by considering the equilibrium of the forces acting on the work roll, from the strip and from the backup roll. (The weight of the work roll is neglected as it is typically less than 0.5°/o of the total roll force).

$$2qF + \frac{4\rho_B F}{3} = 2pw + \frac{4\rho_S w}{3} + 2J$$

$$\text{or} \quad q = p\frac{w}{F} + \frac{2\rho_S w}{3F} + \frac{J}{F} - \frac{2\rho_B}{3} \qquad 2.4.19$$

Substituting for ρ_B from equation 2.4.18, and rearranging gives:

$$q = \frac{1}{1 + \left[\frac{2K_{13}(K_4 - K_1)}{3(1 - K_5 + K_2)}\right]} \left\{ p\left[\frac{w}{F} - \frac{2K_3 K_{13}}{3(1 - K_5 + K_2)}\right] + \rho_S\left[\frac{2w}{3F} - \frac{2K_{13} K_6}{3(1 - K_5 + K_2)}\right] \right.$$

$$\left. + J\left[\frac{1}{F} - \frac{2K_{13} K_7}{3(1 - K_5 + K_2)}\right] - \frac{2K_{13}}{3(1 - K_5 + K_2)}[C_w + C_B] \right\} \qquad 2.4.20$$

or,

$$q = K_{14}p + K_{15}\rho_S + K_{16}J + K_{17}(C_w + C_B) \qquad 2.4.21$$

q can now be eliminated from the expression for ρ_B by combining equations 2.4.21 and 2.4.18. Then,

$$\rho_B = \left[\frac{3K_{13}}{3(1 - K_5 + K_2) + 2K_{13}(K_4 - K_1)}\right] \left\{ \left[K_3 + (K_4 - K_1)\frac{w}{F}\right] p \right.$$

$$\left. + \left[K_6 + \frac{2(K_4 - K_1)w}{3F}\right]\rho_S + \left[K_7 + \frac{(K_4 - K_1)}{F}\right] J + C_w + C_B \right\} \qquad 2.4.22$$

or,

$$\rho_B = K_{18}p + K_{19}\rho_S + K_{20}J + K_{28}(C_w + C_B) \qquad 2.4.23$$

2.5 Work Roll Flattening

Two expressions will be derived for the parabolic component of the work roll flattening. Firstly the flattening caused by the parabolic variation in roll force ρ_S alone will be considered, and then the flattening caused by the uniform roll force distribution p. The total flattening is the sum of these two components.

2.5.1 Flattening due to the parabolic component of roll force ρ_S

In an earlier analysis of strip shape [9] it was shown that there was a strong correlation between the accurate roll flattening and the flattening, given by Hertz's theory, between two infinitely long cylinders[15]. The theory was applied to discrete sections of the roll over which it was assumed the pressure was constant. This method however neglects the interaction, due to shear, between the sections. The effect of neglecting the shear stresses is small except where the rate of change of force is high and hence the results were reasonable except near the strip edges where the force drops to zero.

When considering just the parabolic components of roll force, which is zero at the strip edge, there is no sudden change in force and the Hertzian model will give satisfactory results. Since the loading is parabolic it will be assumed that the deformation will also be parabolic and it is therefore only necessary to derive an expression for the flattening at the roll centre where the force per unit length is ρ_S. Then Hertz's theory states that the flattening of the roll is,

$$\Delta_1 = 2\rho_S \frac{(1-\nu^2)}{\pi E}\left[\frac{1}{3} + \ln\left(1.25\sqrt{\frac{D.E}{2\rho_S(1-\nu^2)}}\right)\right] \qquad 2.5.1$$

This expression for roll flattening is unsuitable since ρ_S can be negative indicating that the force is higher at the edge of the

strip than at the centre. In such a condition the expression will contain a negative square root. The maximum likely variation of ρ_S is from zero to $\pm$ 0.5 tonnes/mm, a graph of Δ_1 against ρ_S for a typical roll diameter is shown in figure 24a. It can be seen that Δ_1 is very nearly linear with respect to ρ_S. Equation 2.5.1 can therefore be replaced by:

$$\Delta_1 \simeq K_{21} \rho_S \qquad 2.5.2$$

where K_{21} = 0.155 mm^2/tonne for a roll diameter of 584 mm.

2.5.2 Flattening due to uniform roll force p

The Hertzian model cannot be used for the uniform component of force as it will ignore the sudden change in force at the strip edge and this is responsible for a significant change in the roll flattening near the strip edges. In the full shape model derivation an influence function was derived for the deformation on the surface of a semi infinite solid caused by a uniform pressure applied over a rectangle, section 1.5. In this case a uniform pressure is applied over a rectangle equal to the arc of contact by the strip width. The flattening at any point across the roll is given therefore by equation 1.5.3,

$$W(x) = \frac{p(1-\nu)}{2\pi G}\left\{ 2a \ln\left[\frac{(x+b) + ((x+b)^2 + a^2)^{1/2}}{(x-b) + ((x-b)^2 + a^2)^{1/2}}\right] + (x+b) \ln\left[\frac{((x+b)^2 + a^2)^{1/2} + a}{((x+b)^2 + a^2)^{1/2} - a}\right] - (x-b) \ln\left[\frac{((x-b)^2 + a^2)^{1/2} + a}{((x-b)^2 + a^2)^{1/2} - a}\right]\right\}$$

where 2b is the strip width w

and 2a is the arc of contact

The variation in the flattening across the strip width for a uniform roll force is shown in figure 24b. We shall assume that the parabolic component of flattening Δ_2 can be approximated by $15^0/o$ of the difference between the flattening at the strip centre and at the strip edge. (This parabolic approximation which ignores the edge effects is also shown in figure 24b). Changing this percentage will alter the fit of the simple model results to the full model results. Then,

$$\Delta_2 = .15(W(o) - W(^w/2))$$

Therefore

$$\Delta_2 = \frac{.15p(1-\nu)}{2\pi G}\left\{2\,a\,\ln\left[\frac{^w/2 + \left(^{w^2}/4 + a^2\right)^{1/2}}{-^w/2 + \left(^{w^2}/4 + a^2\right)^{1/2}}\right] - 2\,a\,\ln\left[\frac{w + \left(w^2 + a^2\right)^{1/2}}{a}\right]\right.$$

$$\left. + w\,\ln\left[\frac{\left(^{w^2}/4 + a^2\right)^{1/2} + a}{\left(^{w^2}/4 + a^2\right)^{1/2} - a}\right] - w\,\ln\left[\frac{\left(w^2 + a^2\right)^{1/2} + a}{\left(w^2 + a^2\right)^{1/2} - a}\right]\right\} \qquad 2.5.3$$

$$\text{or} \quad \Delta_2 = K_{22}p \qquad 2.5.4$$

By combining equations 2.5.2 and 2.5.4 the total parabolic component of roll flattening can be written as

$$\Delta_T = K_{21}\rho_S + K_{22}p \qquad 2.5.5$$

2.6 Transverse Distribution of Stress

In section 1.6 equations were derived for the transverse distribution of stress at the entry and exit of a stand and between stands at a distance greater than one strip width from any stand: This last distribution being equal to the strip shape. The stress distributions are functions of stand entry and exit thickness and slip

distributions. The method of simplification adopted here is to approximate all these distributions by parabolic profiles, again fitted over the central portion of the width of the strip ignoring the rapid changes at the strip edges. In this way simple expressions for the parabolic parameters of the stresses are obtained.

The equation for the stress distribution at the entry to a stand, assuming symmetry about the strip centre line, is derived in section 1.6 as,

$$\sigma_i = E\left\{\frac{h_i \bar{H}(1 + f_i)}{\bar{h} H_i (1 + \bar{f})} - 1\right\} + \Omega' \qquad 2.6.1$$

where H, h are vectors of entry and exit thickness

f is the vector of exit slip

Ω' is the shape vector produced by the previous stand

and $\bar{x}$ denotes the mean value of x

By approximating the variable distributions as parabolas the equation can be rewritten as

$$\sigma_i = E\left\{\frac{\bar{H}}{\bar{h}} \frac{(\bar{h} + C_2 z)(1 + \bar{f} + f_p z)}{(\bar{H} + C_1 z)(1 + \bar{f})} - 1\right\} + \Omega'p \qquad 2.6.2$$

where C_1, C_2, f_p and Ω_p are the magnitudes of the parabolic approximations to the variations across the strip of H, h, f and Ω respectively.

and $z = \left(\frac{2x}{w}\right)^2$, x is the distance from the strip centre line

Rearranging equation 2.6.2 using a first order approximation to the Binomial expansion gives

$$\sigma_i = E\left\{\frac{1}{(1 + \bar{f})}\left(1 + C_{2/\bar{h}}\, z\right)\left(1 - C_{1/\bar{H}}\, z\right)\left(1 + \bar{f} + fpz\right) - 1\right\} + \Omega'p \qquad 2.6.3$$

Expand, neglecting multiple of small terms,

$$\sigma_i = E\left\{\frac{1}{(1+\bar{f})}\left[1 + {}^{C_2}/_{\bar{h}}\, z - {}^{C_1}/_{\bar{H}}\, z + \bar{f} + fpz\right] - 1\right\} + \Omega' p \qquad 2.6.4$$

Finally, since $\bar{f} \ll 1$, the parabolic component of the entry stress distribution at a stand is

$$\sigma_1 = E\left\{\frac{C_2}{\bar{h}} - \frac{C_1}{\bar{H}} + fp\right\} + \Omega' p \qquad 2.6.5$$

The equations for the exit stress distribution (1.6.9) and the shape (1.6.10) can be simplified in a similar way to yield:

Parabolic component of stress,

$$\sigma_2 = E\left\{\frac{\bar{H}}{\bar{h}}\left(\frac{C_2}{\bar{h}} - \frac{C_1}{\bar{H}}\right) - f_p\right\} \qquad 2.6.6$$

Parabolic component of shape,

$$\Omega_p = E\left\{\frac{\bar{H}}{\bar{h}}\left(\frac{C_2}{\bar{h}} - \frac{C_1}{\bar{H}}\right)\right\} \qquad 2.6.7$$

2.7 Exit Slip Variation

The slip at the exit of a rolling stand is a function of entry and exit thickness and stress and the coefficient of friction. It is assumed that the coefficient of friction is a constant across the strip and the transverse variation of the thicknesses and stresses are small enough to enable the slip equation to be linearised. Then the parabolic component of slip can be expressed by,

$$fp = \frac{\partial f}{\partial H} C_1 + \frac{\partial f}{\partial h} C_2 + \frac{\partial f}{\partial \sigma_1} \sigma_{p1} + \frac{\partial f}{\partial \sigma_2} \sigma_{p2}$$

or $$fp = F_1 C_1 + F_2 C_2 + F_3 \sigma_{p1} + F_4 \sigma_{p2} \qquad 2.7.1$$

Substituting equations 2.6.6 and 2.6.7 for σ_{p1} and σ_{p2} and rearranging,

$$f_p = A_1 C_1 + A_2 C_2 + A_3 \Omega' p \qquad 2.7.2$$

where $$A_1 = \left[F_1 - E\left(\frac{F_3}{H} + \frac{F_4}{h}\right)\right] \left[1 - E(F_3 - F_4)\right]^{-1}$$

$$A_2 = \left[F_2 + E\left(\frac{F_3}{h} + \frac{F_4}{h}\frac{\bar{H}}{\bar{h}}\right)\right] [1 - E(F_3 - F_4)]^{-1}$$

$$A_3 = + F_3/[1 - E(F_3 - F_4)]$$

2.8 Roll Force Variation

The parabolic component of roll force ρ_S can be obtained in a similar way to the parabolic component for slip in the previous section.

$$\rho_S = \frac{\partial P}{\partial H} C_1 + \frac{\partial P}{\partial h} C_2 + \frac{\partial P}{\partial \sigma_1} \sigma_{p1} + \frac{\partial P}{\partial \sigma_2} \sigma_{p2}$$

or $$\rho_S = P_1 C_1 + P_2 C_2 + P_3 \sigma_{p1} + P_4 \sigma_{p2} \qquad 2.8.1$$

(Coefficient of friction and hardness are assumed constant across the strip).

Then by substituting for σ_{p1} and σ_{p2} and rearranging we obtain

$$\rho_S = C_1\left[P_1 - \frac{P_3E}{\bar{H}} - \frac{P_4E}{\bar{h}}\right] + C_2\left[P_2 + \frac{P_3E}{\bar{h}} + \frac{P_4E}{\bar{h}} - \frac{\bar{H}}{\bar{h}}\right]$$

$$+ f_p\left[E(P_3 + P_4)\right] + P_3\Omega'p \qquad 2.8.2$$

Finally, substituting for f_p from equation 2.7.2

$$\rho_S = A_4\ C_1 + A_5\ C_2 + A_6\ \Omega p' \qquad 2.8.3$$

where $A_4 = P_1 - \frac{P_3E}{\bar{H}} - \frac{P_4E}{\bar{h}} + A_1E(P_3 - P_4)$

$$A_5 = P_2 + \frac{P_3E}{\bar{h}} + \frac{P_4\ E\bar{H}}{\bar{h}\ \bar{h}} + A_2E(P_3 - P_4)$$

$$A_6 = A_3E(P_3 - P_4) + P_3$$

2.9 The Simple Shape Model

It is assumed that the exit thickness profile is equal to the roll gap profile; that is variations in the elastic recovery across the strip are ignored. The exit thickness profile, C_2, can therefore be expressed as a function of the original (ground) profile of the work rolls, the deflection due to bending and shearing of the work rolls, and the flattening of the work rolls against the strip.

An expression for the bending and shearing deflection in terms of roll force p and ρ_S, the roll bending jack force J, and the work

and backup roll crowns C_w and C_B, can be obtained by substituting for q and ρ_B in 2.3.20 with equations 2.4.21 and 2.4.23. Then

$$y_w = (K_8 + K_9K_{14} + K_{10}K_{18})p + (K_{11} + K_9K_{15} + K_{10}K_{19})\rho_S + (K_{12} + K_9K_{16} + K_{10}K_{20})J + (K_9K_{17} + K_{10}K_{28})(C_w + C_B) \quad 2.9.1$$

An expression for the exit thickness profile C_2 can now be written by combining equations 2.9.1 and 2.5.5, and substituting the roll crown (expressed over the strip width). A factor of two must be included to account for the upper and lower rolls.

$$C_2 = 2\left[K'_{23}p + K_{24}\rho_S + K_{25}J + K'_{26}C_w + K_{27}C_B - C_w\left(\frac{w}{F}\right)^2 + K_{21}\rho_S + K_{22}p\right]$$

Finally substituting equation 2.8.3 for ρ_S and rearranging

$$C_2 = \frac{K_{23}p + K_{25}J + K_{26}C_w + K_{27}C_B + (K_{21} + K_{24})A_4C_1 + (K_{21} + K_{24})A_6\Omega'p}{0.5 - (K_{21} + K_{24})A_5} \quad 2.9.2$$

where $K_{23} = K_{23}' + K_{22}$

$$K_{26} = K_{26}' - \left(\frac{w}{F}\right)^2$$

Then by substituting for C_2 in the shape expression, equation 2.6.7, a simple algebraic expression for the parabolic component of strip shape is obtained.

$$\Omega_p = E\left\{\frac{\bar{H}}{\bar{h}}\left[\frac{(K_{23}p + K_{25}J + K_{26}C_w + K_{27}C_B + (K_{21} + K_{24})A_4C_1 + (K_{21} + K_{24})A_6\Omega'_p)}{\bar{h}(0.5 - (K_{21} + K_{24})A_5)} - \frac{C_1}{\bar{H}}\right]\right\} \qquad 2.9.3$$

The coefficients K_{23} to K_{27} are complicated functions of mill dimensions and the strip width. For any particular mill the dimensions are constant and the only variable is strip width. The variation of each of these coefficients with strip width for a particular mill is shown in the graphs in figure 25. It can be shown that all five curves are closely quadratic and therefore each of the coefficients can be represented by a law of the form

$$K_i = A_1w^2 + A_2w + A_3 \qquad i = 23\text{-}27$$

where the coefficients A_i are chosen to give a good least squares fit to the actual curves. For the mill dimensions used in figure 25 the actual equations are:

$$\begin{aligned}
K_{23} &= -0.275 * 10^{-6}\, w^2 + 0.546 * 10^{-3}\, w - 0.218 \\
K_{24} &= -0.088 * 10^{-6}\, w^2 + 0.271 * 10^{-3}\, w - 0.112 \\
K_{25} &= -0.875 * 10^{-9}\, w^2 + 0.812 * 10^{-6}\, w - 0.298 * 10^{-3} \\
K_{26} &= -0.475 * 10^{-6}\, w^2 - 0.217 * 10^{-3}\, w + 0.082 \\
K_{27} &= \;\;0.025 * 10^{-6}\, w^2 - 0.232 * 10^{-3}\, w + 0.092
\end{aligned} \qquad 2.9.4$$

A simple algebraic expression has been derived for the parabolic component of strip shape. It is interesting to compare this with the complexity of the block diagram for the full shape calculation shown in figure 2. It should be emphasized that the simple expression is not a substitute for the full model since it is only valid for symmetric conditions and only models the parabolic component. This component is particularly important in mill scheduling studies, which will be discussed in the next section, and in designing certain feedback shape control loops.

2.10 Model Verification

The shape distributions computed from the full and simple models for two different widths and two different jack forces are plotted in figure 26. The difference in the full and simple model results is due mainly to the sudden change in stress near the strip edges caused by the work roll flattening in the full model.

2.11 Shape Sensitivity

An understanding of the behaviour of shape to variations in the available controls assists in the design of scheduling algorithms and shape control schemes, both of which will be discussed in later sections. Because the full shape analysis derived in Chapter 1 is iterative, sensitivities of shape to any other variables can only be obtained numerically. The simple expression for the parabolic component of strip shape, equation 2.9.3, can however be differentiated to yield expressions for the required sensitivities as follows.

Sensitivity of shape to roll force:

$$\frac{\partial \Omega}{\partial p} = E \frac{\bar{H}}{\bar{h}} \left[\frac{K_{23}}{\bar{h}(0.5 - (K_{21} + K_{24})A_5)} \right] \qquad 2.10.1$$

The coefficients K_{23} and K_{24} are functions of width which can be approximated by the quadratic equations 2.9.4. The sensitivity of shape to roll force is therefore highly width dependent and the form of this dependency is shown in figure 27. As the strip width decreases the rolls tend to bend more easily because the strip acts as a pivot. For very narrow widths however the sensitivity tends to decrease because the effect of bending over the narrow portion at the centre of the rolls is small. As the strip width increases and more of the roll width is in contact with the strip, the resistance to bending increases and the sensitivity again decreases. The sensitivity is a maximum for about 1000 mm wide strip.

Sensitivity of shape to jack force:

$$\frac{\partial \Omega}{\partial J} = E \frac{\bar{H}}{\bar{h}} \left[\frac{K_{25}}{\bar{h}(0.5 - (K_{21} + K_{24})A_5)} \right]$$

Since K_{25} has a similar width dependency to K_{23}, the variation of this sensitivity with width is similar to that described above.

Sensitivity of shape to roll crown:

$$\frac{\partial \Omega}{\partial C_w} = E \frac{\bar{H}}{\bar{h}} \left[\frac{K_{26}}{\bar{h}(0.5 - (K_{21} + K_{24})A_5)} \right]$$

CHAPTER 3

Tandem Mill Scheduling

In a tandem cold rolling mill, which can consist of up to six stands, the strip is successively reduced in thickness at each stand as it passes through the mill. At each stand the force required to reduce the strip is applied via the rolls by screws situated in the top of the main frame, or by means of hydraulic actuators usually situated below the bottom backup roll. To assist in the reduction process the screw position and motor speeds are adjusted to maintain the strip in tension between the stands. The problem of scheduling is concerned with choosing the proportion of the overall reduction to be carried out at each stand, the levels of interstand tension, the crown to be ground on the rolls at each stand and, if available, the level of roll bending jack forces required for good shape.

In practice scheduling policies are usually based on past experience and trial and error. These procedures are often adequate particularly when backed up with experienced manual interventions and long runs of standard products. However in certain extreme cases when the product is very variable or mill working is erratic, so that the thermal conditions never reach a steady state, it is important to have an understanding of the physical process underlying the scheduling behaviour.

The basis of most existing scheduling policies is said to be to maximise throughput, no account being taken of strip quality. The problem then becomes one of choosing the reductions and tensions so that at any speed the ratio of the power required to the power available, is the same at all stands. With this approach the shape of the strip produced is completely ignored, both in the final product, where it could lead to scrap material, and at intermediate points

through the mill where it could cause operating difficulties and expensive delays. Shape is particularly important on the nose of each coil during threading. If the nose becomes buckled it is difficult to thread it into a stand and roll damage can occur. Clearly the question of throughput cannot be totally ignored and on an existing mill some acceptable compromise must be made between throughput and strip quality. When designing a new mill however the power requirements for each stand should be computed for the ideal scheduling policy first, and this information used when designing the motors. For the discussion which follows we shall ignore the power requirements and investigate scheduling from shape considerations only.

The shape produced by a stand can be considered to be the result of three factors (1) the transmission of shape produced at preceding stands, (2) the effect of roll deformation (bending, shearing and flattening) and the initial ground camber on the work rolls, and (3) the thermal camber on the rolls caused by the friction heating in the roll gap. It is convenient to investigate separately the behaviour of each of these three factors to changes in schedule before combining the effects.

3.1 Shape Transmission

The effect on the shape produced at one stand of that produced at the preceding stand can be demonstrated by referring to the simple expression for the parabolic component of shape (equation 2.9.3) developed in Chapter 2.

$$\Omega_p = E\left\{\frac{\bar{H}}{\bar{h}}\left[\frac{(K_{23}p + K_{25}J + K_{26}C_w + K_{27}C_B + (K_{21} + K_{24})A_4C_1 + (K_{21} + K_{24})A_6\Omega'_p)}{\bar{h}(0.5 - (K_{21} + K_{24})A_5)} - \frac{C_1}{\bar{H}}\right]\right\}$$

Differentiate with respect to $\Omega'p$, then

$$\frac{\partial \Omega p}{\partial \Omega' p} = E \frac{\bar{H}}{\bar{h}} \left[\frac{(K_{21} + K_{24})A_6}{\bar{h}\left(0.5 - (K_{21} + K_{24})A_5\right)} \right] \qquad 3.1.1$$

If this sensitivity is evaluated for a typical schedule, values of approximately -0.54 are obtained. This implies that the magnitude of the shape produced by one stand will be reduced by a half as it passes through the next stand, and the sign will be changed; tensile stresses at the centre of the strip leaving one stand, will cause compressive stresses at the centre after the next stand. (This sensitivity has been verified numerically using the full shape model, a value of -0.6 was obtained).

It is interesting to also investigate the transmission of gauge profile through a stand. The effect of the entry profile C_1 on the exit profile C_2 can be found by rearranging equation 2.9.2,

$$C_2 = \left[\frac{(K_{21} + K_{24})A_4}{0.5 - (K_{21} + K_{24})A_5} \right] C_1 + \left[\frac{K_{23}p + K_{25}J + K_{26}C_w + K_{27}C_B + (K_{21} + K_{24})\Omega'}{0.5 - (K_{21} + K_{24})A_5} \right] \qquad 3.1.2$$

or

$$C_2 = D_1 C_1 + D_2$$

By inserting coefficient values into the first term it is found that the minimum likely value of $(K_{21} + K_{24})A_5$ is 44 and the expression can therefore be reduced to

$$C_2 \doteq -\frac{A_4}{A_5} C_1 + D_2$$

If the equations for A_4 and A_5 from equation 2.8.3 are inserted, and small terms are discarded it can be shown that

$$C_2 \doteqdot \frac{\bar{h}}{H} C_1 + D_2 \qquad 3.1.3$$

The second term D_2 is a function of roll force, jack force, roll crowns and shape from any previous stand. However if typical values for these parameters are inserted it can be shown that D_2 is very small, less than 0.002 mm, compared with strip crowns which are typically at least an order higher. Hence to a first order the strip profile at the exit of a stand is approximately equal to the profile at the entry reduced by the reduction ratio. Hence the ratio of strip profile to thickness remains approximately constant through a mill. (This transmission of strip profile has been verified experimentally as reported in 9).

3.2 Roll Deformation

The effect of schedule changes on the roll deformation can again be investigated using the simple shape model. The controls available at any one stand for modifying the shape via the schedule, are reduction and entry and exit strip tension. However none of these controls has a direct effect on roll deformation. The effect is via roll force and we shall therefore study the effect of roll force changes on roll deformation.

Ideally a schedule is chosen so that the roll forces developed at each stand together with the total crown on the rolls, due to grinding thermal expansion and roll wear, are such that strip with perfect shape is produced. Whatever the roll force developed at a stand, there is a value of roll crown which, to a first order at least, will cancel out the effects of roll deformation and cause strip with

perfect shape to be rolled. The relationship between this "crown for perfect shape" and roll force can be derived by equating equation 2.9.3 to zero,

$$\frac{(K_{23}p + K_{25}J + K_{26}C_w + K_{27}C_B + (K_{21} + K_{24})A_4C_1 + (K_{21} + K_{24})A_6\Omega')}{\bar{h}(0.5 - (K_{21} + K_{24})A_5)} - \frac{C_1}{\bar{H}} = 0$$

3.2.1

and rearranging for roll crown,

$$C_w = D_1 + D_2p \qquad 3.2.2$$

where $D_1 = \frac{1}{K_{26}}\left\{\frac{\bar{h}}{\bar{H}}[0.5 - (K_{21} + K_{24})A_5]C_1 - K_{25}J - K_{27}C_B - (K_{21} + K_{24})A_4C_1 - (K_{21} + K_{24})A_6\Omega'\right\}$

$$D_2 = -\frac{K_{23}}{K_{26}}$$

Hence the relationship is linear and this has been confirmed by results from the full model.

The value (D_1) of C_w when $p = 0$ represents the roll crown required to produce perfect shape when the roll force is zero. Clearly this is not a practical situation since with zero roll force there is no reduction, however zero force implies zero bending shearing and flattening (assuming the jack force is also zero). The roll crown must therefore be the negative of half the exit strip crown. (There

is a factor of a half as the strip crown is produced by the top and bottom rolls). For simplicity let us assume that the jack force J, the backup roll crown C_B, and the shape from the previous stand are all zero, then D_1 in equation 3.2.2 can be rewritten as,

$$D_1 = \frac{C_1}{K_{26}} \left\{ .5 \frac{\bar{h}}{H} - (K_{21} + K_{24}) \left[\frac{\bar{h}}{H} A_5 + A_4 \right] \right\} \qquad 3.2.3$$

A_4 and A_5 are the sensitivities of roll force to entry and exit gauge respectively. These sensitivities are always opposite in sign and of similar magnitude so that

$$\frac{\bar{h}}{H} A_5 + A_4 \doteq 0$$

From equation 2.9.2: $K_{26} = K_{26'} - \left(\frac{w}{F}\right)^2$

If this is evaluated for different widths it is found that $\left(\frac{w}{F}\right)^2$ always dominates. Equation 3.2.3 can therefore be rewritten as,

$$D_1 \doteq -0.5 \frac{\bar{h}}{H} \left(\frac{F}{w}\right)^2 C_1 \qquad 3.2.4$$

The factor $\left(\frac{F}{w}\right)^2$ is required since the strip crown C_1 is defined over the strip width w, and the roll crown C_w is defined over the roll width F; both crowns are assumed to be parabolic. In section 3.1 we have shown that the exit strip crown is approximately equal to the entry crown reduced by the reduction ratio. Therefore

$$D_1 \doteq -0.5 \left(\frac{F}{w}\right)^2 C_2 \qquad 3.2.5$$

As indicated by the full expression for D_1 in equation 3.2.2 the intercept is also dependent on the roll bending jack force J, the backup roll crown C_B, and the shape from the previous stand $\Omega'p$. It should be noted that since none of these parameters appear in the slope D_2, changes to any of them will have the effect of simply shifting the zero shape line of equation 3.2.2 vertically.

The slope of the 'zero shape line',

$$D_2 = -\frac{K_{23}}{K_{26}}$$

is dependent on strip width only. If the approximate representation of K_{23} and K_{26} given in equation 2.9.4 is used, the slope becomes

$$D_2 = \frac{-0.257*10^{-6}w^2 + 0.546*10^{-3}w - 0.218}{-0.475*10^{-6}w^2 - 0.217*10^{-3}w + 0.082} \qquad 3.2.6$$

Using this expression a graph has been drawn for slope D_2 against width, figure 28. It is easier to understand the behaviour of this slope with width if the horizontal axis of the zero shape graph is changed from specific roll force p to total roll force P, where,

$$P = p * w \qquad 3.2.7$$

Then the slope becomes

$$D_2' = -\frac{1}{w}\frac{K_{23}}{K_{26}} \qquad 3.2.8$$

This new slope is also plotted in figure 28 and the result is close to a straight line with negative slope. This implies that for a given <u>total</u> roll force more bending and shearing occurs for narrow strip than for wide strip, since a larger crown is required to cancel the

effect. This is obviously a sensible practical result as when the complete width of the roll gap is full of strip, bending must be severely inhibited.

To summarise, the relationship between roll force and roll crown for zero shape is a straight line. The intercept on the roll crown axis is dependent on the roll bending jack force, backup roll crown, and the shape from the previous stand but when these parameters are zero the intercept is equal,and opposite in sign,to the strip crown. The slope of the line is dependent on strip width only.

3.3 Roll Thermal Crown

As the strip passes through a roll gap heat is generated both by the work done in the reduction and by the friction forces between the strip and the rolls; this heat flows partly into the rolls and partly into the strip. Heat is extracted from the rolls outside the roll bite by coolant sprays acting over the complete roll width and as a result a thermal crown is developed across the rolls. (The heat flows are shown in figure 29).

The magnitude of the thermal crown is affected by entry and exit strip thickness and tension, strip hardness,and the coefficient of friction. If all these variables are fixed and only exit thickness is allowed to vary a graph can be drawn of thermal camber against roll force. A model of thermal crown has been developed in [21] where it is shown that the heat generated Q, is a convex function of the specific roll force p ie

$$Q = b\, p^{[(n+1)/n]}$$

The relationship between roll crown and the heat generated is developed in [22] where it is also shown that the difference in crown from the

roll centre to the roll edge is approximately independent of strip width and bears a linear relationship to the amount of heat generated. The crown profile however is a function of strip width, changing from near parabolic for narrow strip, to near quartic for wide strip. As we are concerned here only with the parabolic components of the distributions, the equivalent thermal crown is width dependent.

A graph of the total roll crown (thermal plus ground) is shown in figure 30. Clearly the intercept on the vertical axis is equal to the ground crown as the thermal crown must be zero for zero roll force.

In the previous section the effects of changes in roll force, and roll bending jack forces on the roll crown required to produce strip with perfect shape, were analysed. If this "zero shape" line and the thermal crown curve are plotted on a common pair of axes, points of intersection between the lines will indicate perfect shape conditions; that is the actual roll crown indicated by the curve is equal to the crown required for perfect shape, indicated by the straight line. Figure 31 shows such a graph drawn for particular entry and exit tensions, strip hardness, strip width, strip crown and roll crown. Under these conditions perfect shape will be produced at roll forces A and B. However as shown in the previous section the zero shape line can be shifted vertically by changes in jack forces, also the thermal crown curve can be shifted vertically by changes in ground crown, it is therefore possible to obtain perfect shape at any roll force.

There are three regions on the graph. For forces below A the thermal crown curve is above the zero shape line. The roll crown generated at these roll forces is therefore greater than that required to produce strip with perfect shape: Strip with full middle shape will be produced. In the second region, roll forces between A and B,

the crown required is greater than that generated: Strip rolled under these conditions will therefore have wavy edges. Roll forces above B will produce strip with full middle since, as with the first region, too large a thermal crown will be generated.

The diagram described is a valuable tool for understanding the behaviour at any one stand of a mill as the schedule parameters are varied. To design an optimum rolling schedule requires only that the thicknesses, tensions, ground crowns and jack forces be chosen so that at the operating roll force for each stand the two curves are, ideally, coincident. Unfortunately the calculation of tensions and reduction at a stand is an iterative procedure owing to the interdependency of roll force, reductions and tensions. Also each stand cannot be treated in isolation because of the requirement to meet a specified mill exit thickness and because of the transmission of shape through the mill. A method of obtaining an optimum solution to this problem is discussed in the next section.

3.4 Solution of the Scheduling Problem

The problem is to derive schedules for given mill entry thicknesses and strip widths which will enable strip to be rolled to the required thickness with good shape at the mill exit, and which will also maintain good shape throughout the mill.

As the mill entry thickness and total reduction are specified it is rarely possible to produce strip with perfect shape at all stands of the mill. The one exception is when roll bending jacks are available on all stands; shape can then be adjusted independently of any other mill variable. Even this observation must be interpreted with caution, since deformation patterns generated from thermal causes do not have the same parabolic characteristics of those generated by roll bending and hence perfect cancellation is not possible. It is

assumed that buckling can not occur unless there are compressive stresses in the strip. Under rolling conditions the strip is under tension between the stands and hence the transverse stress variation must exceed this mean level before buckling can occur. When threading the mill however the nose of the strip is unconstrained and the possibility of buckling is much greater. When designing schedules therefore we are interested in producing strip with good shape at intermediate stands during threading and at the mill exit during rolling.

3.4.1 Mathematical Formulation

Scheduling has been formulated as a non-linear sample data problem where the states are sampled at intervals of space rather than time. The sample points correspond to the stands of the mill where the controls are also specified. It is a two point boundary value problem as the dimensions and physical properties of the incoming strip are fixed, as are the mill exit thickness and tension. The dynamic behaviour of the shape, thermal crown and roll force is incorporated in a sample data state variable description of the mill.

Procedures for specifying the system adjoint equations and the control space gradient for such a problem are well known. As the end point constraints are linear, gradients were suitably projected to obtain constraint satisfactions[23]; the projected gradients were then used with a conjugate gradient iterative procedure[24]. When formulating the equations to represent the mill in this way it is convenient to specify six "states" and four "controls" at each stand. The six states are:

1) entry thickness (mm)
2) entry tension (tonne/mm^2)
3) roll force (tonne/mm)

4) shape parameter (tonne/mm^2)

5) difference in roll force developed between threading and running (tonne/mm)

6) thermal crown (mm)

The four controls are:

1) reduction (mm)

2) exit tension (tonne/mm^2)

3) roll bending jack force (tonne)

4) work-roll ground crown (mm)

The six states are chosen as mill variables which might be either constrained or costed at some point through the mill. The change in roll force from the threading to the rolling condition is required to calculate the value of shape while threading, from that while rolling. The reason for tension appearing as both a state and a control will become clear as the six state equations are derived.

(1) The entry thickness at one stand is equal to the entry thickness to the previous stand minus the reduction at that stand:

$$x_1^{i+1} = x_1^i - U_1^i \qquad 3.3.1$$

(2) The entry tension at one stand is equal to the exit tension at the previous stand, hence the need for tension as both a state and a control:

$$x_2^{i+1} = U_2^i \qquad 3.3.2$$

N.B. In the above two equations sample point i refers to the stand number.

(3) The roll force at a stand is a complex non-linear function of several states and controls at that stand, ie. entry and exit tension and thickness, and strip hardness which is a function of total reduction. For a state variable formulation, the value of a state at one sample point must be a function of states and controls at the previous sample point. To overcome this the roll force at sample point i is defined as the roll force at stand i-1. Therefore,

$$x_3^{i+1} = \text{roll force at stand } i$$

To assist in the calculation of gradients in the optimisation routine the roll force model is linearised[17]. The state equation is therefore,

$$x_3^{i+1} = A_1 x_2^i + A_2 U_2^i + A_3 x_1^i + A_4[x_1^i - U_1^i] + \text{constant} \qquad 3.3.3$$

States 4, 5 and 6 are similarly defined at sample point i as being the values at stand i+1.

(4) The strip shape, and hence the shape parameter at the exit of a stand, is a function of stand roll force, thermal crown, ground crown, jack force, and shape from the previous stand. As with the roll force the function is linearised and, incorporating the equation for the roll force, 3.3.3, the state equation for shape becomes,

$$x_4^{i+1} = K_1 x_2^i + K_2 U_2^i + K_3 x_1^i + K_4[x_1^i - U_1^i] + K_5 U_4^i$$

$$+ K_6 U_5^i + K_7 x_4^i + \text{constant} \qquad 3.3.4$$

(5) The difference in the roll force at stand i between the threading and rolling condition, represented by state 5 at sample point i+1, is brought about by the absence of exit tension during threading. The result is an increase in the roll force and the exit thickness. The total roll force change at a stand is due therefore, to the zero exit tension and to the increase in entry thickness caused when threading the previous stand. The increase in entry thickness is a function of the roll force difference at the previous stand. The state equation which is derived using linear coefficients of roll force is therefore,

$$x_5^{i+1} = \left[\frac{mA_2}{m - A_4 w}\right] U_2^i + \left[\frac{A_3 w}{m - A_4 w}\right] x_5^i \qquad 3.3.5$$

where m is the mill stiffness.

(6) The final state x_6 is defined at sample point i as being the work roll thermal crown at stand i-1. Thermal crown is a non linear function of stand entry and exit tensions and thicknesses[22], but as with roll force and shape a linearised expression will be used to assist in the gradient calculation. Therefore,

$$x_6^{i+1} = B_1 x_2^i + B_2 U_2^i + B_3 x_1^i + B_4 (x_1^i - U_1^i) + \text{constant} \qquad 3.3.6$$

The practical aspects of the scheduling problem dictate that the endpoints of some of the states are constrained. At the first sample point the first state, x_1, represents the mill entry thickness. In finding the solution to a normal scheduling problem this would be specified, however it could be left free to obtain the optimum mill entry thickness for a required mill exit thickness. The mill entry strip tension (x_2 at the first sample point) is fixed at zero on most mills, but it could be controlled in the same way as the other tensions.

The remaining states are constrained to zero at the first sample point (i=1) to give the correct initial conditions at stand 1.

The last sample point corresponds to the mill exit and hence the finished strip. The definition of states 3 to 6 dictates that there shall be one more sample point than there are stands, in order to accommodate the values of these states at all stands. Because of this, at the last sample point the first two states represent the entry thickness and tension to an imaginary stand after the last stand. However, by definition, these must be equal to the thickness and tension at the exit of the previous stand, ie the final thickness and tension between the last stand and the coiler. The two states are therefore fixed, the thickness for obvious reasons and the tension to facilitate satisfactory coiling of the strip. At the last sample point states 3 to 6 represent the values of certain mill variables at the last stand. The roll force (x_3) is normally constrained by considerations of surface finish and shape. It is desirable that the final strip shape (x_4) shall be zero. If roll bending jacks are installed it is possible to force the shape parameter to zero and hence x_4 would be fixed. The remaining states are free, their final value being chosen to satisfy a cost function. The constraints are summarised in table 3.3.1.

3.4.2 Cost function

The unconstrained controls are chosen to satisfy the endpoints and to minimize a cost function. A quadratic cost function was derived from practical considerations of the mill and the strip. The cost function is divided into three sections: (1) A cost on the shape during threading each stand, this has a weighting which increases through the mill to account for the increased likelihood of buckling as the thickness decreases. (2) A cost on the tension which must be

State	Sample Point	Definition	Endpoint condition
1	First	Mill entry thickness	Constrained or free
2	First	Mill entry tension	Constrained or free (normally zero)
3	First	Meaningless	Constrained to zero
4	First		Constrained to zero
5	First		Constrained to zero
6	First		Constrained to zero
1	Last	Mill exit thickness	Constrained
2	Last	Coiler tension	Constrained
3	Last	Last stand roll force	Constrained
4	Last	Final strip shape	Constrained or free
5	Last	Difference in roll force between threading and rolling on the last stand	Free
6	Last	Thermal crown on last stand	Free

Table 3.3.1 Summary of Endpoint Constraints

held to within limits imposed by consideration of skidding in the roll gap or loss of tension,with expected disturbances. (3) A cost on thermal crown. If a schedule is designed with a large crown on any stand, the loss of that crown after a roll change may lead to unacceptable strip being produced. The form of the complete cost function is,

$$\text{Cost} = \sum_{i=1}^{5} K_1^i \left(x_4^{i+1} + S^i x_5^{i+1}\right)^2 + K_2 \sum_{i=1}^{5} \left[x_2^{i+1} - \left(\frac{T_1^i + T_2^i}{2}\right)\right]^2$$

$$+ K_3 \sum_{\substack{i,j=2 \\ i \neq j}}^{5} \left(x_6^i - x_6^j\right)^2$$

where S^i is the linear coefficient of shape to roll force at stand i

T_1^i is the lower tension limit at stand i

T_2^i is the upper tension limit at stand i

A digital computer program for solving the scheduling problem has been written for use on a CDC 6400 computer. Examples of the results obtainable are shown and discussed in reference 25. Scheduling policies derived in this way are now in use on two five stand tandem cold mills.

In theory the scheduling problem can be solved using the above technique without the physical understanding of the complex interactions between roll force, shape and thermal crown developed in sections 3.2 and 3.3. This understanding is however necessary in order to design the best form of cost function which has a strong influence on the results produced. The physical understanding also assists in interpreting the results from the optimiser in terms that can be appreciated by practicing engineers and plant personnel.

CHAPTER 4

Shape Control

The primary aim of any shape control scheme is to produce strip with an acceptably low transverse stress variation at the mill exit. The shape produced at one stand is improved by a factor of approximately 0.5 as the strip passes through the next stand (section 3.1), hence in most cases only the conditions at the last two stands have any appreciable effect on the mill exit shape. The shape at all intermediate stands must however be good enough to avoid either high edge stresses, leading to strip breakage, or manifest shape which could produce roll damage.

4.1 Means of Control

The foregoing analysis has shown that the means of affecting the shape produced at any stand are (a) by changing the roll deformation, (b) by changing the roll thermal crown and (c) by changing the entry strip crown.

In section 3.2 the ratio of strip crown to thickness was shown to be approximately constant through a mill irrespective of schedule or jack forces, this can therefore be discounted as a possible control. Roll deformation can be controlled by jack forces, and reductions or tensions causing roll forces changes. Thermal crown is also affected by reductions and tensions but also by changes in the roll coolant distribution across the roll width. The suitability of each of these controls will now be discussed in more detail.

4.1.1 Roll bending jack forces

The most direct way of altering the roll deformation is by the use of hydraulic jacks situated at the ends of the rolls. There are three possible configurations for these jacks[26] (a) between the work and backup rolls, figure 32a, (b) between the work rolls, figure 32b and (c) between the backup rolls, figure 32c. All three configurations have essentially a parabolic effect on the strip shape being produced although for very wide strip, relative to the roll barrel length, the effects tend to be restricted to the edges of the strip. The degree of control available for work and work / backup roll jacks tends to be similar as both operate by bending the work rolls. The backup roll jacks have much less effect on shape because of the large diameter to length ratio and bending stiffness of the backup rolls.

All three jack configurations affect, by different degrees, the thickness of strip being produced which is generally taken to be the thickness at the strip centre line. This nominal thickness can only be affected therefore by changes in work roll flattening and inter roll squashing at the centre line, changes in the deflection of the backup roll relative to the screws, and changes in the reaction on the screws (S in figure 32) causing a change in the frame stretch. The first three of these effects are small and thickness changes are dominated by changes to the reaction S.

Consider the forces acting when jacks are applied between the work and backup rolls (figure 32a). An increase in jack force from J to $J + \Delta J$ will cause an increase in the total roll force $P(= \Sigma p)$ because the rolls are bent towards the strip at the strip edges, and a decrease in the inter roll force $Q(= \Sigma q)$ as the work rolls are bent away from the backup rolls at the roll ends. Therefore the equilibrium equation of the work roll is,

$$J + \Delta J = (P + \Delta P) - (Q + \Delta Q) \qquad 4.1.1$$

To maintain equilibrium the change in P and Q must cancel the change in J, hence equation 4.1.1 can be rewritten as

$$J + \Delta J = P + n\,\Delta J - (Q - (1 - n)\Delta J) \qquad 4.1.2$$

where $0 \leqslant n \leqslant 1$

Considering the equilibrium of the combined work and backup roll,

$$\Delta S = \Delta P$$

therefore

$$\Delta S = n\,\Delta J \qquad 4.1.3$$

In the case of work roll jacks (figure 32b) the change in jack force ΔJ is again shared between the changes in P and Q,

$$J + \Delta J = (Q + \Delta Q) - (P + \Delta P) \qquad 4.1.4$$

and again to maintain equilibrium

$$\Delta P = -\,n'\,\Delta J$$

and $\Delta Q = (1 - n')\,\Delta J$

where $0 \leqslant n' \leqslant 1$

For equilibrium of the backup roll

$$\Delta S = \Delta Q$$

Therefore, $\Delta S = (1 - n')\,\Delta J$ 4.1.5

An increase in the backup roll jack force will cause an increase in Q as the roll will bend about the screws towards the work roll. Therefore

$$\Delta S = \Delta J + \Delta Q \qquad 4.1.6$$

The increase in Q will depend upon the relative stiffnesses of the stand frame and the backup roll bending.

Comparison of equations 4.1.3, 4.1.5 and 4.1.6 shows that change in the screw reaction and therefore in the centre line strip thickness is much greater in the case of the backup roll jacks than for the other two configurations. The relative effects of work roll and work / backup roll jacks on the centre line thickness depends on the value of the constants n and n' and this will depend on the dimensions of the rolls. For all mills investigated the work / backup roll jacks have been found to affect the centre line thickness the least, however they do not afford a "non interactive" control for shape as is often assumed in the literature.

4.1.2 Roll force

The deformation of the work rolls is highly sensitive to changes in roll force. However changes in roll force obviously have a direct effect on the strip thickness and there is no way of correcting for this. The only situation when roll force can be used as an effective form of shape control is when the strip is very hard so that the sensitivity of thickness to roll force is very much smaller than the sensitivity of shape to roll force; the latter being unaffected by the hardness. This condition would apply on the last stand of a 5 or 6 stand tandem mill.

As well as affecting the deformation of the work rolls, changes in roll force also modify the thermal camber. The sensitivity of thermal crown to roll force was described in section 3.3 and is shown in figure 30; as the roll force increases so does the thermal crown. Changes in roll force therefore cause changes in shape by changing the deformation of the rolls (section 3.2) and by changing the thermal crown. Unfortunately these two effects oppose one another; the

combined effect can be described with reference to the combined graph of figure 31. For operating roll forces below A and greater than B, the roll crown (ground plus thermal) is greater than the crown required for perfect shape (indicated by the straight line) and the shape is therefore compressive at the centre and tensile at the edges. However in order to correct the shape the operating roll force must be changed to either A or B and this will require an increase in one case and a decrease in the other.

A difficulty of using roll force as a control for shape therefore is that on line it is not possible to know, from shape or roll force measurements, whether an increase or a decrease in roll force is required to correct shape in the steady state.

Because the strip thickness is defined at the centre line, differential roll force (the difference in the roll force at each edge of the strip) may be used as a control for asymmetric shape errors.

4.1.3 Coolant spray distribution

The thermal crown developed on the work rolls during rolling is a result of the balance between the heat input across the strip width in the roll gap and the heat lost to the coolant. By varying the intensity of the coolant on different parts of the rolls, the thermal expansion and hence the strip shape can be modified. This form of control has not been widely used on mills to date because as yet there are no instruments available for measuring thermal crown on line. With the advent of shape measuring instruments, however, it will be possible to infer the thermal crown from the shape readings and more sophisticated forms of spray control may be developed to thermally contour the rolls to correct bad shape. Such equipment[27] will be particularly advantageous in tinplate and aluminium rolling where more heat is generated and the shape tolerances are much tighter.

Coolant spray control has the advantage over the other shape controls discussed that a wide range of roll profiles and therefore stress distributions can be developed. For example, if the strip entering the mill has a thick band at some position across the width, shown exaggerated in figure 33, a band of compressive stress will be set up in the strip after rolling. This cannot be corrected by roll deformation. However if a coolant flow at that position across the roll is increased relative to the rest of the roll, the inverse profile can be generated on the roll and the shape corrected.

There are two disadvantages of spray control. On some mills the coolant and the lubricant are combined so that reducing the coolant will also reduce the lubrication: this can cause a bad surface finish to be produced on the strip and rolls. Secondly there is a long time constant of several minutes involved in changing the thermal crown.

4.2 Measuring Instruments

Over the last 15 years a variety of instruments have been developed for measuring strip shape. The instruments can be conveniently divided into two categories, contact and non contact.

The non contact instruments operate on one of three principles: a) The reflection of a straight line source of light on the strip surface[28]; if the surface is buckled the reflection will not be straight. Latent shape is not detected by this method. (b) An electromagnetic measurement, at several points across the strip, of the amplitude or frequency of vibrations induced in the strip by some resonator. The amplitude and frequency are both functions of the local tension and hence are an indication of stress and shape. c) Steel changes its magnetic permeability when subjected to mechanical stress. A measurement of this permeability can be used therefore at several points across the strip to detect stress changes.

With the exception of the IHI light source instrument which is useful for detecting the shape in hot rolling where contact instruments are not practical, the non contact instruments have had very limited success. The biggest problem is the effect of the large vibrations in the strip at the exit of a high speed tandem mill, also the instrument working on the magnetic principle can obviously only be used for steel rolling.

Contact instruments work on the principle of measuring the downwards force at several points across the strip as it passes over a segmented roll. Two of this type of instrument are now commercially available; the Loevy Robertson "Videmon" and the ASEA "Stressometer". In the ASEA instrument the forces are measured by pressductors, and in the Loevy Robertson by the difference in pressure at the top and bottom of gas bearings on which the segments are mounted. The only apparent disadvantage with ~~the~~ this type of instrument is the degree of resolution attainable since the instrument measures the average stress over each segment and the segments cannot be made arbitrarily thin. This is probably adequate for the central 75% of the strip width, but the sudden changes in stress possible near the strip edges due to the work roll flattening (section 1.5) may not be detected by the instrument.

4.3 Parameterisation

Parameterisation of the shape signal has already been discussed in section 2.1 in relation to the development of the simple shape model. The parameterisation choice for shape control is dictated by the controls available. The two main controls are roll bending jacks and roll coolant sprays. The roll bending jacks predominantly affect the parabolic component of shape; a parabolic parameter is therefore required for control of the jacks. The degree of spray

control available varies considerably between mills. On steel mills rolling sheet material the sprays are typically divided into 3 or 5 banks across the roll and in this case it may only be possible to utilise information on the parabolic parameter. On some aluminium mills however coolant jets at a 2 inch pitch across the roll are individually controllable. In this case parameterisation may be unnecessary, it may be more convenient to use the actual output from the shape instrument. Lastly it is convenient to filter any asymmetric or "skew" component from the shape reading and control this by a differential screw movement.

The output from the shape instrument may therefore be parameterised by a quadratic function,

$$\Omega = A + B\left[\frac{x}{W} - 0.5\right] + 4C\left[\frac{x}{W} - 0.5\right]^2$$

where A is the mean stress level

B is the asymmetric component

C is the parabolic component

W is the strip width

and x is the distance across the strip from one edge, $0 \leq x \leq W$

Having chosen a set of suitable parameters, it is equally as important to adopt a practical fitting criterion. The problem of choosing an incorrect fitting criterion can be illustrated by considering a shape distribution with a rapid change near the strip edges as shown in figure 34a. Suppose the method of fitting for the parabolic parameter was simply to take the two edge and the centre values; the resulting parabola is shown dotted. A control scheme which reduced this parabola to zero would produce the shape shown in figure 34b and this may not be the optimum result.

The best fitting criterion to use may be mill dependent because it is strongly affected by any edge effects caused by the work roll flattening. The degree of this edge effect is affected by the thickness profile of the incoming strip as illustrated by the results shown in 1.10. For the purposes of this control design we will assume the parameters are fitted by least squares over the central 75^{o}/o of the strip width thus ignoring the edge effects. The edge effects will be controlled separately.

4.4 Open Loop Control

It is not feasible either mechanically or economically to install shape instruments after every stand of a rolling mill. As the shape at the intermediate stands is less critical it is sufficient to provide an open loop predictive form of control.

Changes in shape during rolling are caused by changes in strip profile, roll profiles and roll force. Any change in strip profile will tend to be slow except possibly at a weld. Strip thickness profile cannot be measured on line and therefore shape variations caused by this can only be corrected manually from a visual shape assessment. (Strip profile produced on a hot mill will normally tend to be fairly constant throughout the length of a coil.) Changes in roll crown due to roll wear and thermal expansion also tend to be very slow. Again roll profiles cannot be measured on line at present and correction must be applied manually. Manual corrections to the jack forces are indications of the offsets in the strip or roll profiles. If the applied corrections are consistent therefore over a long period they can be used to update the crown estimates. Most of the shape changes along the length of a coil stem from changes in roll force which can be caused by changes in thickness or hardness of the strip entering the mill, or by changes to the motor speeds, or

screw positions resulting from the operation of thickness and tension control circuits.

Changes in roll force are measured by load cells on each stand. Changes in shape due to roll force can therefore be eliminated by a control loop from the roll force measurement to the roll bending jack force. The circuit for this control is given in figure 35. The gain G_1 can be obtained from the sensitivities of shape to roll force and of shape to jack force ie

$$G_1 = \left[\frac{\partial \Omega}{\partial P}\right]\left[\frac{\partial \Omega}{\partial J}\right]^{-1}$$

Expressions for these sensitivities, obtained from the simple shape model, are given in section 2.9. Combining the two we obtain:

$$G_1 = \frac{K_{23}}{K_{25}}$$

where K_{23} and K_{25} are defined in chapter 2.
It is assumed that both work roll and work / backup roll jacks are installed so that both positive and negative changes in roll bending can be effected.

As we have already discussed in section 4.1.1, changes in the force applied by roll bending jacks will affect the strip thickness by changing the frame stretch. To correct for this a compensating signal must be applied to the screw position via gains G_2 and G_3 as shown in the circuit in figure 35. The values of these gains are given by equations 4.1.3 and 4.1.5: G_2, the compensation for work roll jacks is $(n' - 1)$ and G_3, for the work backup roll jacks is $-n$. The exact values of n and n' are dependent on the mill dimensions and must be determined from results from the full shape model for each particular mill.

4.5 Feedback Control

An automatic feedback control of shape at the exit of all rolling mills is by no means a necessity. Except possibly at a weld (where two hot roll coils have been joined to form one coil for cold rolling) the rate of change of strip and roll parameters will be fairly slow. Furthermore roll force disturbances can probably be adequately controlled with an open loop jack force control as described above. When rolling steel sheet material the thermal crown on the final stand is small due to a low reduction and in this case manual control may well be adequate. When rolling steel for tinplate material where the final stand reduction is much larger or when rolling aluminium, the thermal crown is comparatively large and a coolant spray control will usually be required to maintain the precise shape required for these products. In this case the essential difficulty is that of processing information rather than speed of response and automatic shape control would seem to offer real advantages.

The structure of a feedback shape control scheme is shown in figure 36. The readings from the shape instrument will be of the stress at several points across the strip. These readings are first parameterised to give signals suitable for deriving the various control functions. The three control functions are (a) a signal to the screws to correct for asymmetry, (b) a signal to the roll bending jacks to correct the parabolic component of the shape and (c) a signal to the coolant sprays to (1) correct possible components in the stress distribution which cannot be controlled by the jacks and (2) to change the thermal crown so that in the event of a long term error, the jack forces will slowly be reduced; large jack forces promote roll and bearing wear. Parameters 1 and 2 in figure 36 are obtained therefore by fitting a quadratic function to the shape signal, as discussed in

section 4.3. The third parameter is for the coolant spray control and assuming that individual jet control is available, the signals from the instrument can be filtered to remove noise before being fed direct to the jet controls.

Any asymmetric component in the shape is fed to cause a differential movement of the screws. Since the strip thickness is defined at the strip centre line, there should be no interference with output thickness.

The parabolic parameter (2) is fed to either the work roll or the work / backup roll jacks depending on the sign of the correction required. As explained earlier, both of these jack forces will affect the strip thickness and therefore compensating signals must be fed to the screws.

The coolant sprays are controlled by parameter 3 and also by parameter 2 fed through a slow filter to correct long term roll profile errors by thermal crown changes rather than steady state jack forces. The changes in the coolant spray distribution are recorded and used to improve the on line estimation of the thermal crown.

Incorporated in the control scheme discussed above are two loops involving proportional plus integral controllers and the gains in these loops must be chosen to ensure optimum response. The problem is more complicated because the gains involved in the process dynamics in both loops are schedule dependent. Consider the loop to the roll bending jacks shown in isolation in figure 37. The shape parameter 2 is fed via the P + I and gain G_1 to the roll bending jacks. The shape being produced by the stand is then affected via the jack and process dynamics and after a transport delay the shape change is measured by the instrument and fed back to the parameterisation. The dynamics of the jacks and the instrument will be very fast and

can probably be ignored. The steady state gains of these items will be specified. The process dynamics will also be very fast but the steady state gain of the process will be highly schedule dependent and this will complicate the design of the P + I gains. The schedule dependency has been modelled by the shape analysis. Therefore by incorporating in G_1 the inverse of the process dynamics, the design is trivialised to that of a loop with unity gain. The transfer required is of jacks to shape and therefore,

$$G_1 = \left[\frac{\partial S}{\partial J}\right]^{-1}$$

$$= \frac{\bar{h}}{\bar{EH}}\left[\frac{\bar{h}(0.5 - (K_{21} + K_{24})A_5}{K_{25}}\right]$$

where A_5 and K_i are as defined in chapter 2.

The compensating gains to the screws are the same as for the open loop control and are mill dependent. Therefore from section 4.1.1,

$$G_2 = n' - 1$$

$$G_3 = -n.$$

CONCLUSIONS AND FUTURE RESEARCH

The phenomenon of strip shape has been analysed in depth and a detailed model developed. The relevance of shape to associated problems in control and scheduling has been investigated. A digital computer simulation of this model has been developed and results have shown encouraging agreement with plant data. The model is iterative and complex and therefore unsuitable for use on-line in shape control and scheduling. For this purpose a simple algebraic expression for strip shape is developed from the full model.

The simple model has been used to explain the complex interactions at a rolling stand which strongly affect the design of tandem mill schedules. A full procedure has been developed for designing tandem mill schedules. A shape control scheme has been developed and the problem of schedule dependency solved using the results of the simple shape model.

The most urgent piece of future work must be further experimental verification of the model. This requires only a fairly modest program of trials on a mill equipped with a shape instrument, and rolling a fairly wide range of product thicknesses and widths.

In order to proceed further with the shape control, two areas need attention. Firstly the problem of parameterisation choice for the purposes of dynamic control design needs careful study. Secondly before coolant spray control can be fully exploited it will be necessary to develop an accurate model of the effects of coolant spray patterns on the thermal profile. The theoretical analysis will certainly need the backing of plant trials particularly as the process contains parameters that are difficult to forecast from theory.

REFERENCES

1. McPhearson D.J., "Contributions to the Theory and Practice of Cold Rolling". Metallurgical Transactions, Vol. 5, Dec. 1974
2. Research of the Rolling of Strip, A Symposium of Selected Papers 1948–58, British Iron and Steel Research Association
3. Sivilotti O.G. et al, U.S. Patent No 3,534,571
4. Saxl K., "Transverse Gauge Variation in Strip and Sheet Rolling". Proc. Inst. Mech. Eng., 1958, 172, 727
5. Harguchi S., Kajawara T., Hata K., "Shape of Steel Strip in the Cold Rolling Process". Bulletin of the JSME, V. 14, No 67, 1971
6. Wilmotte S., Mignon J., Econopoulos M., "A Study of the Cross Profile in Hot Rolled Strip". C.R.M. No 30, March 1972
7. Sabatini B., "An Investigation into the Use of Tension and Roll Bending for Control of Strip Shape". BISRA Report
8. O'Connor H.W., Weinstein A.S., "Shape and Flatness in Thin Strip Rolling". Trans. ASME Jnl. of Engineering for Industry, November 1972
9. Edwards W.J., Spooner P.D., "Analysis of Strip Shape" *
10. Oliver B.R., Bowers J.E., "A Simplified Method of Deriving Cold-Rolling Schedules". J. Inst. Met., 1964–5, 93, 218–22
11. Suzuki et al, "New Methods of Calculating Pass Schedules for Tandem Strip Mill Rolling". Rep. Inst. Ind. Sci. Univ. Tokyo 1971, 21, (3), Sep.
12. Ford H. et al, "Cold Rolling with Strip Tension". JISI, 1951, 168, 57
13. Ryder G.H., "Strength of Materials". London. Cleaver Hume Press 1963
14. Spooner P.D., "Preliminary Investigation into the Control of Strip Shape". M.Sc. Thesis, Imperial College, 1969

15. Roark R.J., "Formulas for Stress and Strain". McGraw-Hill

16. Bryant G.F., Osborn R., "Derivation and Assessment of Roll Force Models". *

17. Bryant G.F. et al, "Evaluation of Linear Roll-Gap Coefficients" *

18. Mendelson A., "Plasticity; Theory and Application". London, Collier Macmillan, 1968

19. Prescott J., "Applied Elasticity". Dover Publications, New York

20. Boley B.A., Weiner J.H., "Theory of Thermal Stresses". New York Wiley 1960

21. Bryant G.F., Spooner P.D., "Basic Principles of Tandem Mill Scheduling". *

22. Beeston J.W., Edwards W.J., "Thermal Camber Analysis in Cold Rolling". *

23. Polak E., "Computational Methods of Optimisation". Academic Press, New York (1971)

24. Mitter S., Lasdon L.S., Waren A.D., "The Method of Conjugate Gradients for Optimal Control Problems". Proc. IEEE (1966)

25. Bryant G.F., Halliday J.M., Spooner P.D., "Tandem Mill Scheduling as a Two Point Boundary Value Problem". Automatica, Vol. 9, Pergamon Press 1973

26. Shohet K.N., "Preliminary Study of Profile Control on Plate Mills by Roll Bending Methods". BISRA Report

27. Sivilotti O.G., "Automatic Thermal Crown Control of Strip Mill Rolls". US Patent 3,587,265

28. Ishikavajima-Havima Heavy Industries, Tokyo, Japan. IHI Shape Meter (Strip Shape Detector)

* Bryant G.F. (Editor), "Automation of Tandem Mills", 1973, The Metals Soc. London

SYMBOL TABLE

A	Cross sectional area
a	Distance from roll bending jack to end of roll barrel
	Half the arc of contact
C_W	Work roll crown
C_B	Backup roll crown
C_1	Entry strip crown
C_2	Exit strip crown
D	Roll diameter
E	Youngs modulus of elasticity
F	Half the roll barrel length
f	Slip
G	Modulus of rigidity
h	Strip thickness
I	Moment of inertia
J	Roll bending jack force
K	Yield stress
L	Half the distance between the screws
L_J	Half the distance between the jacks
M	Bending moment
P	Total roll force
p	Roll force per unit length
q	Force per unit length between the work and the backup rolls
R	Roll radius
t	Thickness
U_d	Distortion energy
V	Stand entry velocity
	Shear force
v	Stand exit velocity

W	Work roll flattening
w	Strip width
y	Deflection
ε	Strain
ν	Poissons ratio
σ	Stress
ω	Roll speed
p_S	Parabolic component of force between the work roll and the strip
p_B	Parabolic component of force between the work and backup roll
$\bar{\cdot}$	Mean value

APPENDIX 1

Derivation of the Relationships between Forces Applied, Stresses and Displacement of an Element in an Elastic Body[19]

A1.1 Strain in terms of displacements in two dimensions

Suppose that a plane body is strained so that all particles remain in one plane after the strain, and refer all displacements to a pair of axes fixed relative to some particles of the body; (see figure 38) Let the origin 0 be situated at one of the particles of the body, and if that particle moves, 0 is supposed to move with it. Let the axis OX pass through one other given particle of the body and axis OY be perpendicular to OX or in the plane of the particles.

Let the particle situated at (x, y) before the strain move to $(x + u, y + v)$ after strain. Both u and v are functions of x and y. We shall investigate the change in the size and shape of the element which, before strain, was a rectangle dx by dy.

In figure 38 the rectangle CDHK is displaced relative to the axes to C'D'H'K'. The displacement of C has components u, v.

Now $u = f(x, y)$

The point D moves a distance $u + \delta u$ in the direction of the OX axis and, since the coordinates of D are $x + \delta x$,

$$u + \delta u = f(x + \delta x, y)$$

hence $$\delta u = f(x + \delta x, y) - f(x, y)$$

Expanding by Taylors series and neglecting terms in δx^2 and higher powers gives:

$$\delta u = \frac{\partial f(x, y)}{\partial x} \delta x = \frac{\partial u}{\partial x} \delta x$$

Since δu is the increase in length of the face CD relative to the OX axis,

the extensional strain $\epsilon_x = \frac{\delta u}{\delta x} = \frac{\partial u}{\partial x}$

Similarly the extensional strain in the direction OY,

$$\epsilon_y = \frac{\partial v}{\partial y}$$

The shear strain for the lines C'D' and C'H' is, by definition, the whole change in the angle at C; therefore shear strain = $\phi_1 + \phi_2$.

$$\phi_1 = \frac{ND'}{C'N}$$

$$= \frac{\partial v}{\partial x}$$

and $$\phi_2 = \frac{\partial u}{\partial y}$$

$$\text{Shear strain} = \frac{\partial v}{\partial x} + \frac{\partial u}{\partial y}$$

A1.2 Strain in terms of displacement in 3 dimensions

Let a particle originally at (x, y, z) move to (x + u, y + v, z + w). The displacements parallel to the x, y plane are the same as if w were zero, therefore the extensional strains parallel to OX and OY and the shear strain perpendicular to the axis OZ are as for the two dimensional case.

For three dimensions therefore the three extensional strains are

$$\frac{\partial u}{\partial x}, \frac{\partial v}{\partial y} \text{ and } \frac{\partial w}{\partial z}$$

and the three component shear strains are

$$\left(\frac{\partial v}{\partial z} + \frac{\partial w}{\partial y}\right), \left(\frac{\partial w}{\partial x} + \frac{\partial u}{\partial z}\right), \left(\frac{\partial u}{\partial y} + \frac{\partial v}{\partial x}\right)$$

For convenience, denote the extensional strains by α, β and γ and the shear strains by a, b and c

$$\alpha = \frac{\partial u}{\partial x} \qquad \beta = \frac{\partial v}{\partial y} \qquad \gamma = \frac{\partial w}{\partial z} \qquad \text{A1.1}$$

$$a = \left(\frac{\partial v}{\partial z} + \frac{\partial w}{\partial y}\right), \quad b = \left(\frac{\partial w}{\partial x} + \frac{\partial u}{\partial z}\right), \quad c = \left(\frac{\partial u}{\partial y} + \frac{\partial v}{\partial x}\right) \qquad \text{A1.2}$$

A1.3 Stress strain relationships

In figure 39 one view of a small rectangular block under tensional stresses P_1, P_2, P_3 and shear stresses S_1, S_2 and S_3 is shown.

The strain in the direction of $P_1 = \alpha = \frac{P_1}{E}$ due to P_1

$$- \nu \frac{P_2}{E} \text{ due to } P_2$$

$$- \nu \frac{P_3}{E} \text{ due to } P_3$$

where ν = Poissons ratio

E = Youngs modulus

$$\text{Therefore } \alpha = \frac{1}{E}[P_1 - \nu(P_2 + P_3)] \qquad \text{A1.3}$$

$$\text{and similarly } \beta = \frac{1}{E}[P_2 - \nu(P_1 + P_3)] \qquad \text{A1.4}$$

$$\gamma = \frac{1}{E}[P_3 - \nu(P_1 + P_2)] \qquad \text{A1.5}$$

The shear stress and shear strain are related simply by the modulus of rigidity G,

$$S_1 = G\,a = G\left(\frac{\partial v}{\partial z} + \frac{\partial w}{\partial y}\right) \qquad \text{A1.6}$$

$$S_2 = G\,b \qquad \text{A1.7}$$

$$\text{and } S_3 = G\,c \qquad \text{A1.8}$$

A1.4 Tensional stresses in terms of strains

By addition of equations A1.3, A1.4 and A1.5 and rearranging we get

$$P_1 + P_2 + P_3 = \frac{E}{1 - 2\nu}(\alpha + \beta + \gamma) = 3K(\alpha + \beta + \gamma) \qquad \text{A1.9}$$

where K is the bulk modulus

If a block of dimensions δx, δy, δz is strained in three directions, the new volume becomes,

$$\delta x(1 + \alpha) * \delta y(1 + \beta) * \delta z(1 + \gamma) = \delta x \delta y \delta z(1 + \alpha + \beta + \gamma)$$

neglecting products of α, β, and γ. The ratio of the increased volume to the original volume, that is the volumetric strain (Δ), is $(\alpha + \beta + \gamma)$. Therefore equation A1.9 can be rewritten,

$$P_1 + P_2 + P_3 = 3K\Delta \qquad \text{A1.10}$$

By combining equation A1.10 with A1.3, A1.4 and A1.5 respectively, expressions for P_1, P_2, and P_3 in terms of the strains can be found:

$$P_1 = 2G\left[\frac{\nu}{1-2\nu}\Delta + \partial u/\partial x\right]$$

$$P_2 = 2G\left[\frac{\nu}{1-2\nu}\Delta + \partial v/\partial y\right] \qquad \text{A1.11}$$

$$P_3 = 2G\left[\frac{\nu}{1-2\nu}\Delta + \partial w/\partial z\right]$$

where $\Delta = \alpha + \beta + \gamma = \dfrac{\partial u}{\partial x} + \dfrac{\partial v}{\partial y} + \dfrac{\partial w}{\partial z}$

A1.5 Relation between stresses and external forces

Consider the block shown in figure 40 with its centre at x, y, z and external dimensions δx, δy, δz. Let the body force per unit mass acting at x, y, z be X, Y, Z. The mass of the block is $\rho \delta x \delta y \delta z$, where ρ is the density. The body force on the block has components therefore of,

$X\rho\delta x\delta y\delta z$

$Y\rho\delta x\delta y\delta z$

$Z\rho\delta x\delta y\delta z$

Suppose also that the element has component accelerations of f_1, f_2 and f_3.

Let P_1, P_2, P_3 and S_1, S_2, S_3 denote the stresses at (x, y, z). Then

$$P_1'' = P_1 + \frac{\partial P_1}{\partial x} \cdot \frac{1}{2} \delta x$$

$$\text{and } P_1' = P_1 + \frac{\partial P_1}{\partial x}\left(-\frac{1}{2} \delta x\right)$$

$$\text{hence } P_1'' - P_1' = \frac{\partial P_1}{\partial x} \delta x \qquad \text{A1.12}$$

$$\text{Similarly, } S_3'' - S_3' = \frac{\partial S_3}{\partial y} \delta y$$

$$S_2'' - S_2' = \frac{\partial S_2}{\partial z} \delta z$$

Therefore the total force acting in the direction OX as a result of the stresses on the faces of the block is

$$\left(\frac{\partial P_1}{\partial x} \delta x\right)\delta y \delta z + \left(\frac{\partial S_3}{\partial y} \delta y\right)\delta x \delta z + \left(\frac{\partial S_2}{\partial z} \delta z\right)\delta y \delta z$$

$$= \left(\frac{\partial P_1}{\partial x} + \frac{\partial S_3}{\partial y} + \frac{\partial S_2}{\partial z}\right)\delta x \delta y \delta z \qquad \text{A1.13}$$

Hence the equation of motion can be written as

$$\delta x\delta y\delta z\left[\frac{\partial P_1}{\partial x}+\frac{\partial S_3}{\partial y}+\frac{\partial S_2}{\partial z}+\rho X\right]=\text{mass}*\text{acceleration}=\rho\delta x\delta y\delta z * f_1$$

$$\text{or}\quad \frac{\partial P_1}{\partial x}+\frac{\partial S_3}{\partial y}+\frac{\partial S_2}{\partial z}+\rho X=\rho f_1 \qquad \text{A1.14}$$

Similarly,

$$\frac{\partial P_2}{\partial y}+\frac{\partial S_1}{\partial z}+\frac{\partial S_3}{\partial x}+\rho Y=\rho f_2 \qquad \text{A1.15}$$

$$\text{and}\ \frac{\partial P_3}{\partial z}+\frac{\partial S_2}{\partial x}+\frac{\partial S_1}{\partial y}+\rho Z=\rho f_3 \qquad \text{A1.16}$$

Also the accelerations can be expressed in terms of the displacements

$$f_1=\frac{\partial^2 u}{\partial x^2}\qquad f_2=\frac{\partial^2 v}{\partial y^2}\qquad f_3=\frac{\partial^2 w}{\partial z^2} \qquad \text{A1.17}$$

A1.6 Equations of motion in terms of displacements

By combining equations A1.6 to A1.8 and A1.11 with equations A1.14 to A1.16 and rearranging the equations of motion can be expressed in terms of displacements:

$$\left[\frac{G}{(1-2\nu)}\right]\frac{\partial\Delta}{\partial x}+G\nabla^2 u+\rho X=\rho f_1 \qquad \text{A1.18}$$

$$\left[\frac{G}{(1-2\nu)}\right]\frac{\partial\Delta}{\partial y}+G\nabla^2 v+\rho Y=\rho f_2 \qquad \text{A1.19}$$

$$\left[\frac{G}{(1-2\nu)}\right]\frac{\partial\Delta}{\partial z}+G\nabla^2 w+\rho Z=\rho f_3 \qquad \text{A1.20}$$

APPENDIX 2

Displacement on the Surface of a Semi Infinite Solid due to a Pressure Applied at a Point[19]

The expression for the displacement dw caused by a pressure p applied at a point can be derived from the general equations relating the forces applied to, the stresses in, and the displacements of, an element in an elastic body. The relevant equations, which are derived in appendix 1 are,

a) Equations of motion:

$$\left[\frac{G}{1-2\nu}\right]\frac{\partial \Delta}{\partial x} + G\nabla^2 u + \rho X = \rho f_1$$

$$\left[\frac{G}{1-2\nu}\right]\frac{\partial \Delta}{\partial y} + G\nabla^2 v + \rho Y = \rho f_2 \qquad \text{A2.1}$$

$$\left[\frac{G}{1-2\nu}\right]\frac{\partial \Delta}{\partial z} + G\nabla^2 w + \rho Z = \rho f_3$$

where Δ = volumetric strain $= \dfrac{\partial u}{\partial x} + \dfrac{\partial v}{\partial y} + \dfrac{\partial w}{\partial z}$

u, v, w = the displacement in the x, y and z directions

X, Y, Z = body forces

f_1, f_2, f_3 = acceleration in the x, y and z directions

ρ = density

G = modulus of rigidity

$$\nabla^2 = \frac{\partial^2}{\partial x^2} + \frac{\partial^2}{\partial y^2} + \frac{\partial^2}{\partial z^2}$$

b) Stress strain relationships

$$P_1 = 2G\left[\frac{\nu}{1-2\nu}\Delta + \frac{\partial u}{\partial x}\right]$$

$$P_2 = 2G\left[\frac{\nu}{1-2\nu}\Delta + \frac{\partial v}{\partial y}\right] \qquad \text{A2.2}$$

$$P_3 = 2G\left[\frac{\nu}{1-2\nu}\Delta + \frac{\partial w}{\partial z}\right]$$

$$S_1 = G\left[\frac{\partial w}{\partial y} + \frac{\partial v}{\partial z}\right]$$

$$S_2 = G\left[\frac{\partial u}{\partial z} + \frac{\partial w}{\partial x}\right] \qquad \text{A2.3}$$

$$S_3 = G\left[\frac{\partial v}{\partial x} + \frac{\partial u}{\partial y}\right]$$

where P_i are the normal stresses

and S_i are the shear stresses

In this particular problem the accelerations are zero and there are no body forces. Equations A2.1 therefore reduce to:

$$\frac{\partial \Delta}{\partial x} + (1-2\nu)\nabla^2 u = 0$$

$$\frac{\partial \Delta}{\partial y} + (1-2\nu)\nabla^2 v = 0 \qquad \text{A2.4}$$

$$\frac{\partial \Delta}{\partial z} + (1-2\nu)\nabla^2 w = 0$$

By differentiating equations A2.4 with respect to x, y and z respectively and adding the results we get a differential equation for Δ alone ie

$$\nabla^2\Delta = 0 \text{ , (Laplaces equation)} \qquad \text{A2.5}$$

There are many known solutions to Laplaces equation, among the simplest and most useful are the spherical harmonics:

$$\text{If } r^2 = x^2 + y^2 + z^2 \qquad \text{A2.6}$$

then it can be shown that

$$\nabla^2\left(\frac{1}{r}\right) = 0 \qquad \text{A2.7}$$

Differentiating equation A2.7 with respect to x gives:

$$\frac{\partial}{\partial x}\ \nabla^2\left(\frac{1}{r}\right) = 0$$

$$\text{or} \quad \nabla^2\left[\frac{\partial}{\partial x}\left(\frac{1}{r}\right)\right] = 0 \qquad \text{A2.8}$$

Repeating this process l times gives

$$\nabla^2\left[\frac{\partial^l}{\partial x^l}\left(\frac{1}{r}\right)\right] = 0$$

Similarly it follows that,

$$\nabla^2\left[\frac{\partial^l}{\partial x^l}\ \frac{\partial^m}{\partial y^m}\ \frac{\partial^n}{\partial z^n}\left(\frac{1}{r}\right)\right] = 0 \qquad \text{A2.9}$$

l, m and n being integers.

Therefore one solution of the equation

$$\nabla^2 \phi = 0 \qquad \text{A2.10}$$

is $$\phi = \frac{\partial^l}{\partial x^l} \frac{\partial^m}{\partial y^m} \frac{\partial^n}{\partial z^n} \left(\frac{1}{r} \right) \qquad \text{A2.11}$$

Let ϕ be any solution of equation A2.10, then

$$\text{if} \quad \Delta = 2(1 - 2\nu) \frac{\partial \phi}{\partial z} \qquad \text{A2.12}$$

Δ satisfies A2.6 and substituting this into A2.4 gives

$$\nabla^2 u = - 2 \frac{\partial^2 \phi}{\partial x \partial z} \qquad \text{A2.13}$$

A particular integral of this is

$$u = - z \frac{\partial \phi}{\partial x} \qquad \text{A2.14}$$

since

$$\nabla^2 \left(- z \frac{\partial \phi}{\partial x} \right) = - \frac{\partial^2}{\partial x^2} \left(z \frac{\partial \phi}{\partial x} \right) - \frac{\partial^2}{\partial y^2} \left(z \frac{\partial \phi}{\partial x} \right) - \frac{\partial^2}{\partial z^2} \left(z \frac{\partial \phi}{\partial x} \right)$$

$$= - z \frac{\partial^3 \phi}{\partial x^3} - z \frac{\partial^3 \phi}{\partial y^2 \partial x} - z \frac{\partial^3 \phi}{\partial z^2 \partial x} - 2 \frac{\partial^2 \phi}{\partial z \partial x}$$

$$= - z \nabla^2 \frac{\partial \phi}{\partial x} - 2 \frac{\partial^2 \phi}{\partial z \partial x}$$

but from equations A2.10 and A2.11, $\nabla^2 \frac{\partial \phi}{\partial x} = 0$

$$\nabla^2\left(- z \frac{\partial \phi}{\partial x}\right) = - 2 \frac{\partial^2 \phi}{\partial z \partial x}$$

A more general solution to A2.13 is

$$u = - z \frac{\partial \phi}{\partial x} + \psi_1 \qquad \text{A2.15}$$

where ψ is also a solution to Laplaces equation

ie $\nabla^2 \psi_1 = 0$

Likewise the values of v and w corresponding to the assumed value of Δ are

$$v = - z \frac{\partial \phi}{\partial y} + \psi_2 \qquad \text{A2.16}$$

$$w = - z \frac{\partial \phi}{\partial z} = \psi_3' \qquad \text{A2.17}$$

ψ_2 and ψ_3' also being solutions of Laplaces equation.

Now Δ = volumetric strain $= \frac{\partial u}{\partial x} + \frac{\partial v}{\partial y} + \frac{\partial w}{\partial z}$

Inserting equations A2.15 to A2.17 gives

$$\Delta = - \frac{\partial \phi}{\partial z} + \frac{\partial \psi_1}{\partial x} + \frac{\partial \psi_2}{\partial y} + \frac{\partial \psi_3'}{\partial z}$$

therefore $$\frac{\partial \psi_1}{\partial x} + \frac{\partial \psi_2}{\partial y} + \frac{\partial \psi_3}{\partial z} = \Delta + \frac{\partial \phi}{\partial z} = (3 - 4\nu)\frac{\partial \phi}{\partial z}$$ A2.18

For convenience let $\psi_3' = \psi_3 + (3 - 4\sigma)\phi$ then equation A2.18 becomes

$$\frac{\partial \psi_1}{\partial x} + \frac{\partial \psi_2}{\partial y} + \frac{\partial \psi_3}{\partial z} = 0$$ A2.19

and $$w = -z\frac{\partial \phi}{\partial z} + (3 - 4\nu)\phi + \psi_3$$ A2.20

A particular solution is obtained by putting

$$\psi_1 = \frac{\partial \psi}{\partial x}, \quad \psi_2 = \frac{\partial \psi}{\partial y}, \quad \psi_3 = \frac{\partial \psi}{\partial z}$$

Substituting these values into A2.19 gives

$$\nabla^2 \psi = 0$$

therefore ψ is another solution to Laplaces equation. The equations for u, v, w and Δ become

$$u = \frac{\partial \psi}{\partial x} - z\frac{\partial \phi}{\partial x}$$

$$v = \frac{\partial \psi}{\partial y} - z\frac{\partial \phi}{\partial y}$$ A2.21

$$w = \frac{\partial \psi}{\partial z} - z\frac{\partial \phi}{\partial z} + (3 - 4\nu)\phi$$

$$\Delta = (2 - 4\nu)\frac{\partial \phi}{\partial z}$$ A2.22

By substitution into equations A2.2 and A2.3 the stresses corresponding to these displacements are,

$$P_1 = 2G\left[2\nu \frac{\partial \phi}{\partial z} - z \frac{\partial^2 \phi}{\partial x^2} + \frac{\partial^2 \psi}{\partial x^2}\right]$$

$$P_2 = 2G\left[2\nu \frac{\partial \phi}{\partial z} - z \frac{\partial^2 \phi}{\partial y^2} + \frac{\partial^2 \psi}{\partial y^2}\right] \qquad \text{A2.23}$$

$$P_3 = 2G\left[(2 - 2\nu) \frac{\partial \phi}{\partial z} - z \frac{\partial^2 \phi}{\partial z^2} + \frac{\partial^2 \chi}{\partial z^2}\right]$$

$$S_1 = 2G\left[\frac{\partial^2 \chi}{\partial y \partial z} - z \frac{\partial^2 \phi}{\partial y \partial z} + (1 - 2\nu) \frac{\partial \phi}{\partial y}\right]$$

$$S_2 = 2G\left[\frac{\partial^2 \chi}{\partial x \partial z} - z \frac{\partial^2 \phi}{\partial x \partial z} + (1 - 2\nu) \frac{\partial \phi}{\partial x}\right] \qquad \text{A2.24}$$

$$S_3 = 2G\left[\frac{\partial^2 \psi}{\partial x \partial y} - z \frac{\partial^2 \phi}{\partial x \partial y}\right]$$

Now consider the case of a concentrated normal force W applied at the origin on the surface of a semi infinite elastic solid bounded by z = 0. On the surface (z = 0) the shear stresses S_1 and S_2 (see figure 41) must be zero. Referring to equations A2.24 this condition is satisfied if

$$\frac{\partial \chi}{\partial z} = - (1 - 2\nu)\phi \qquad \text{A2.25}$$

(it is assumed that $\frac{\partial \phi}{\partial z}$ is finite over the surface).

Then

$$S_1 = -2G\,z\,\frac{\partial^2\phi}{\partial y \partial z} \qquad S_2 = -2G\,z\,\frac{\partial^2\phi}{\partial x \partial z} \qquad \text{A2.26}$$

and the stress normal to the surface,

$$P_3 = 2G\left[\frac{\partial\phi}{\partial z} - z\,\frac{\partial^2\phi}{\partial z^2}\right] \qquad \text{A2.27}$$

Now P_3 must be zero all over the surface except directly under the force W at the origin. To satisfy this condition it is necessary that $\frac{\partial\phi}{\partial z}$ shall contain a factor z.

Suppose $\phi = \frac{1}{r}$

then $\frac{\partial\phi}{\partial z} = -\frac{z}{r^3} \qquad \frac{\partial^2\phi}{\partial z^2} = -\frac{1}{r^3} + \frac{3z^2}{r^5}$

and

$$S_1 = -6G\,\frac{y\,z^2}{r^5} \qquad S_2 = -6G\,\frac{x\,z^2}{r^5} \qquad \text{A2.28}$$

$$P_3 = -6G\,\frac{z^3}{r^5} \qquad \text{A2.29}$$

These stresses are all zero therefore except possibly at the origin where r is also zero.

Let S equal the resultant of the two component shear stresses, then,

$$S^2 = 36G^2(x^2 + y^2)\left(\frac{z^2}{r^5}\right)^2$$

$$S^2 = 36G^2\, r^2\left(\frac{z^2}{r^5}\right)^2 \qquad \text{A2.30}$$

because $r^2 = x^2 + y^2$ in the plane $z = 0$.

Therefore $$S = 6\, G\, \frac{z^2}{r^4} \qquad \text{A2.31}$$

which acts on the surface along a radius vector from the origin, hence the stress system is symmetric about the z axis.

In order to verify the choice of ϕ equal to $1/r$ we must find the resultant force at the origin and this must be equal and opposite to the applied force W.

Consider the equilibrium of a small cylindrical portion of the solid having the z axis as its axis of symmetry. Let the faces of the cylinder be in the planes $z = 0$ and $z = C$ and let the radius equal a (figure 42). If we assume that a/C is infinite while a itself is finite, then the resultant of the shear stresses S acting on the curved area is zero. The resultant of the stresses P_3 on the circle of radius a must therefore be equal to -F.

$$F = -\int_0^a 2\pi\rho\, d\rho\, P_3 \qquad \text{A2.32}$$

where $\rho^2 = x^2 + y^2$.

But, from A2.29,

$$P_3 = -6G\frac{z^3}{r^5} = -6G\frac{c^3}{(\rho^2 + c^2)^{5/2}}$$

Therefore

$$F = 12\pi G\int_0^a \frac{\rho c^3}{(\rho^2 + c^2)^{5/2}}\,d\rho$$

$$= 12\pi G\left[\frac{-c^3}{3(\rho^2 + c^2)^{3/2}}\right]_0^a = 4\pi G\left[1 - \frac{c^3}{(a^2 + c^2)^{3/2}}\right] \qquad \text{A2.33}$$

but since $c/a = 0$

Equation A2.33 becomes

$$F = 4\pi G \qquad \text{A2.34}$$

But we require that F must equal W, the applied force. Therefore we should have taken

$$\phi = \frac{W}{4\pi G}\cdot\frac{1}{r} \qquad \text{A2.35}$$

The displacement w in terms of ϕ is given by combining equations A2.21 and A2.25,

$$w = 2(1-\nu)\phi - z\frac{\partial\phi}{\partial z} \qquad \text{A2.36}$$

By inserting the expression for ϕ from equation A2.35, the expression for w becomes

$$w = \frac{W}{4\pi G}\left[\frac{2(1-\nu)}{r} + \frac{z^2}{r^3}\right] \qquad \text{A2.37}$$

which at the surface becomes,

$$w = \frac{W}{2\pi G}\,\frac{(1-\nu)}{r} \qquad \text{A2.38}$$

Equation A2.38 gives the displacement at any point over the surface of a semi infinite elastic body caused by a single force acting at the origin. We require an expression for the displacement at any point on the surface caused by a pressure applied over some area. Suppose a pressure of p per unit area is applied at some point in the plane z = 0 denoted by the co ordinates x_1, y_1. The force on the area dx_1, dy_1 is therefore $pdx_1\,dy_1$. From equation A2.38 the displacement at some point x, y in the plane caused by this force is,

$$dw = \frac{(1-\nu)}{2\pi G}\,\frac{pdx_1\,dy_1}{R} \qquad \text{A2.39}$$

where R is the distance between the point at which the force is applied (x_1, y_1) and the point at which the displacement is measured (x, y).

$$R^2 = (x - x_1)^2 + (y - y_1)^2.$$

APPENDIX 3

Solution of the Integral

$$I = \int_p^q \ln\left[A + (A^2 + Y^2)^{1/2}\right] dY$$

Integrate by parts:

$$\text{let} \quad u = \ln\left[A + (A^2 + Y^2)^{1/2}\right] \qquad dV = dY$$

$$du = \frac{Y(A^2 + Y^2)^{-1/2}}{A + (A^2 + Y^2)^{1/2}}\, dY \qquad V = Y$$

$$I = \left[Y \ln\left(A + (A^2 + Y^2)^{1/2}\right)\right]_p^q - \int_p^q \frac{Y^2\, dY}{\left[A + (A^2 + Y^2)^{1/2}\right]\left[A^2 + Y^2\right]^{1/2}}$$

$$= I_1 - I_2$$

$$I_2 = \int_p^q \frac{Y^2\, dY}{A^2 + Y^2 + A(A^2 + Y^2)^{1/2}}$$

$$\text{let} \quad Y = A \tan z \qquad \text{therefore } z = \tan^{-1} Y/A$$

$$dY = A \sec^2 z\, dz$$

$$\text{when } Y = p \qquad z = \tan^{-1} p/A = c$$

$$Y = q \qquad z = \tan^{-1} q/A = d$$

Therefore

$$I_2 = \int_c^d \frac{A^2 \tan^2 z \cdot A \sec^2 z \, dz}{A^2 + A^2 \tan^2 z + A\left(A^2 + A^2 \tan^2 z\right)^{1/2}}$$

$$I_2 = \int_c^d \frac{A \tan^2 z \sec^2 z \, dz}{1 + \tan^2 z + \left(1 + \tan^2 z\right)^{1/2}}$$

Using the identity $\tan^2 z = \sec^2 z - 1$, this reduces to

$$I_2 = A \int_c^d (\sec z - 1) \sec z \, dz$$

$$= A \int_c^d \sec^2 dz - A \int_c^d \sec z \, dz$$

$$= A[\tan z - \ln (\sec z + \tan z)]_c^d$$

Therefore

$$\int_p^q \ln \left[A + \left(A^2 + Y^2\right)^{1/2}\right] dY =$$

$$\left[Y \ln\left(A + \left(A^2 + Y^2\right)^{1/2}\right)\right]_p^q - A \left[\tan z - \ln\left(\sec z + \tan z\right)\right]_{\tan^{-1}\left(\frac{p}{A}\right)}^{\tan^{-1}\left(\frac{q}{A}\right)}$$

APPENDIX 4

The Variation in the Stress Distribution at the End of a Plate

The various aspects of the problem can be approximated by the behaviour of the simple structural model shown in figure 43[20]. The model consists of three rods connected by two thin plates, thickness t width b. Quantities relating to the centre rod are denoted by a subscript c and those of the side rods by a subscript s. At the ends of the rods, $x = 0$, they are attached to a beam of moment of inertia I. Quantities related to the beam are denoted by subscript B. The entire structure is assumed to be of the same material with modulus of rigidity G and Youngs modulus E.

The forces in the body are assumed to be in equilibrium, therefore

$$2F_s(x) + F_c(x) = 0 \qquad \text{A4.1}$$

and, considering a small element in one of the side rods,

$$\frac{dF_s(x)}{dx} + t\,\tau(x) = 0 \qquad \text{A4.2}$$

where $\tau(x)$ is the shear stress in the plate.

For equilibrium in the beam, the force in the beam at $y = b$ must equal the difference between the force applied and the force in the side rod at that point,

$$F_B = F - F_s(0) \qquad \text{A4.3}$$

The total strain energy U is the sum of the strain energies in the two side rods, the centre rod, the two plates and the beam,

$$U = \frac{2}{2A_sE}\int_0^L F_s^2 dx + \frac{1}{2A_cE}\int_0^L F_c^2 dx + \frac{2bt}{2G}\int_0^L \tau^2 dx$$

$$+ \frac{2}{2EI}\int_0^b M^2 dy \qquad \text{A4.4}$$

where M is the bending moment in the beam,

$$M = F_B(b - y) \qquad 0 \leqslant y \leqslant b$$

Substituting for F_c, τ and M gives

$$EU = \left(\frac{1}{A_s} + \frac{2}{A_c}\right)\int_0^L F_s^2 dx + \frac{Eb}{Gt}\int_0^L \left(\frac{dF_s}{dx}\right)^2 dx + \frac{b^3}{3I}[F - F_s(0)]^2 \qquad \text{A4.5}$$

A solution to this will be found by using the principle of least work which states that the strain energy of any system must be a minimum. A solution for F can be found therefore by differentiating equation A4.5 and equating to zero.

$$2E\delta U = 0 = \left(\frac{1}{A_s} + \frac{2}{A_c}\right)\int_0^L F_s \delta F_s dx + \frac{Eb}{Gt}\int_0^L \left(\frac{dF_s}{dx}\right)\delta\left(\frac{dF_s}{dx}\right)dx$$

$$- \frac{b^3}{3I}(F - F_s(0))\delta F_s(0) \qquad \text{A4.6}$$

which by integrating the second term by parts becomes:

$$\int_0^L \left\{ \left(\frac{1}{A_s} + \frac{2}{A_c} \right) F_s - \frac{Eb}{Gt} \frac{d^2 F_s}{dx^2} \right\} \delta F_s \, dx + \frac{Eb}{Gt} \left\{ \frac{dF_s}{dx} \right\}_{x=L} \delta F_s(L)$$

$$- \left\{ \frac{b^3}{3I} (F - F_s) + \frac{Eb}{Gt} \left(\frac{dF_s}{dx} \right) \right\}_{x=0} \delta F_s(0) = 0 \qquad \text{A4.7}$$

Since the variation δF_s is arbitrary, F_s must satisfy the differential equation,

$$\frac{d^2 F_s}{d\left(\frac{x}{2b}\right)^2} - K_1^2 F_s = 0 \qquad \text{A4.8}$$

with the following boundary conditions:

$$\text{either } \frac{dF_s}{d\left(\frac{x}{2b}\right)} = 0 \quad \text{or} \quad \delta F_s = 0 \text{ at } x = L \qquad \text{A4.9}$$

$$\text{and either } -\frac{K_2}{K_1} \frac{dF_2}{d\left(x/2b\right)} + F_s = F \quad \text{or} \quad \delta F_s = 0 \text{ at } x = 0 \qquad \text{A4.10}$$

$$\text{where } K_1 = 2\sqrt{\frac{Gtb}{EA_s}\left(1 + 2\frac{A_s}{A_c}\right)} \; ; \quad K_2 = \frac{3I}{b^3}\sqrt{\frac{Eb}{GtA_s}\left(1 + 2\frac{A_s}{A_c}\right)}$$

The two possible boundary conditions at $x = L$ in A4.9 correspond to a fixed end ($\tau = 0$, from equation A4.2, because relative end displacements are prevented) or prescribed end forces. The two possibilities at $x = 0$ (A4.10) correspond to the case where the end forces in the rods are determined by the presence of the beam (as in the present problem) or are prescribed.

Consider the case of a fixed end at x = L, the solution is

$$F_s(x) = -\frac{F_c(x)}{2} = \frac{Fe^{-[K_1 x/(2b)]}}{1 + K_2 + (1 - K_2)e^{-[K_1(L/b)]}}\left\{1 + e^{-[K_1(L - x)/b]}\right\} \qquad \text{A4.11}$$

and from A4.2

$$(2bt)\tau(x) = \frac{FK_1 e^{-[K_1 x/(2b)]}}{1 + K_2 + (1 - K_2)e^{-K_1(L/b)}}\left\{1 - e^{-[K_1(L - x)/b]}\right\} \qquad \text{A4.12}$$

Equations A4.11 and A4.12 give the solution for the variation of the forces F_2 and the shear stresses τ along the length of the body. By observation, if the structure is sufficiently long, that is, if

$$L/b \gg 1$$

then $F_s(x)$ and $\tau(x)$ will be approximately independent of F and hence of y provided that x is not too close to zero or L. The exact variation of $F_s(x)$ and $\tau(x)$ in the regions close to the ends will depend on the parameter K_1. Since K_1 will have the same effect at both ends, the equations can be simplified by considering only the region close to x equal zero, and setting L to infinity. Then equations A4.11 and A4.12 become

$$F_s(x) = -\frac{1}{2} F_c(x) = \frac{F}{(1 + K_2)} e^{-[K_1 x/(2b)]} \qquad \text{A4.13}$$

and

$$\tau(x) = \frac{F K_1}{(1 + K_2)} e^{-[K_1 x/(2b)]} \qquad \text{A4.14}$$

We require a solution for a solid structure of uniform cross section (a plate). So that the behaviour of the structure considered above will approximate that of a solid plate,

$$\text{let } A_s = A_c = tb = A$$

$$\text{then } K_1 = 2\sqrt{\frac{3G}{E}} \doteq 2.2$$

$$\text{Therefore } F_s(x) = -\frac{1}{2} F_c(x) = Fe^{-[2.2\ x/(2b)]} = .91\ bt\tau(x) \qquad \text{A4.15}$$

$$\text{or } \frac{F_s(x)}{F} = e^{-[2.2\ x/(2b)]} \qquad \text{A4.16}$$

A plot of equation A4.16 is shown in figure 17 and this shows that the effects of forces applied to the end of a plate may be considered negligible for $x > 2b$.

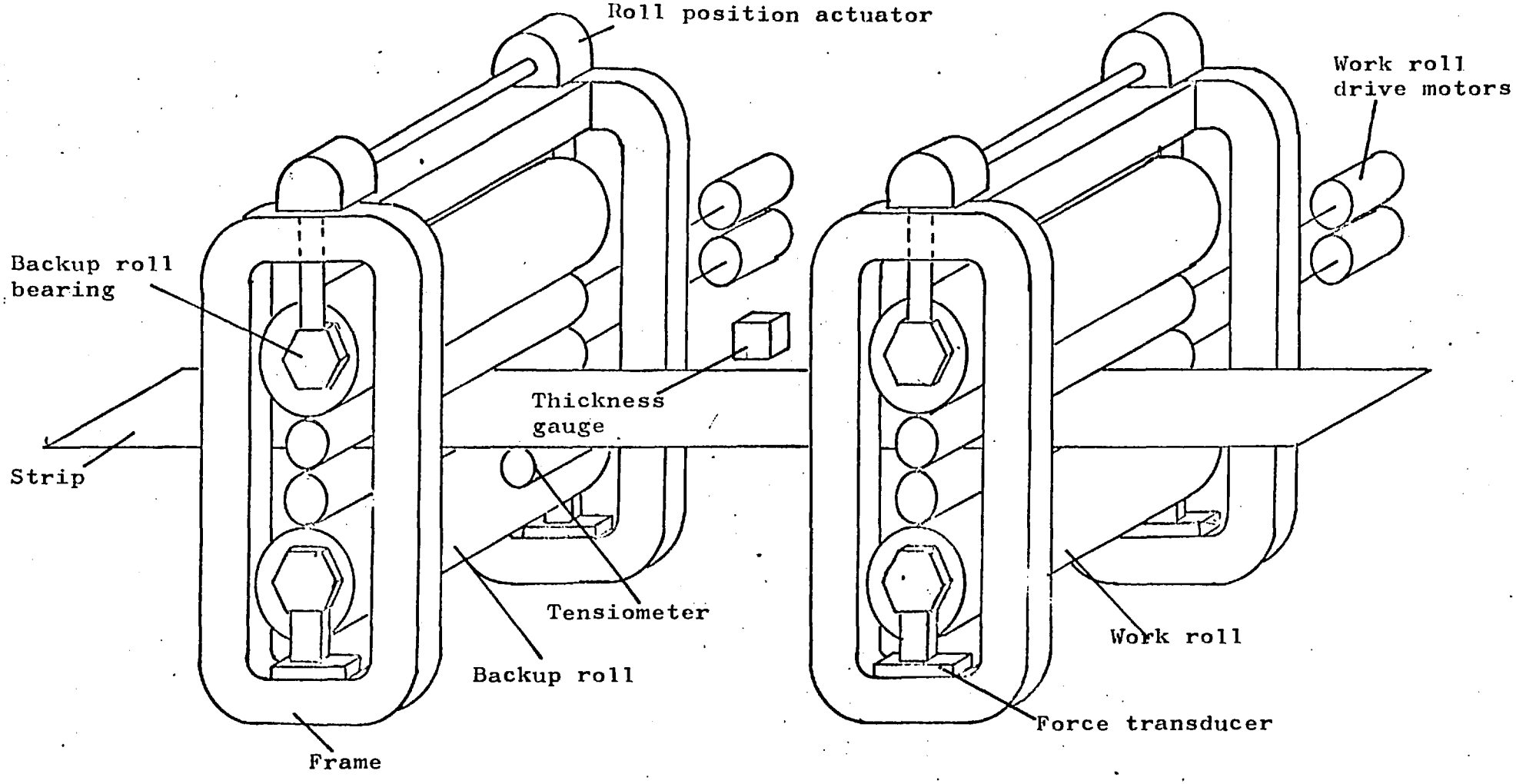

Figure 1. Two Stands of a Rolling Mill.

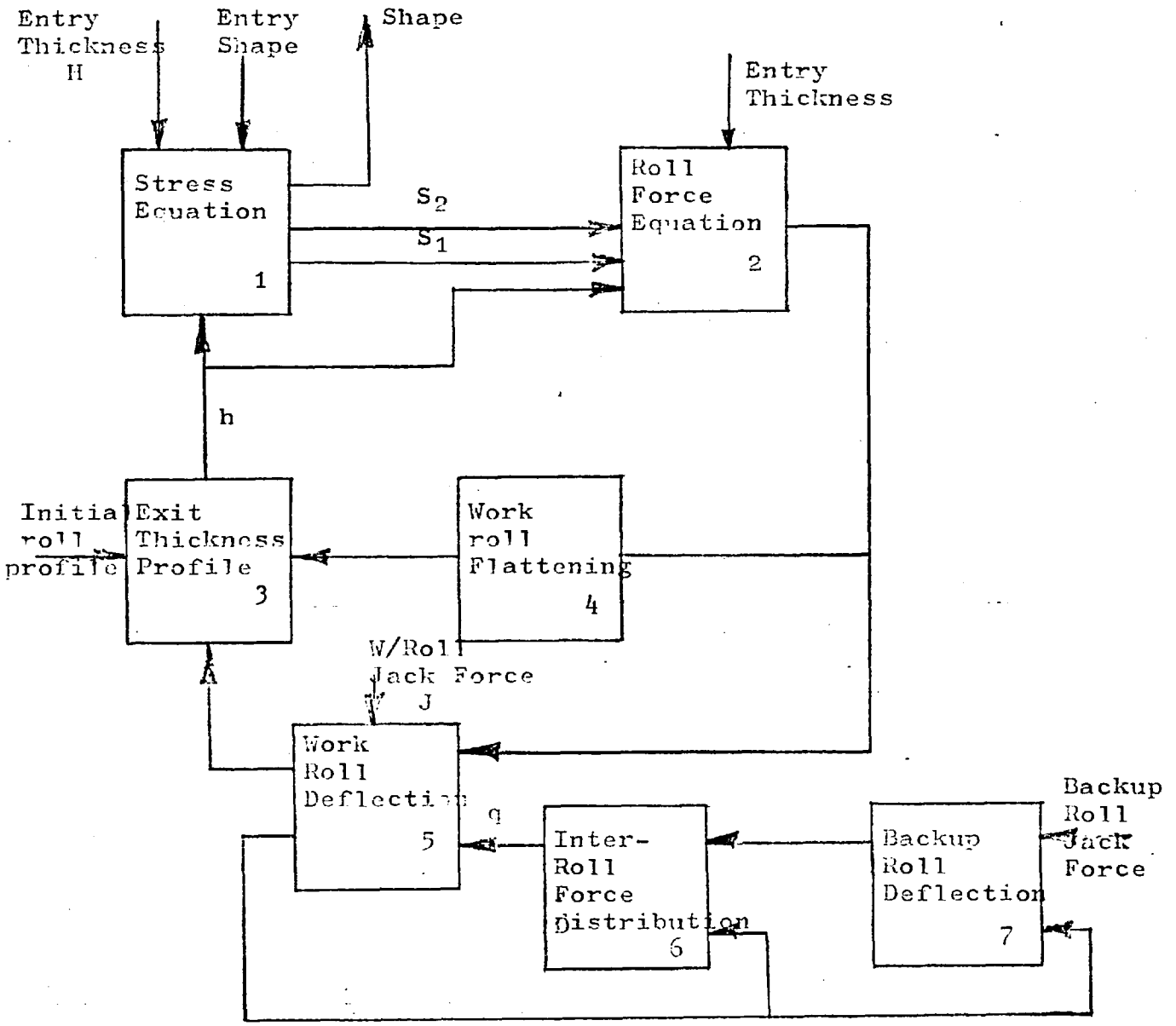

Figure 2. Structure of the Shape Model

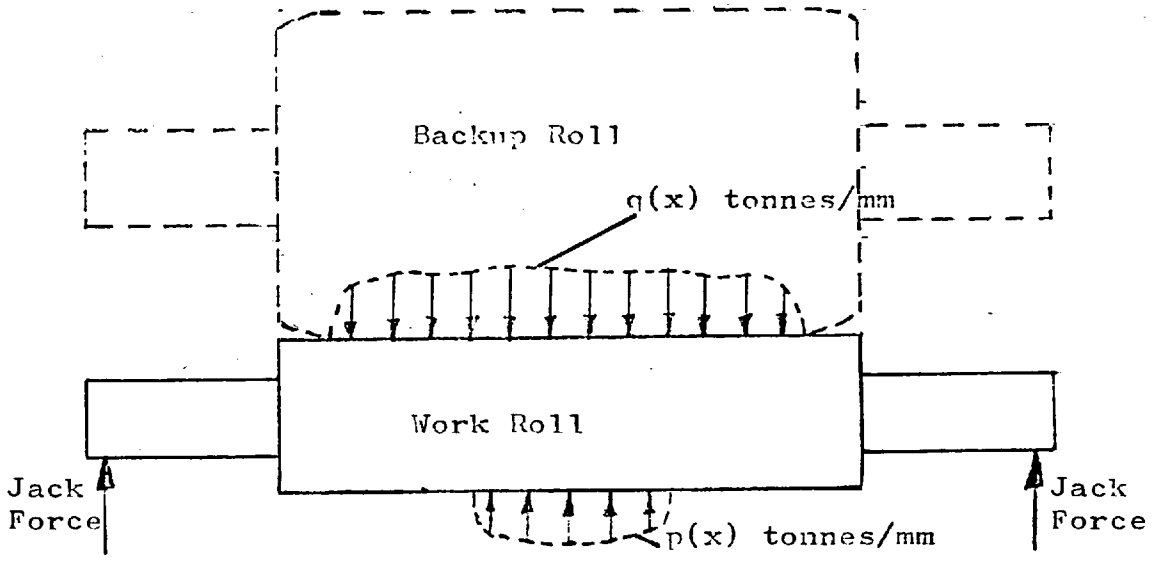

Figure 3a. Forces Acting on the Work Roll.

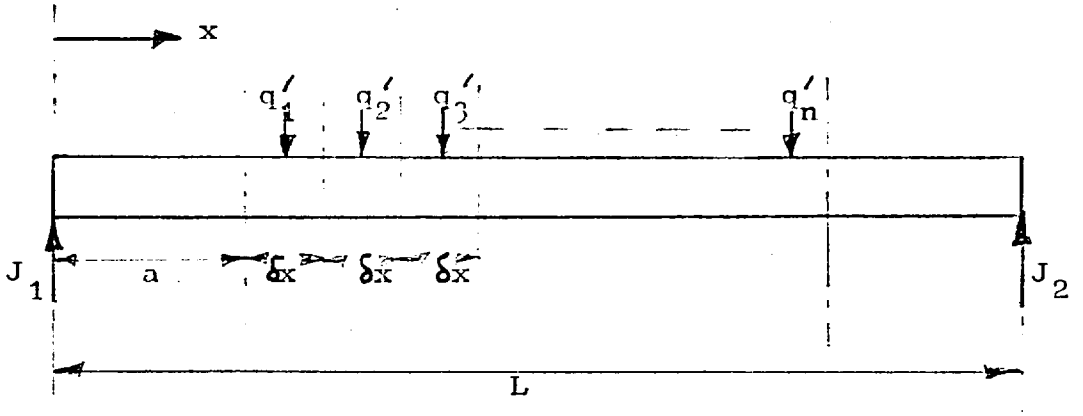

Figure 3b. Work Roll , Equivalent Beam.

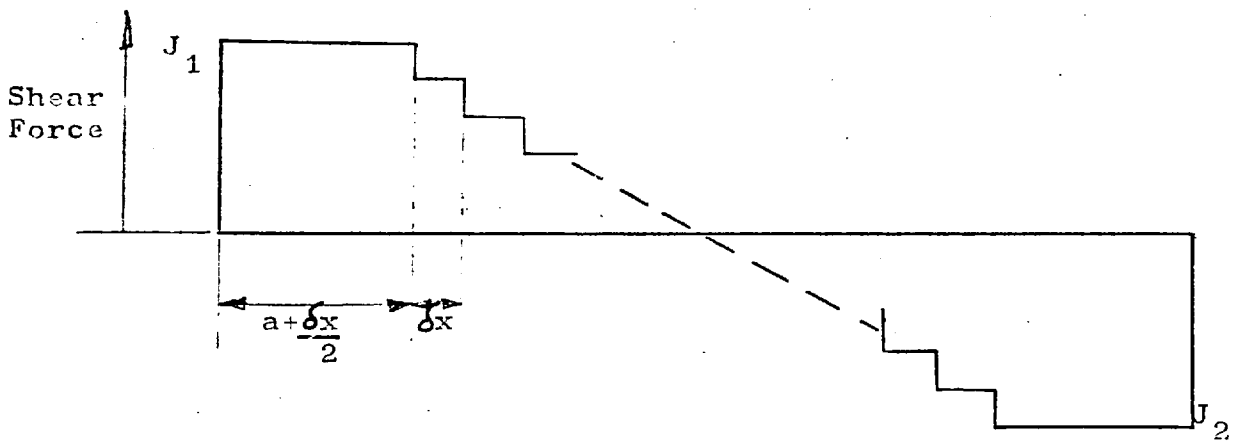

Figure 4. Shear Force Diagram.

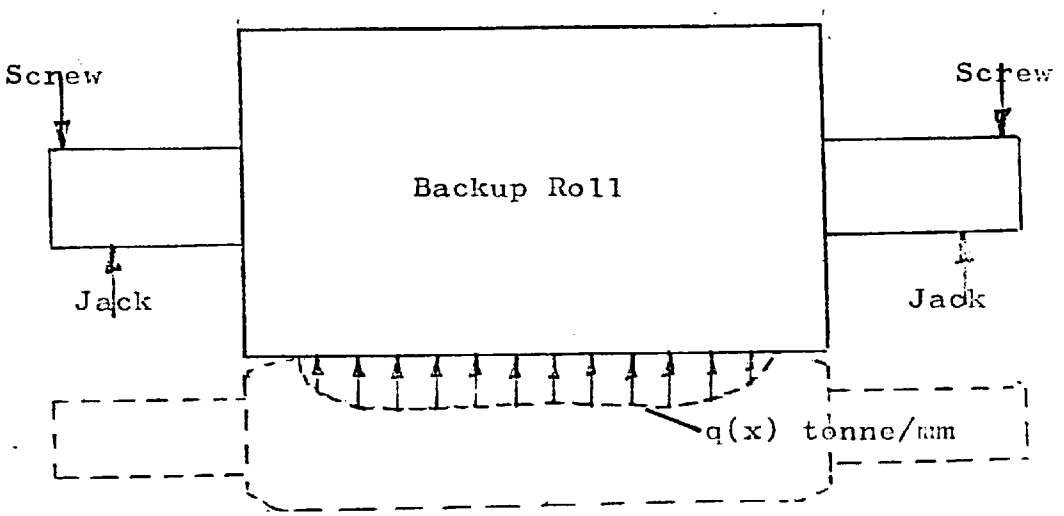

Figure 5. Forces Acting on the Backup Roll.

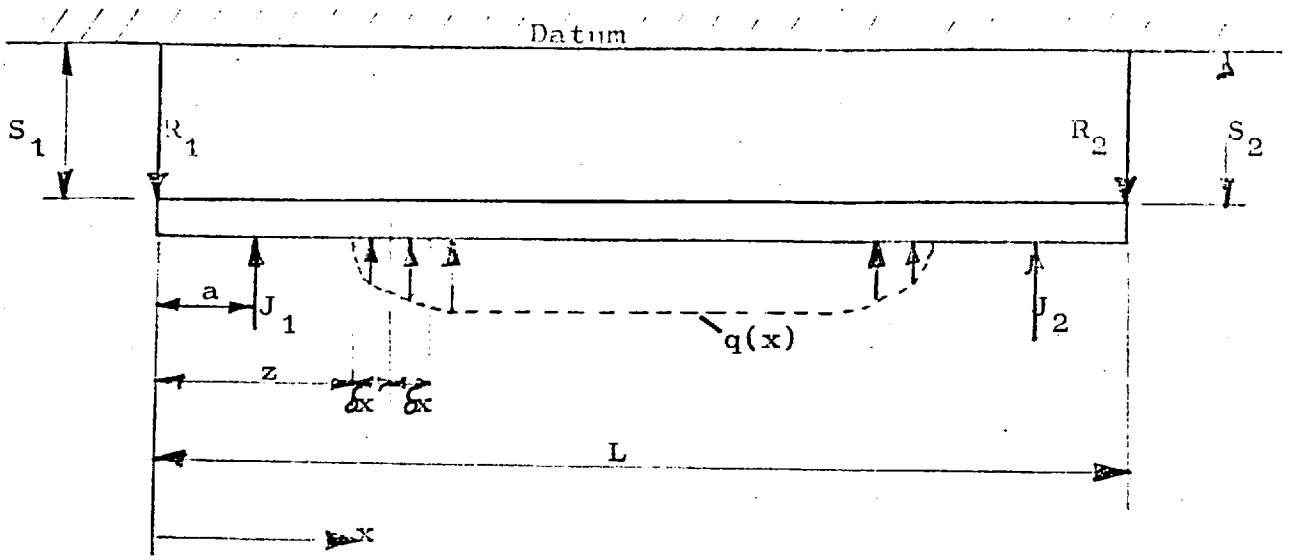

Figure 6. Backup Roll , Equivalent Beam.

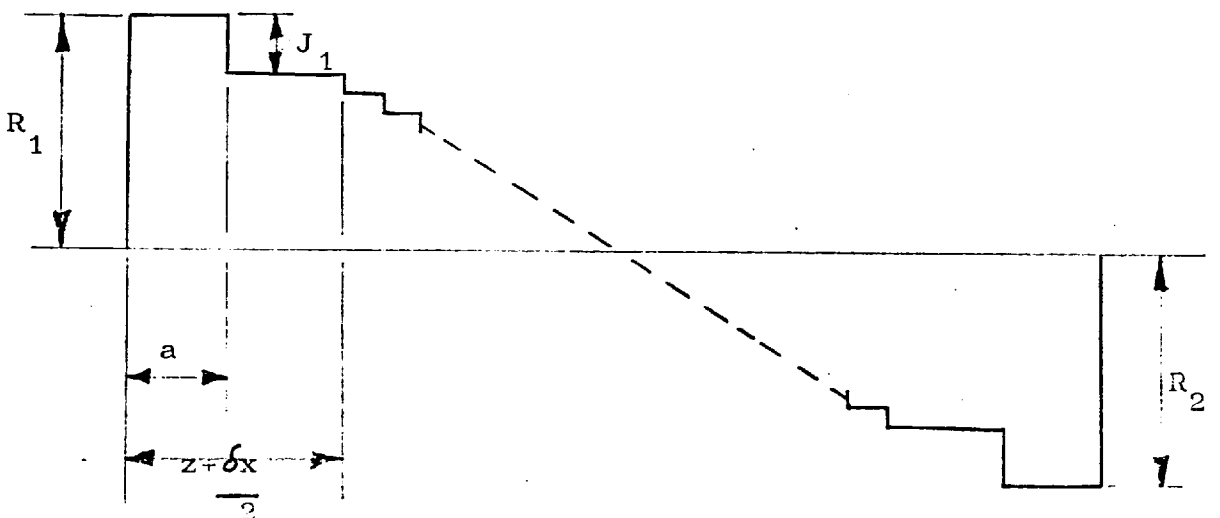

Figure 7. Shear Force Diagram.

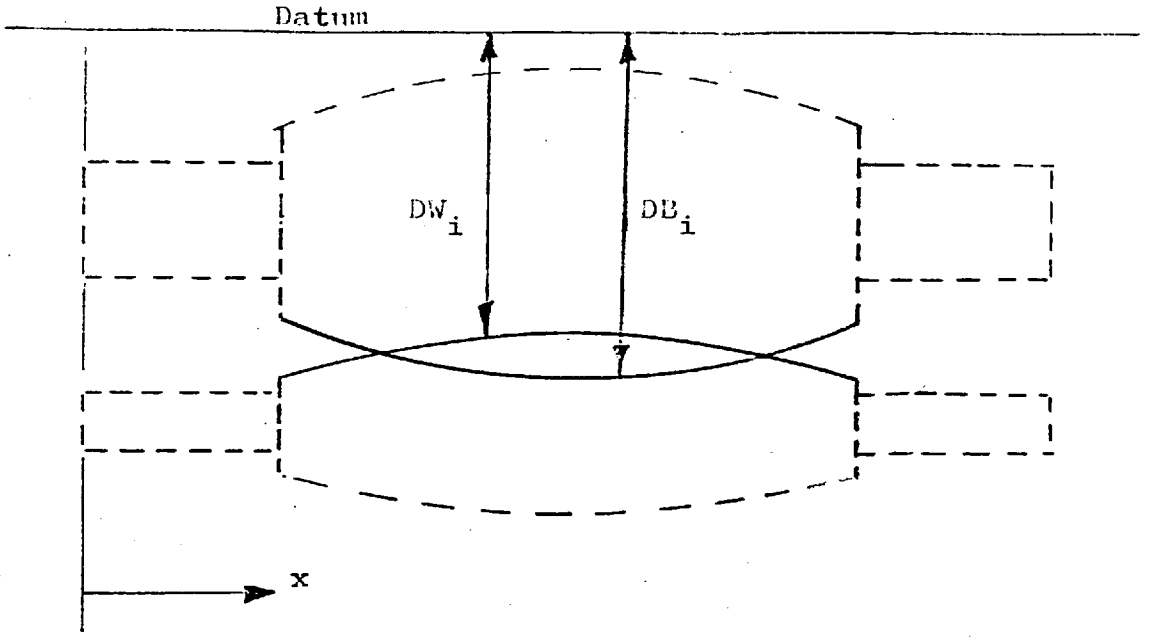

Figure 8. Work Roll/Backup Roll Deformation.

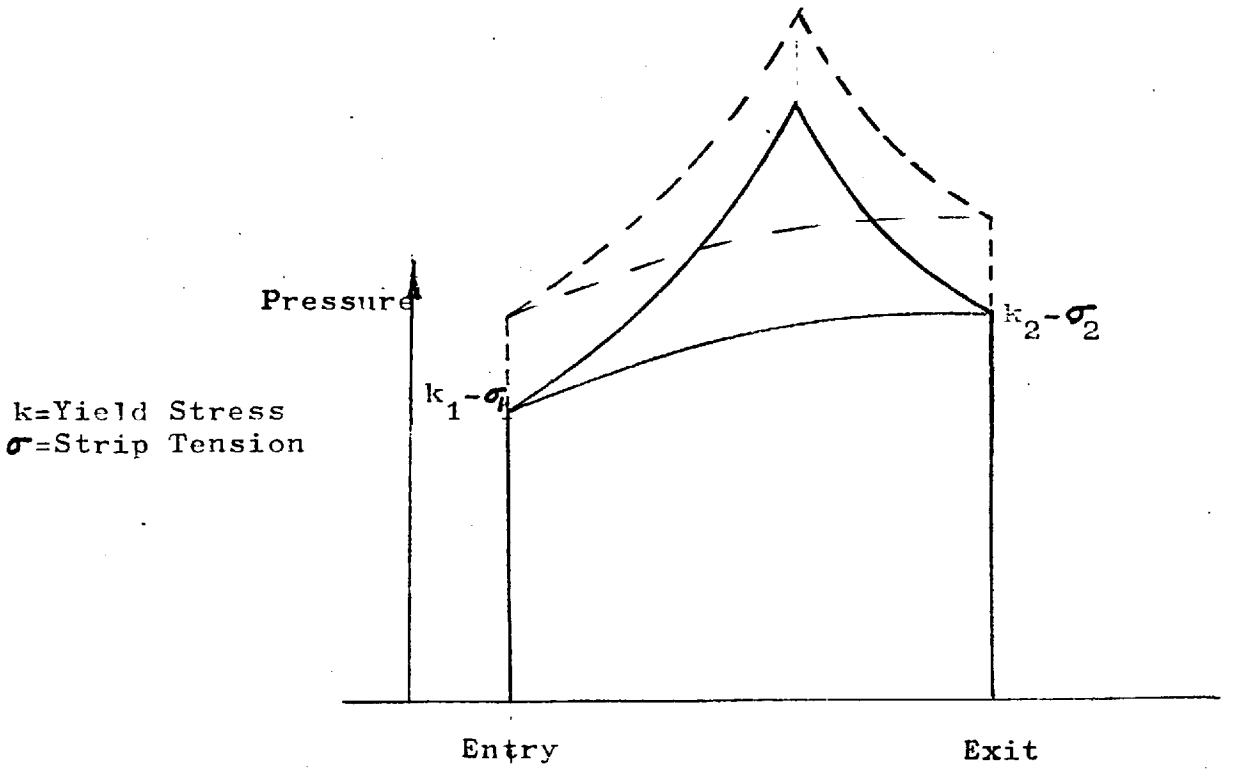

Figure 9. Pressure Variation Through The Roll Gap.

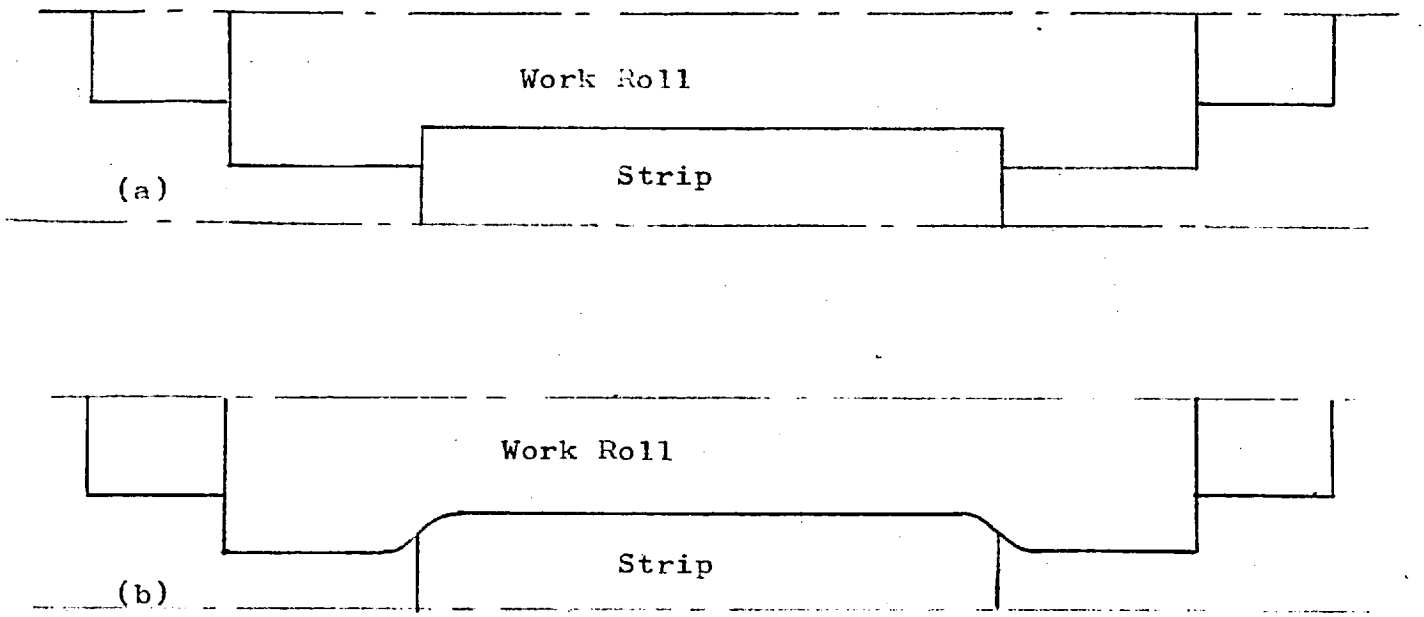

Figure 10. Work Roll Flattening.

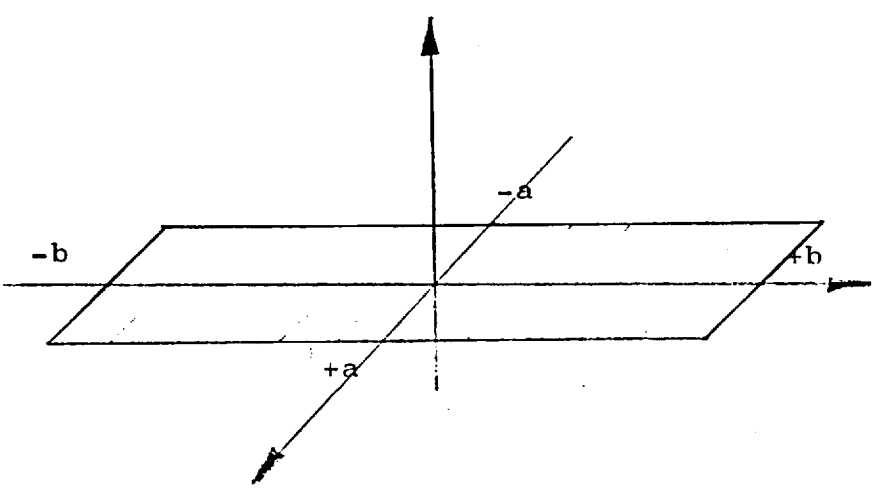

Figure 11. Band of Pressure on Semi-Infinite Solid.

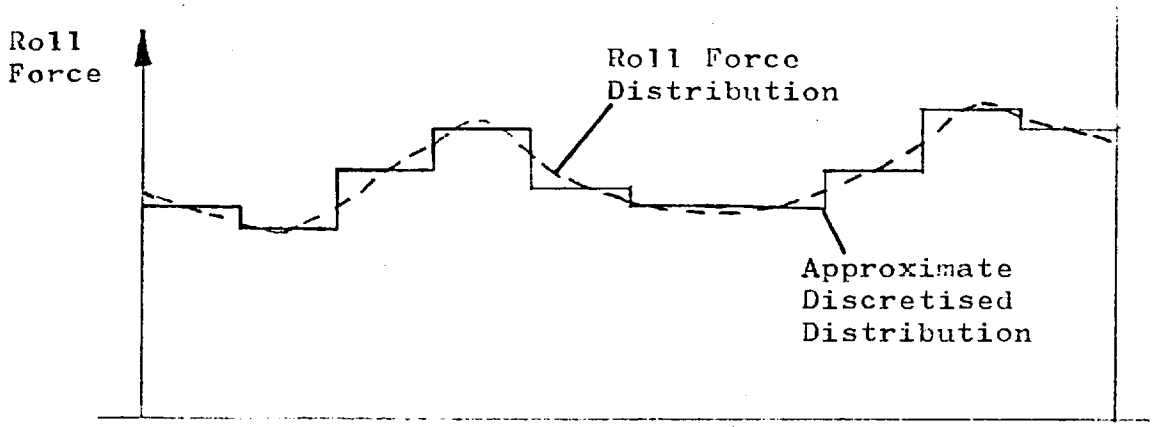

Figure 12. Approximate Discretised Roll Force Distribution.

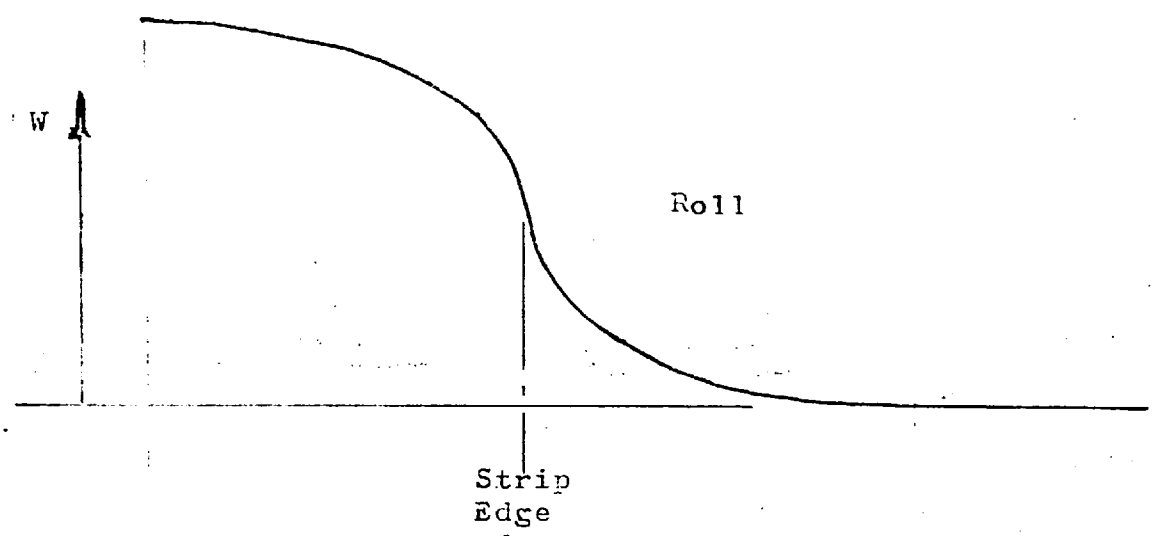

Figure 13. Indentation of Roll by a Uniform Pressure

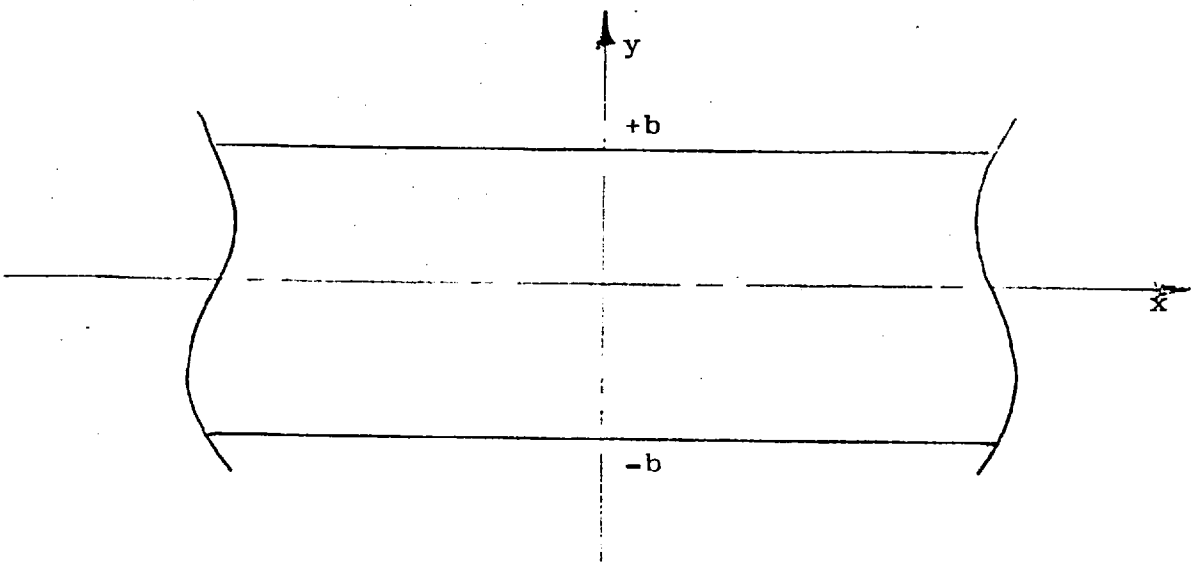

Figure 14. Strip Between Stands.

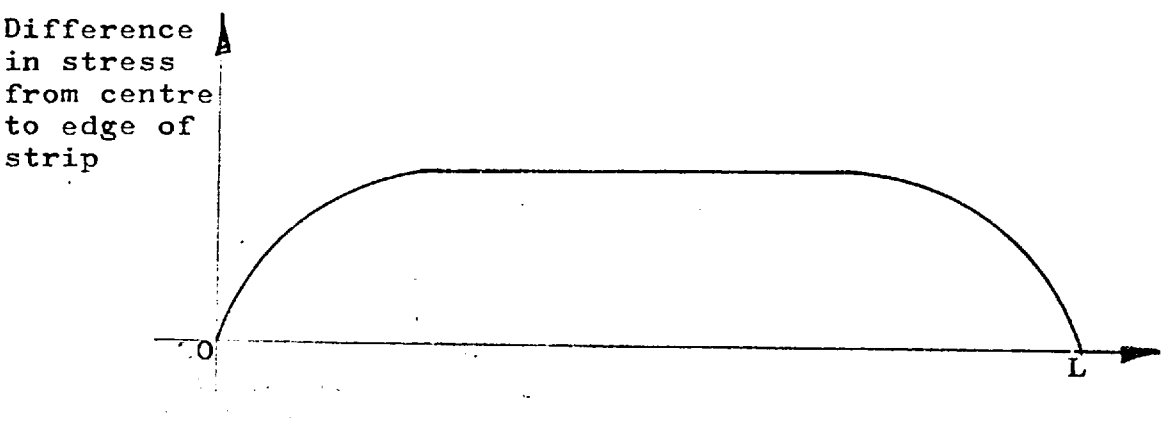

Figure 15. Longitudinal Variation of Transverse Stress Distribution.

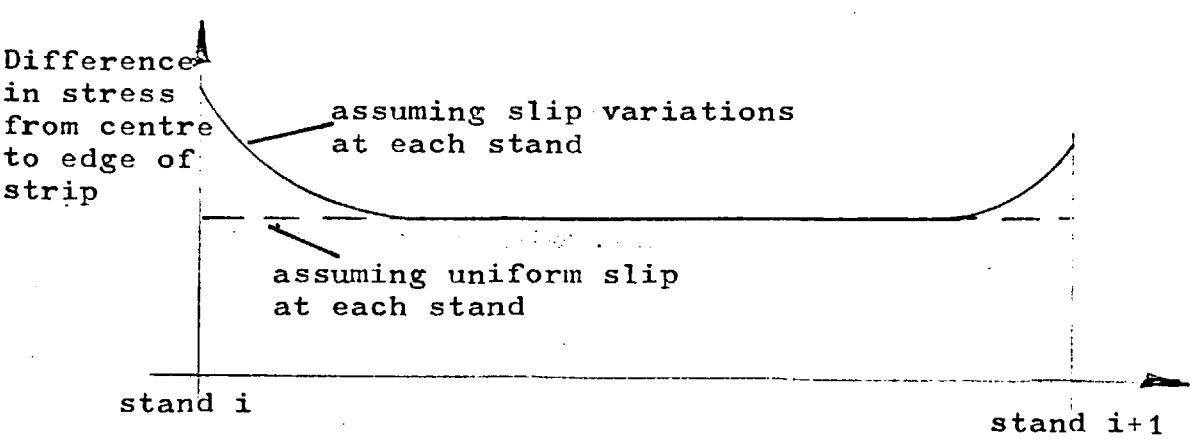

Figure 16. Effect of Slip Variations on the Strip Between Stands.

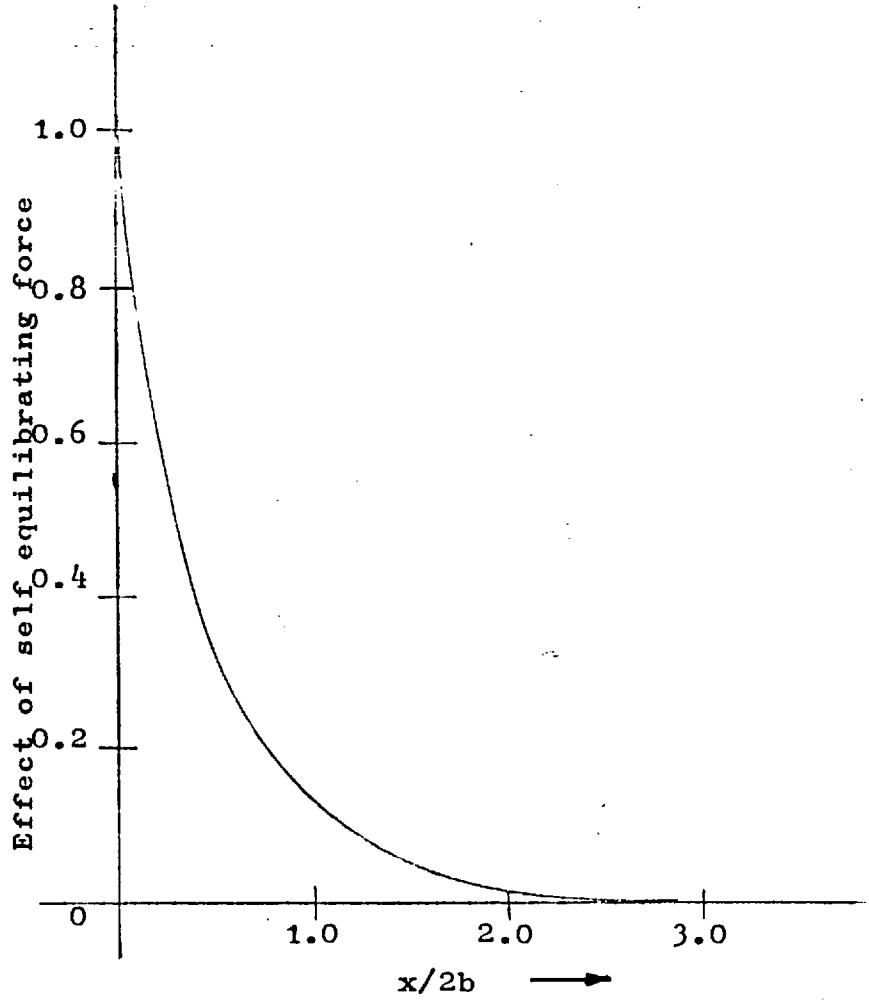

Figure 17. Graph of Decay of Stress due to a Self Equilibrating End Load

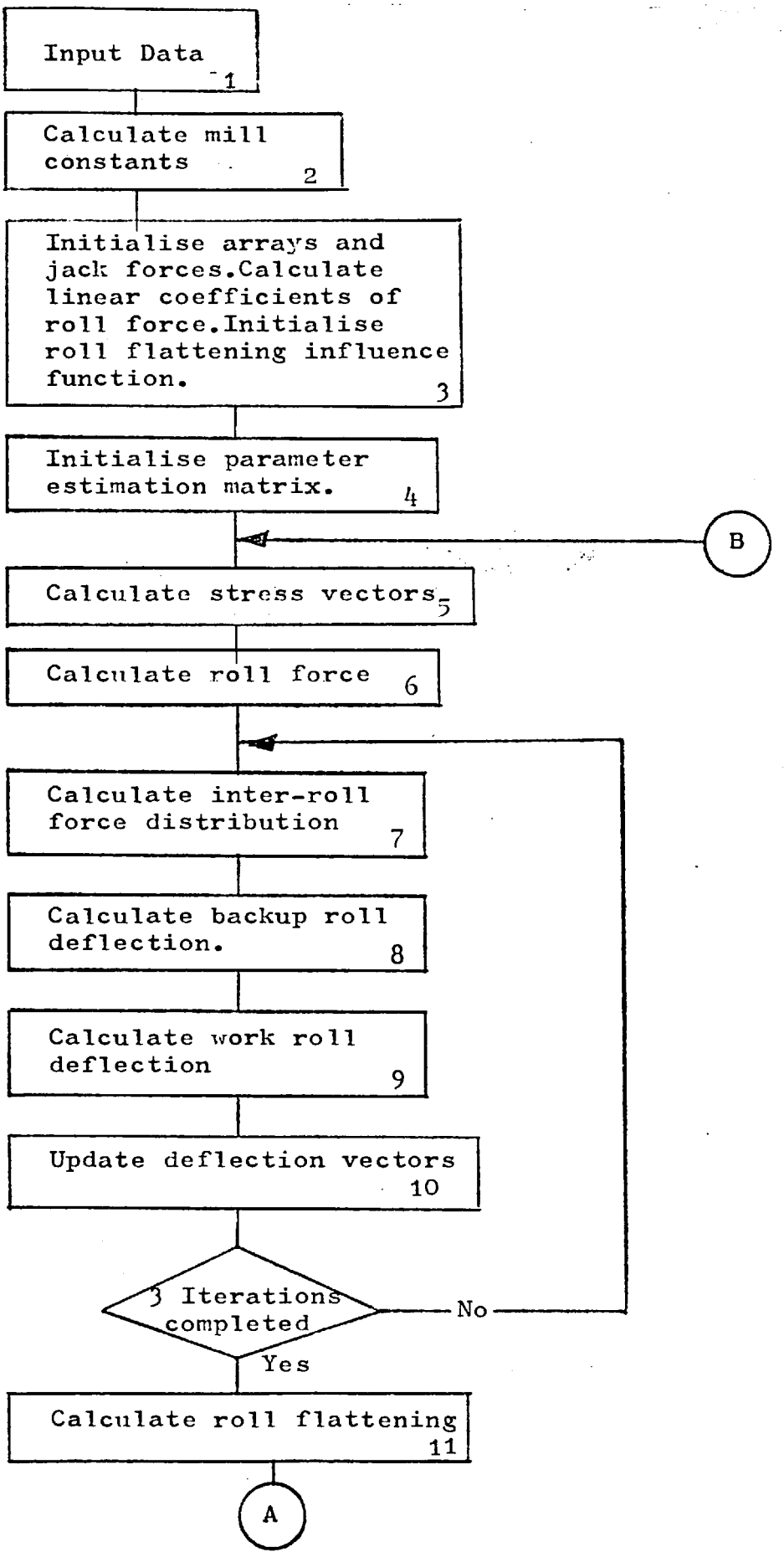

Figure 18a. Flow Diagram of Shape Simulation.

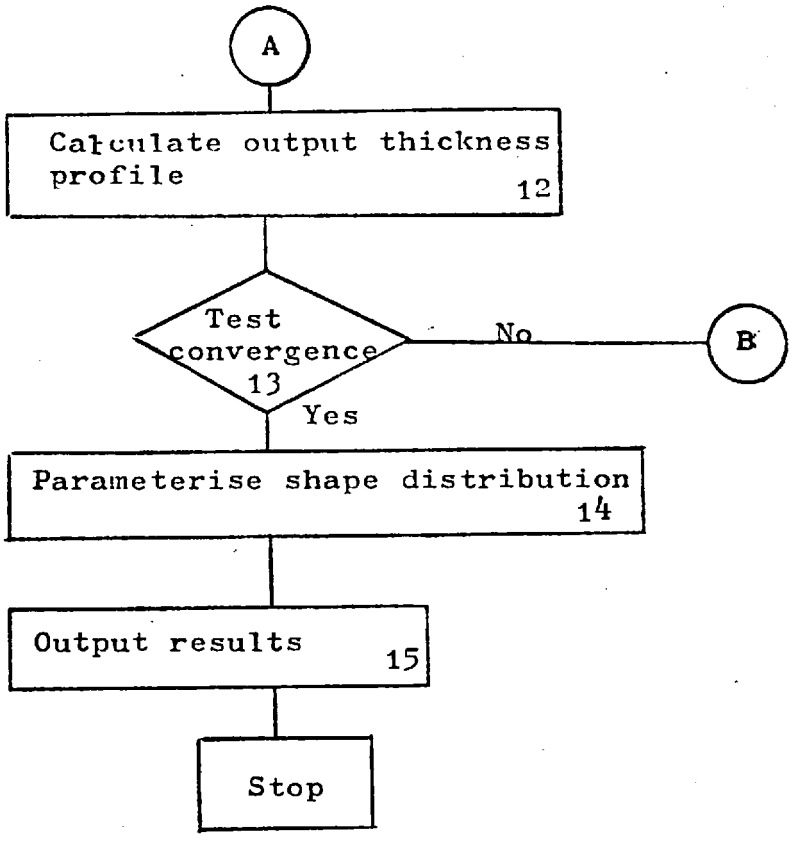

Figure 18b. Flow Diagram of Shape Simulation.

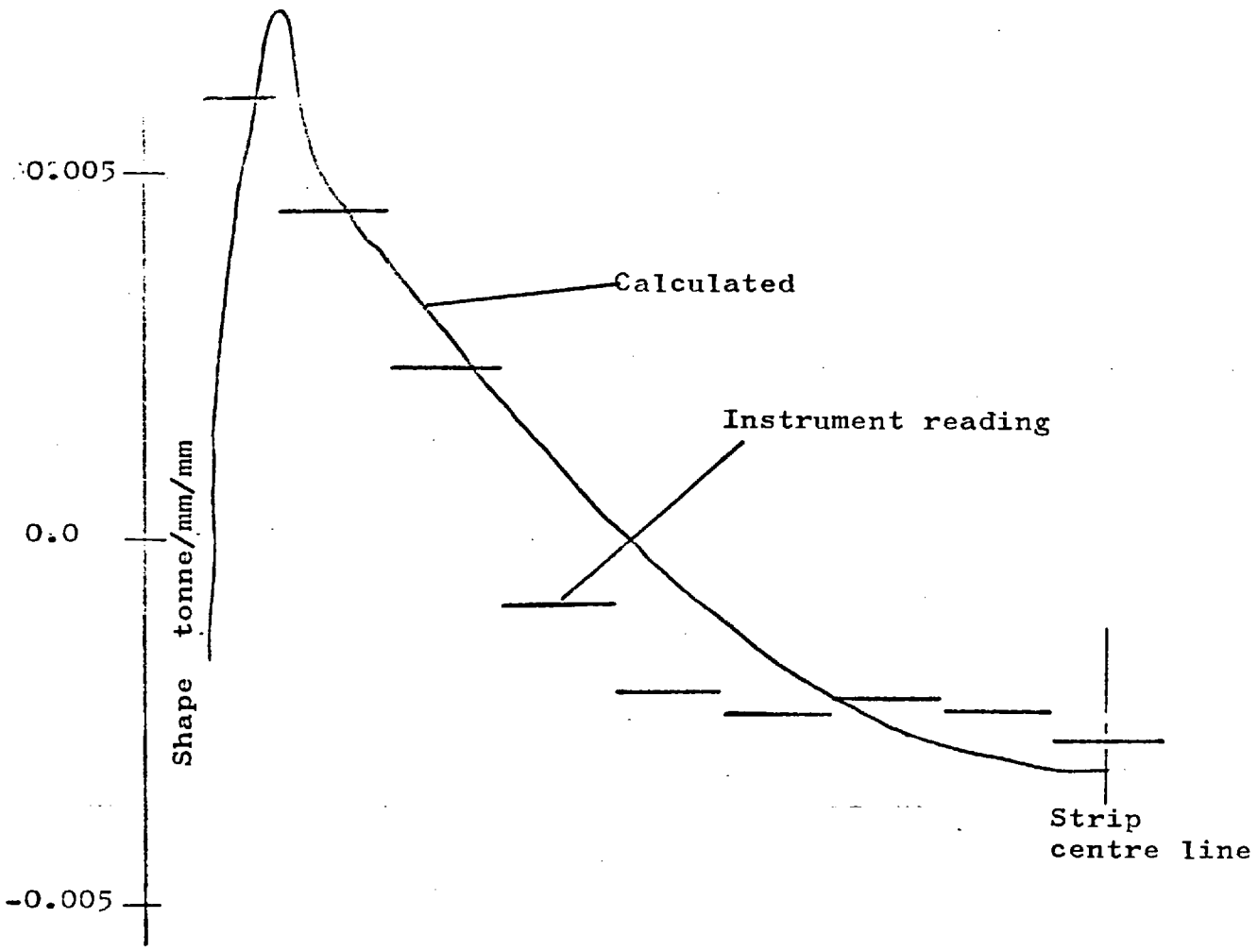

Figure 19a. Comparison of Calculated and Measured Shape , Jack Force=3 tonnes.

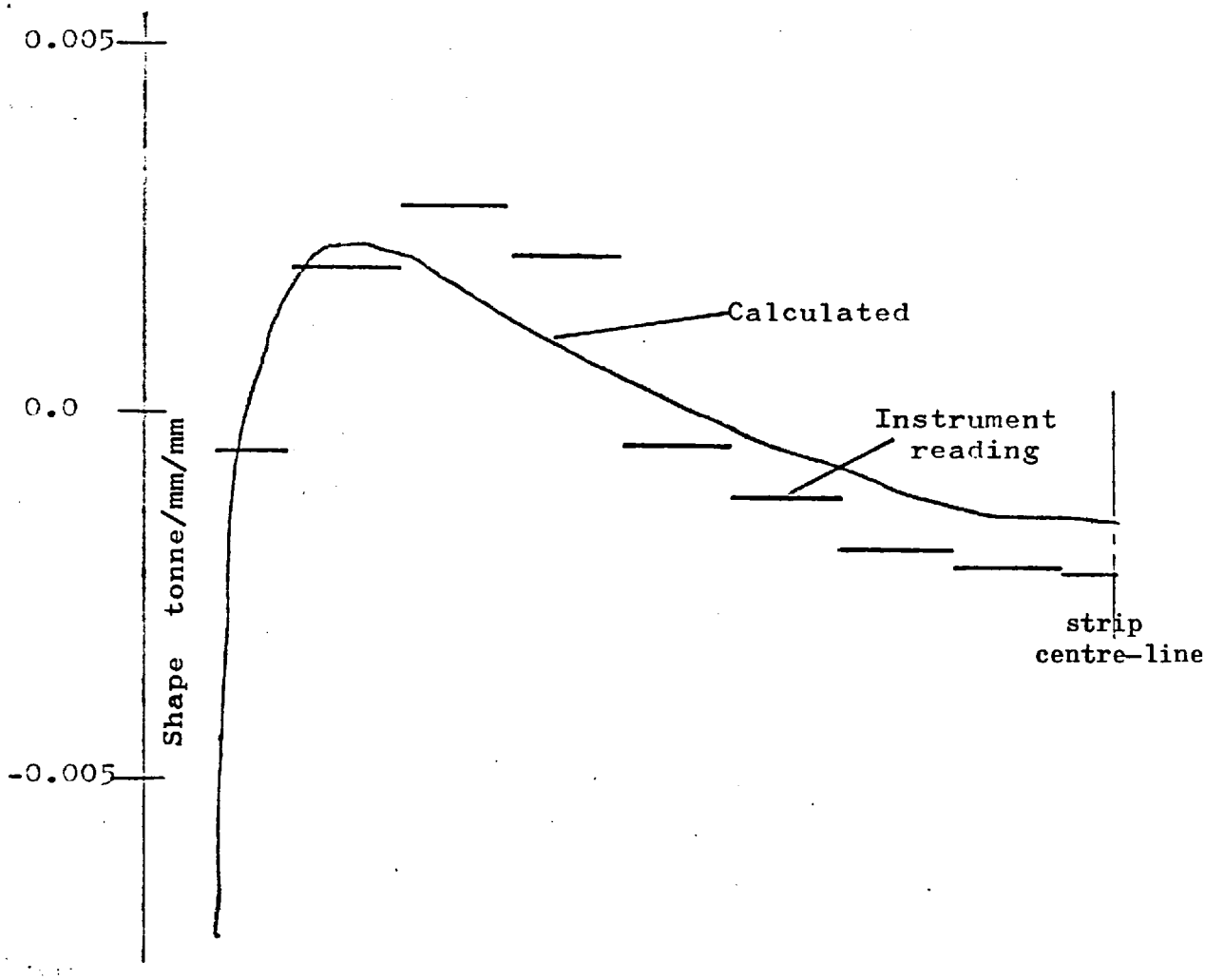

Figure 19b. Comparison of Calculated and Measured Shape , Jack Force=30 tonnes.

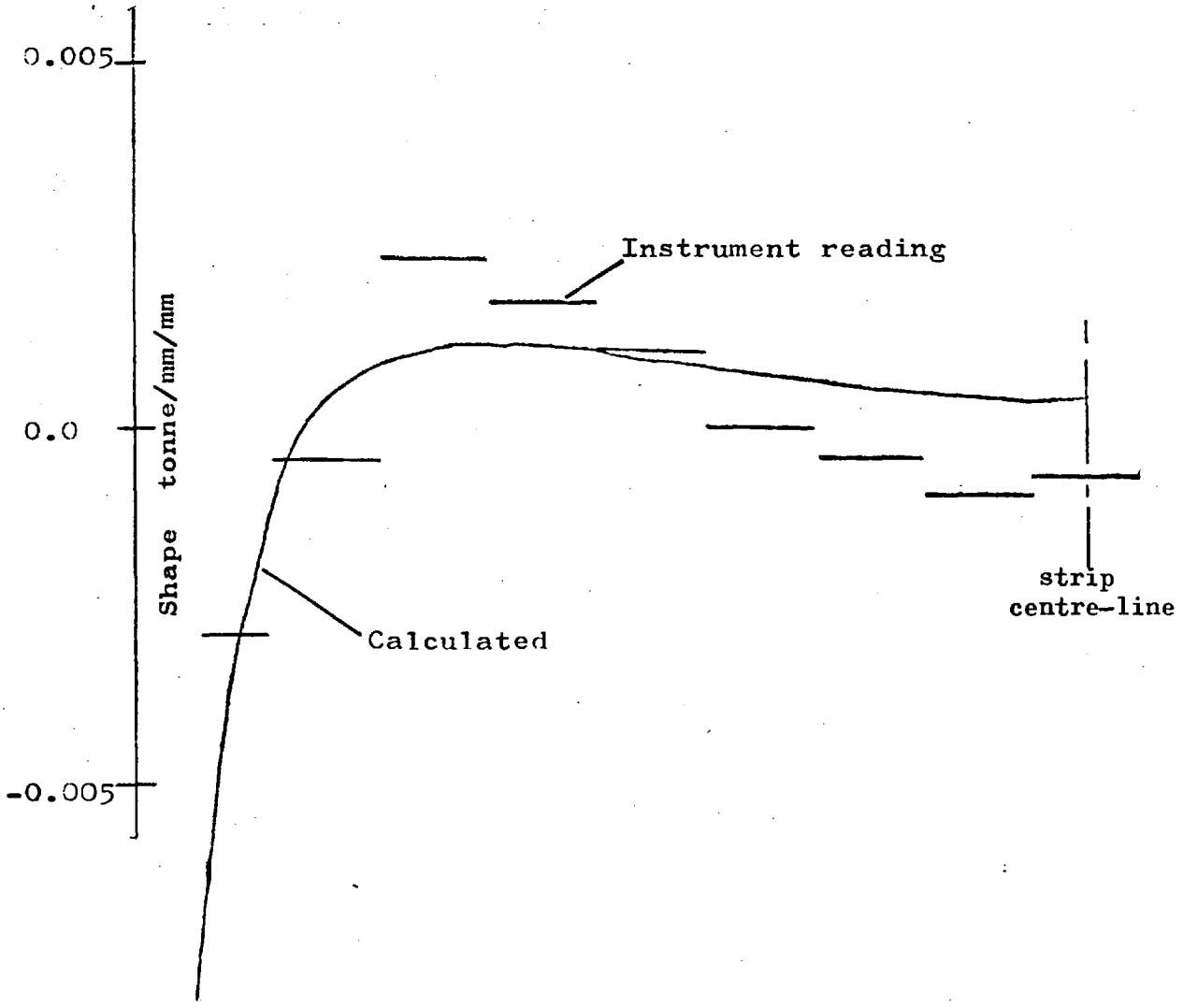

Figure 19c. Comparison of Calculated and Measured Shape , Jack Force=54 tonnes.

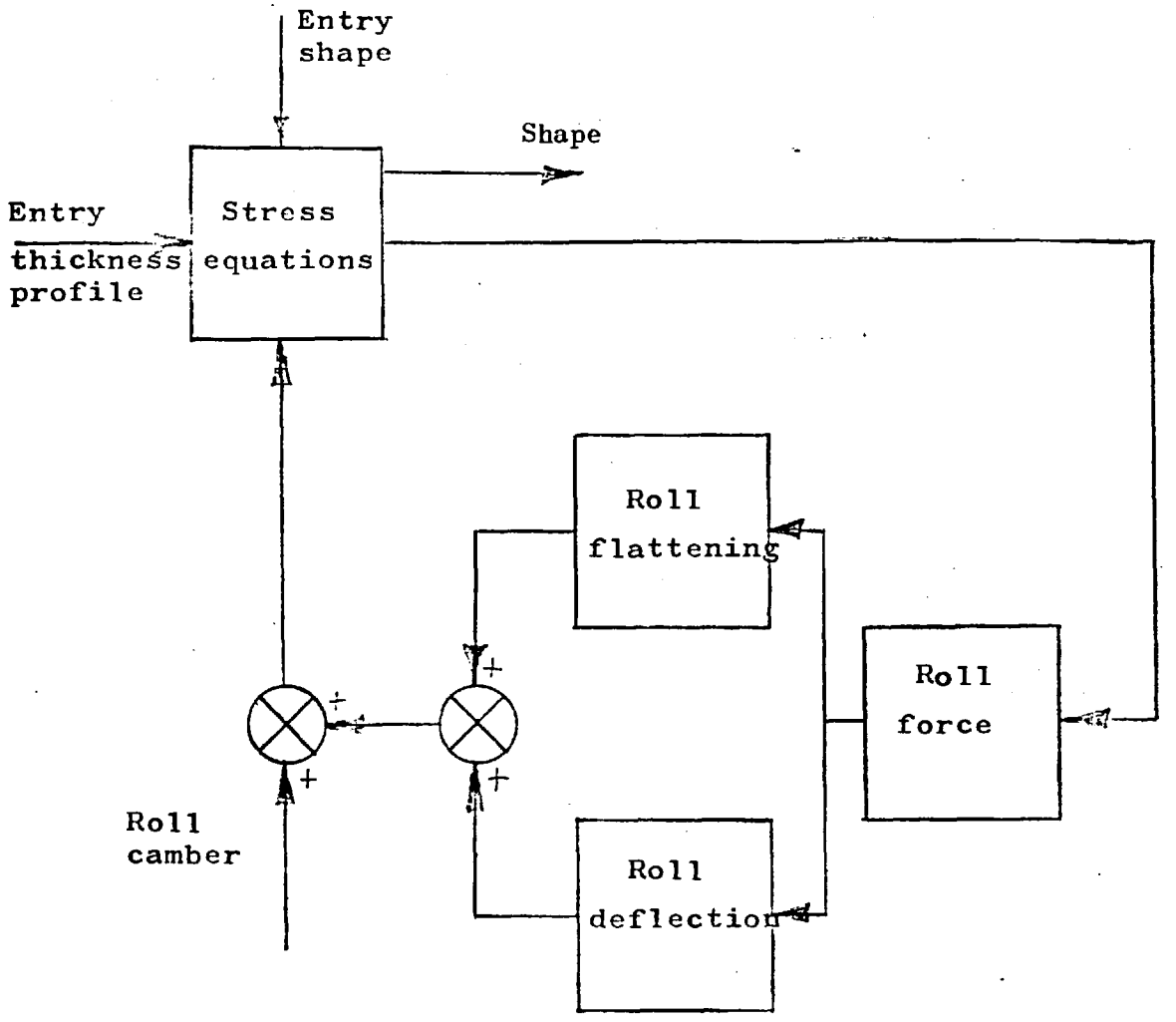

Figure 20. Block Diagram of the Simple Shape Model.

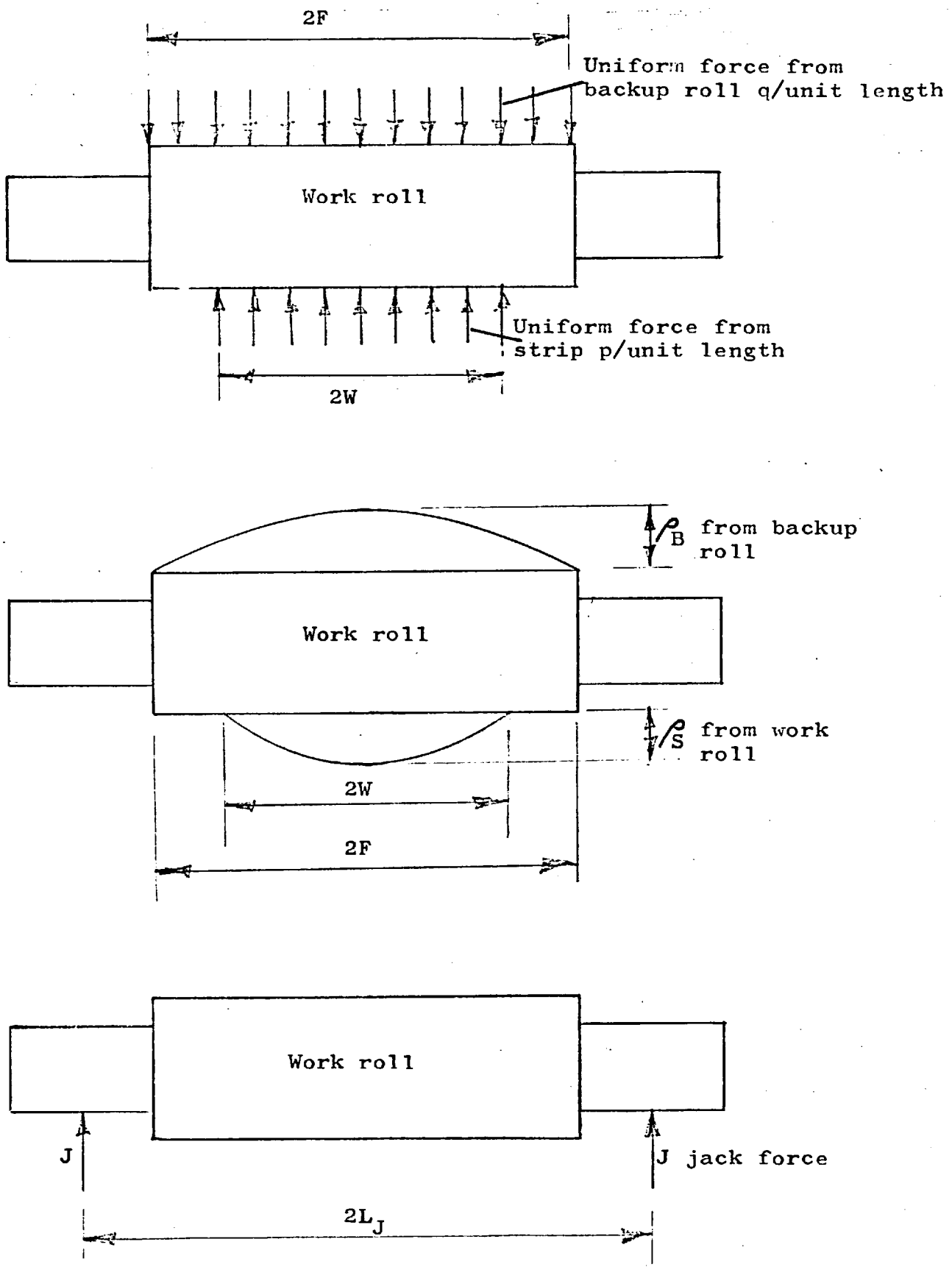

Figure 21. Forces Acting on the Work Roll.

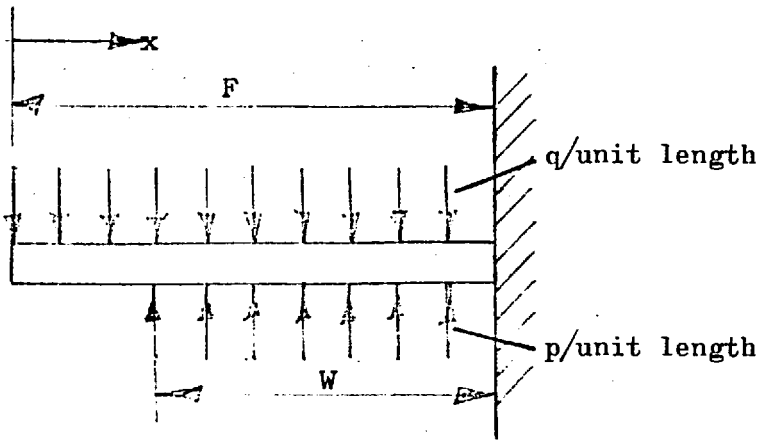

a) Equivalent Cantelever Subjected to Uniform Loading.

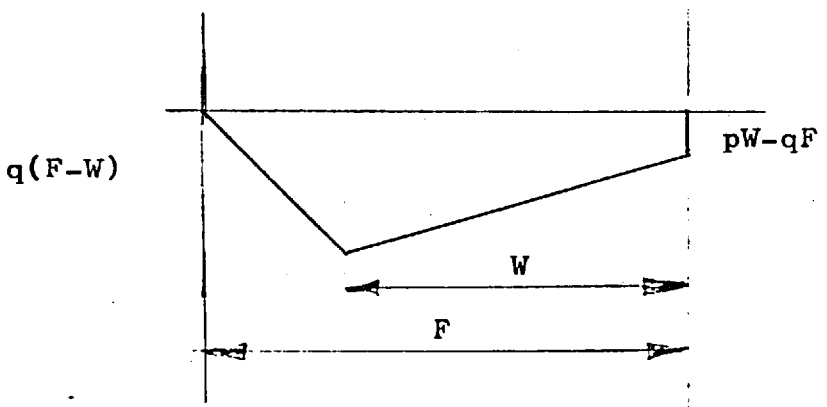

b) Shear Force Diagram.

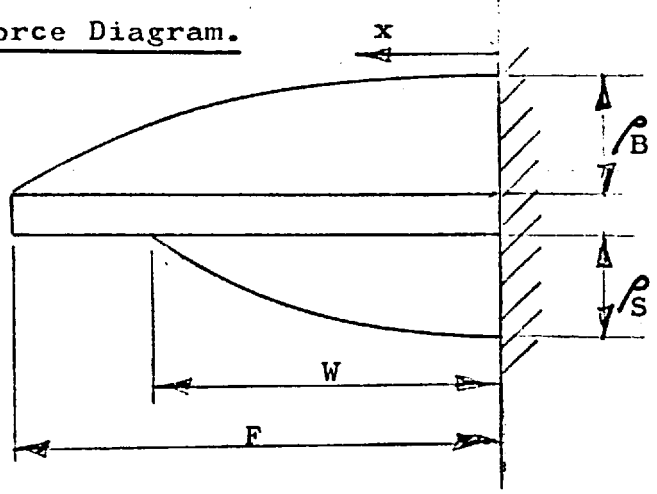

c) Equivalent Cantelever Subjected to Parabolic Loading.

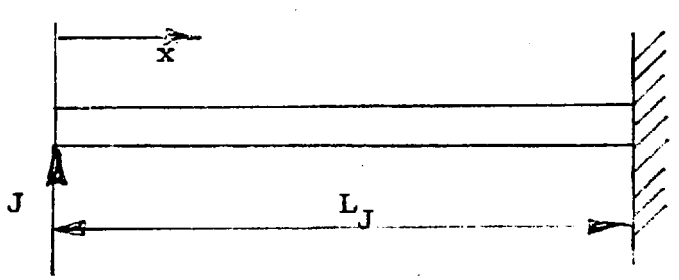

d) Equivalent Cantelever Subjected to Jack Loading.

Figure 22.

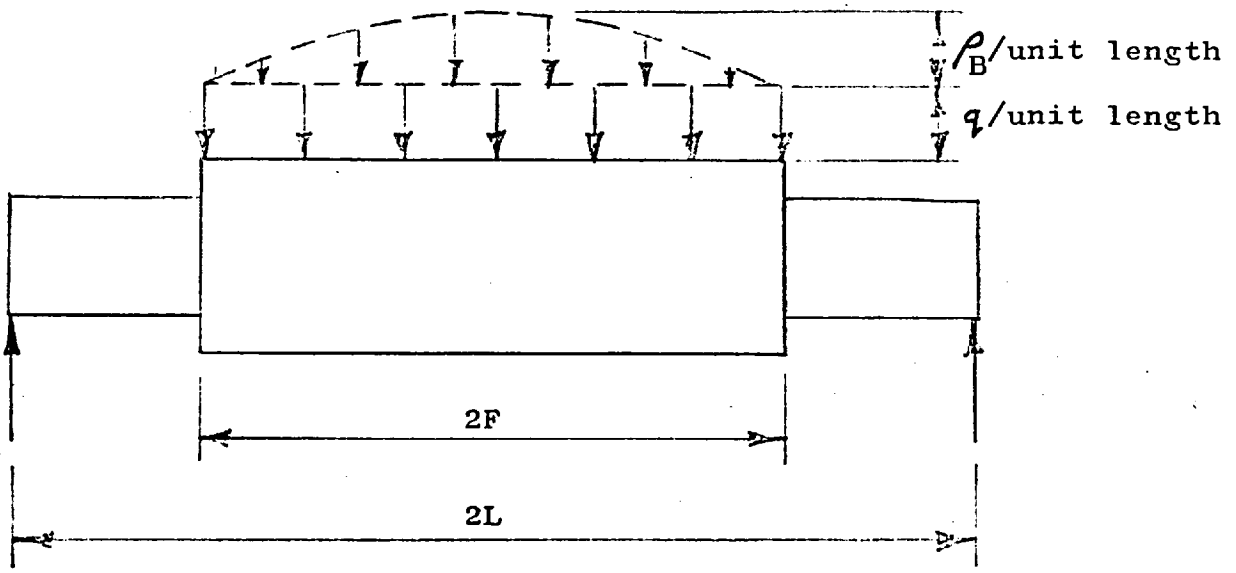

Figure 23. Loading on the Backup Roll.

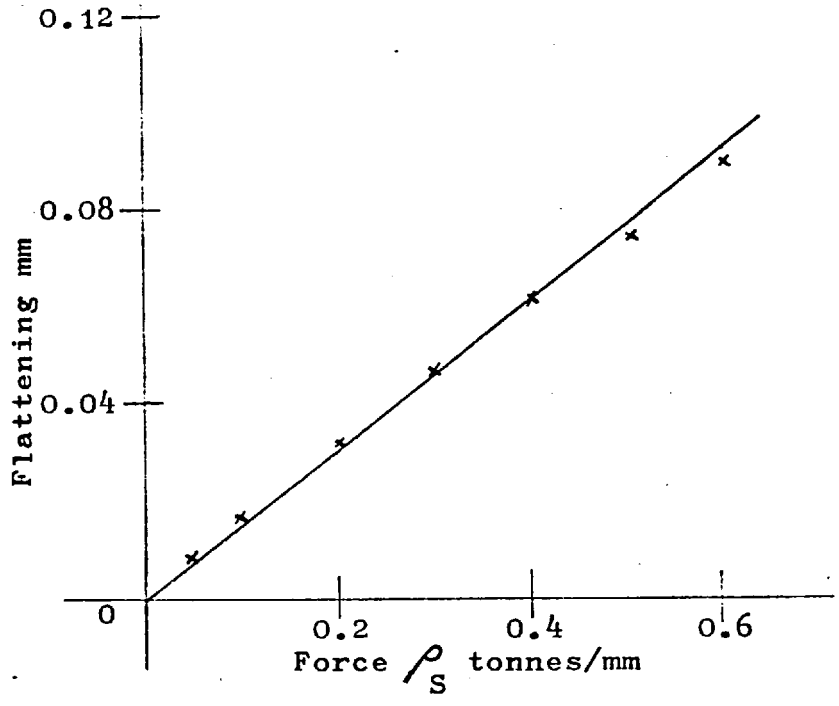

Figure 24a: Graph of Flattening Between Two Cylinders against Force.

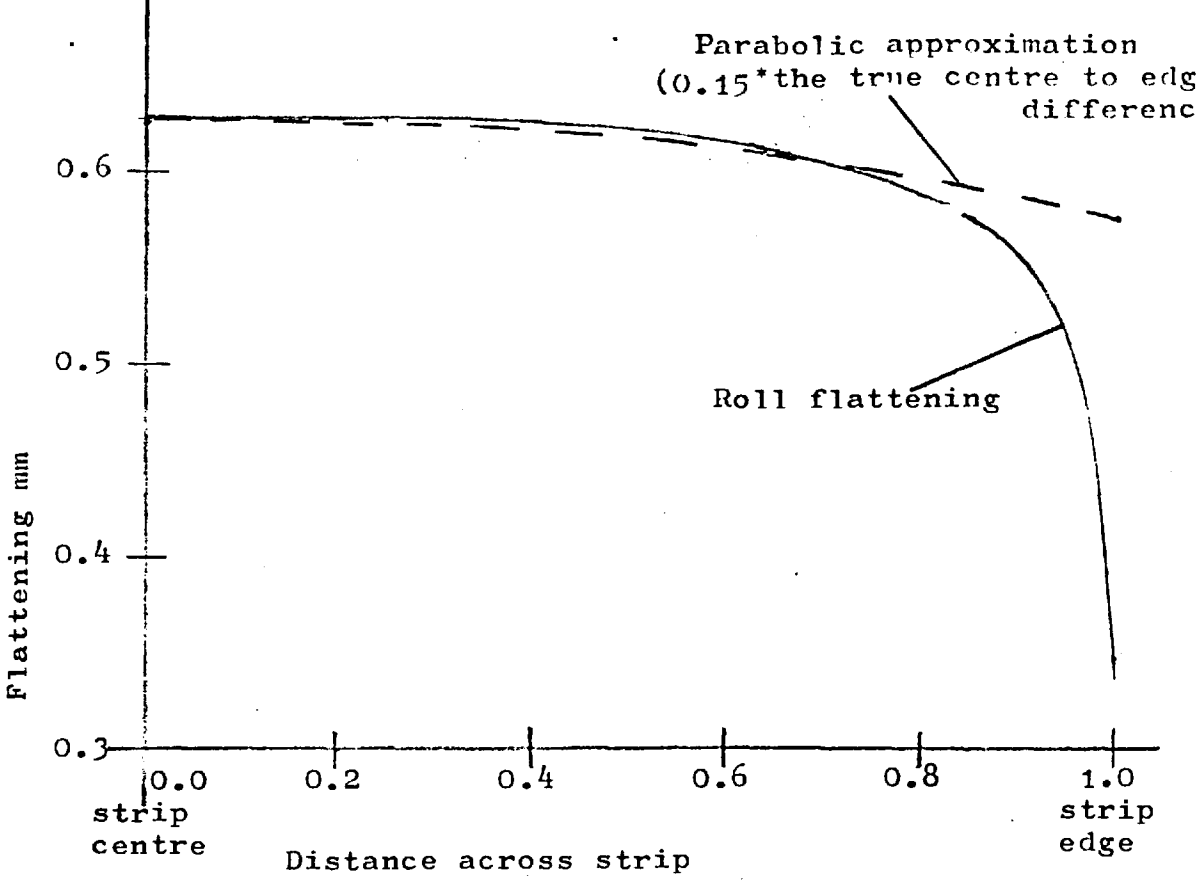

Figure 24b. Parabolic Approximation to the Work Roll Flattening.

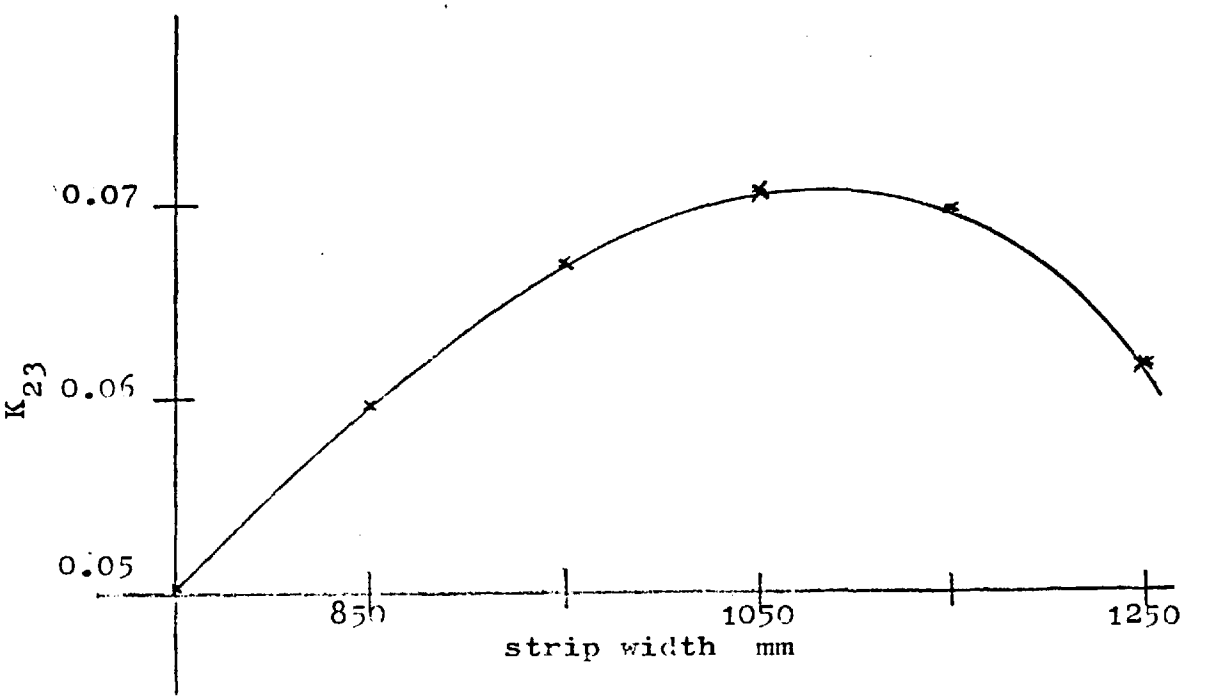

Figure 25a. Graph of K_{23} against Width.

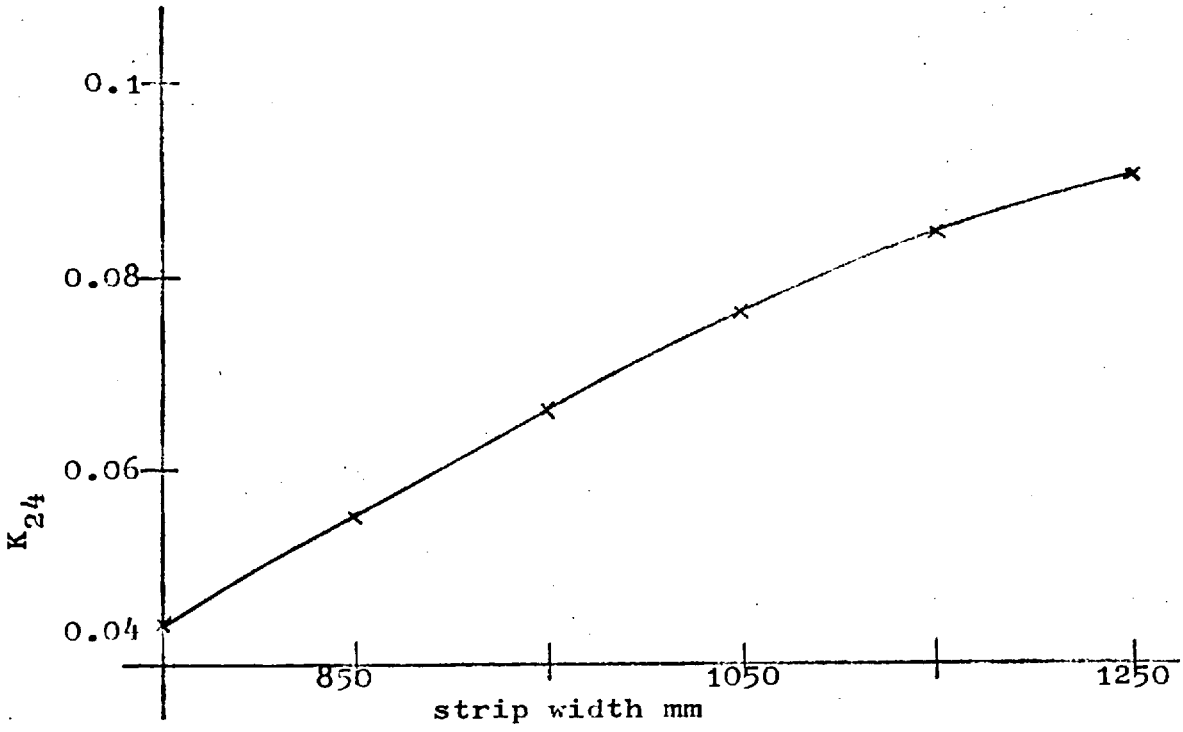

Figure 25b. Graph of K_{24} against Strip Width.

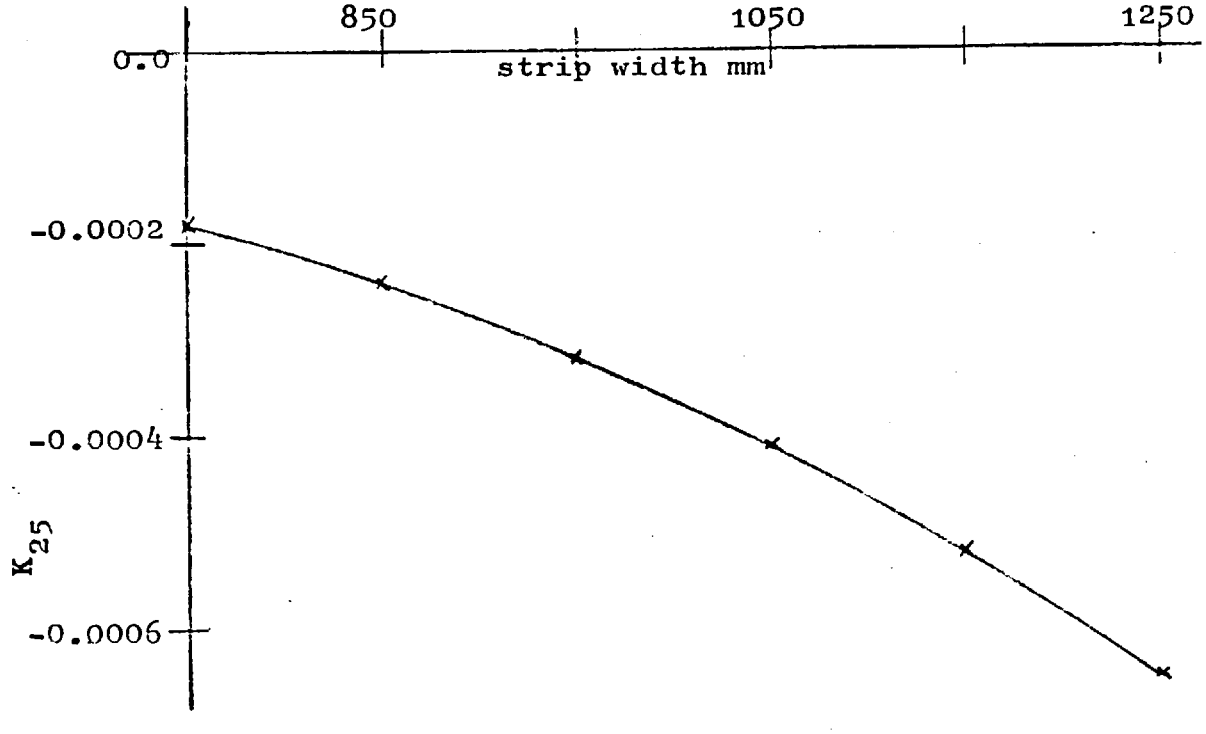

Figure 25c. Graph of K_{25} against Strip Width.

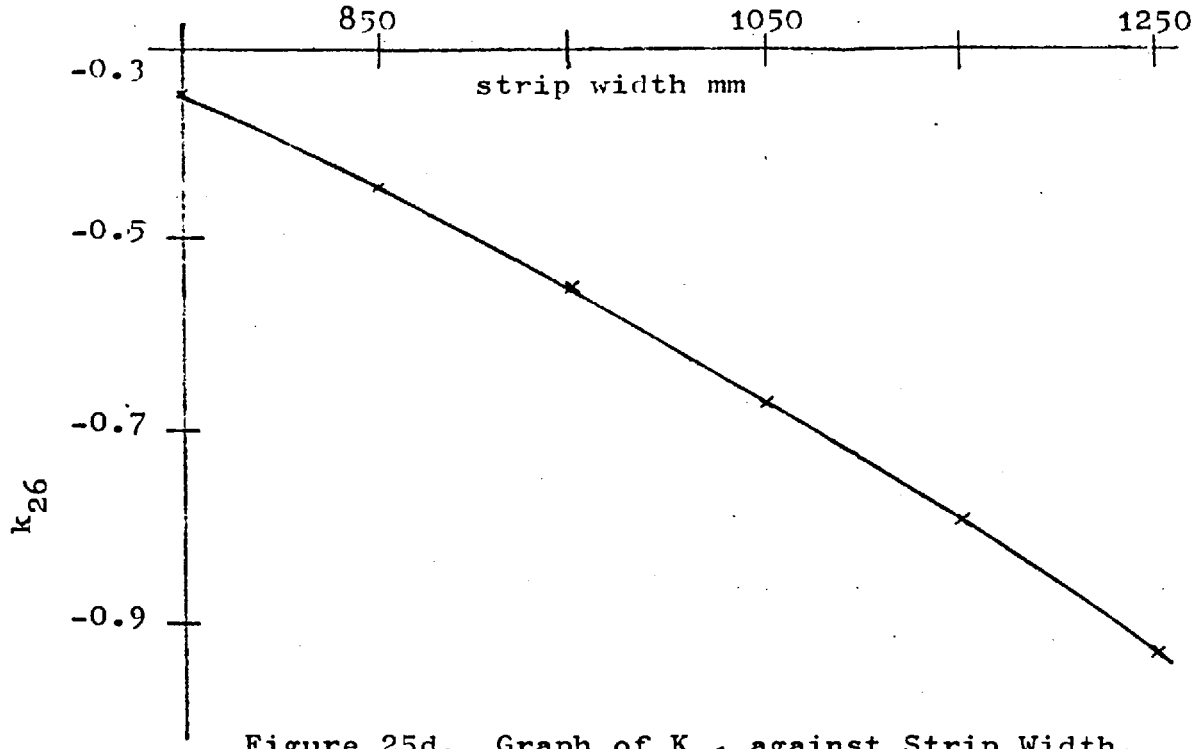

Figure 25d. Graph of K_{26} against Strip Width.

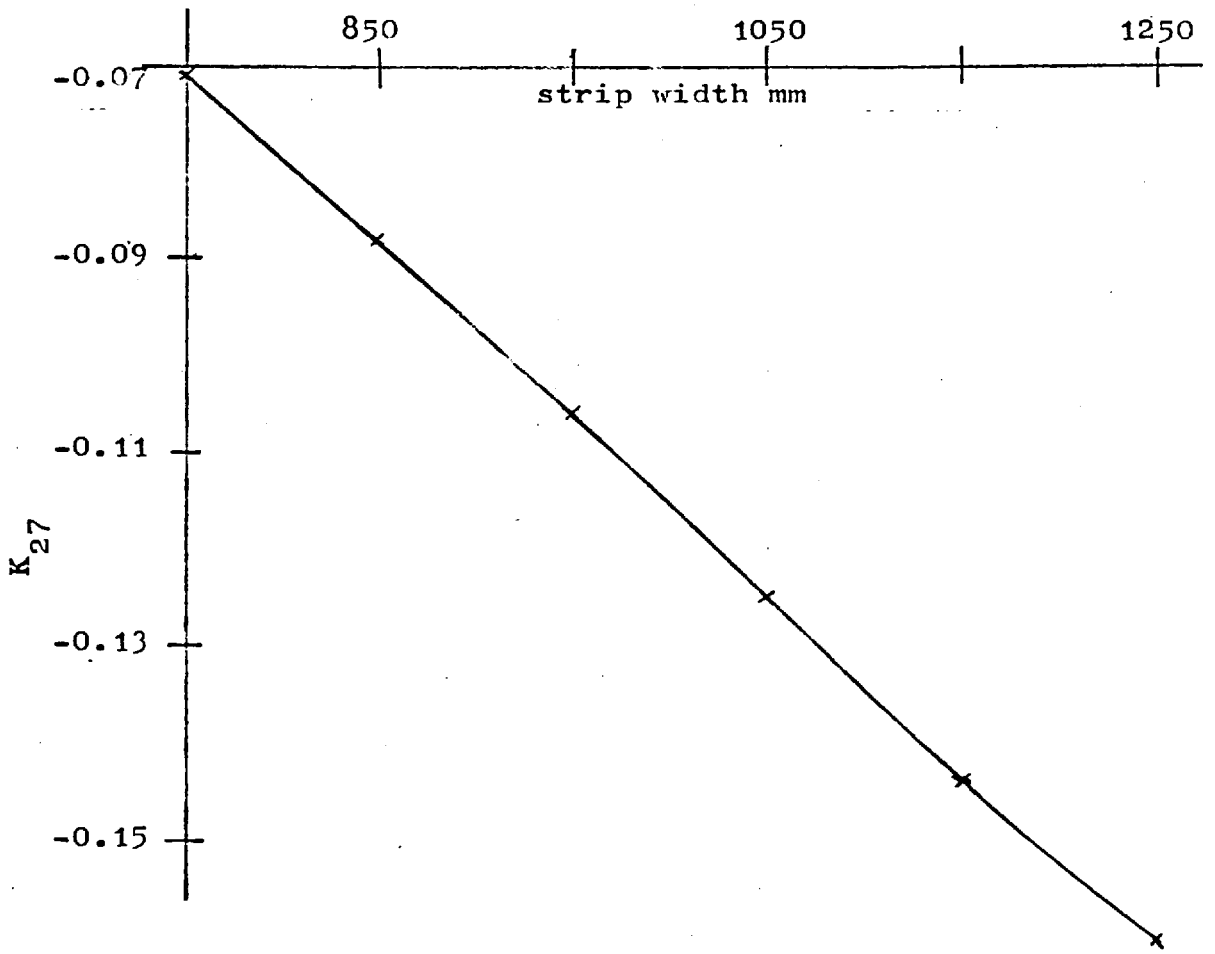

Figure 25e. Graph of K_{27} against Strip Width.

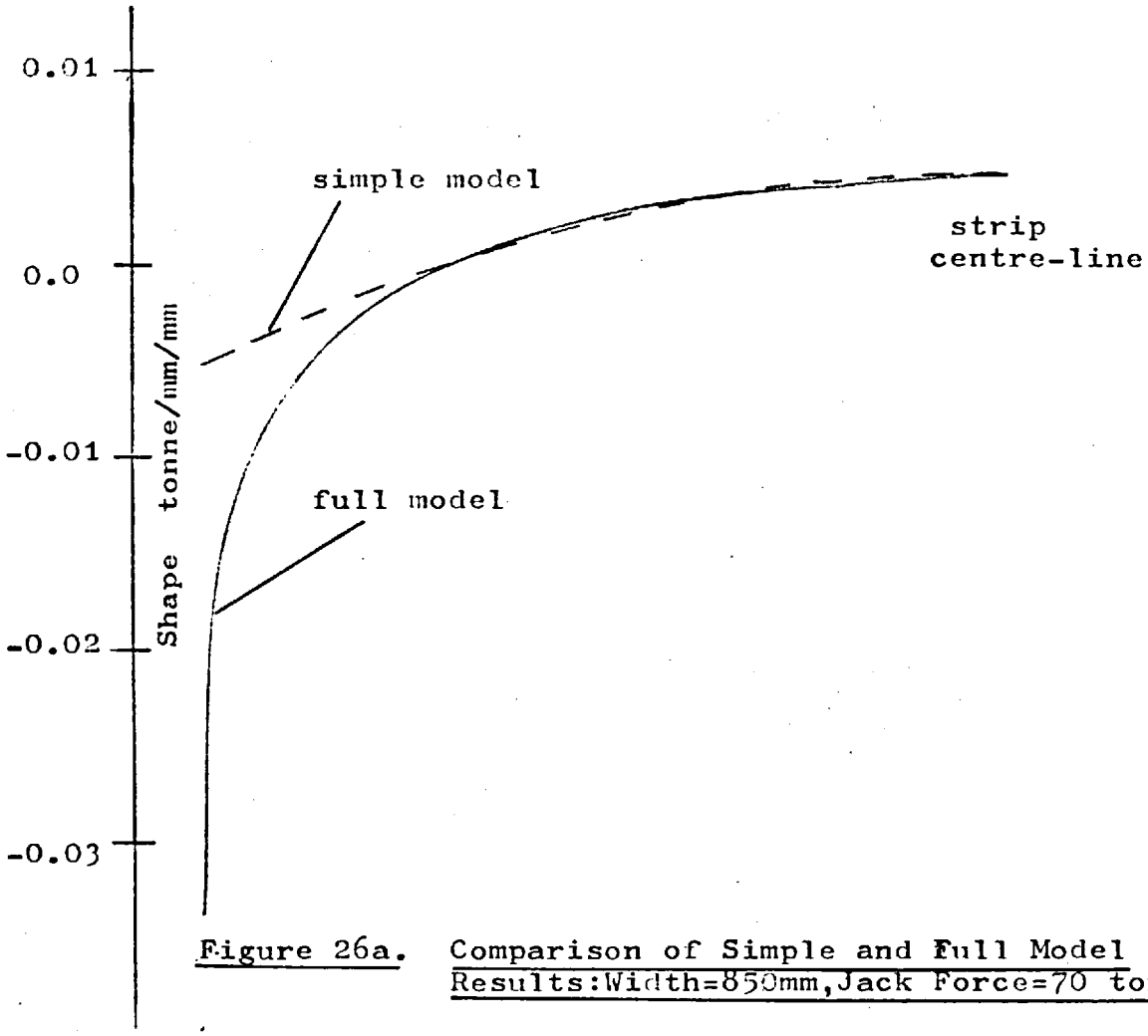

Figure 26a. Comparison of Simple and Full Model Results:Width=850mm,Jack Force=70 tonnes.

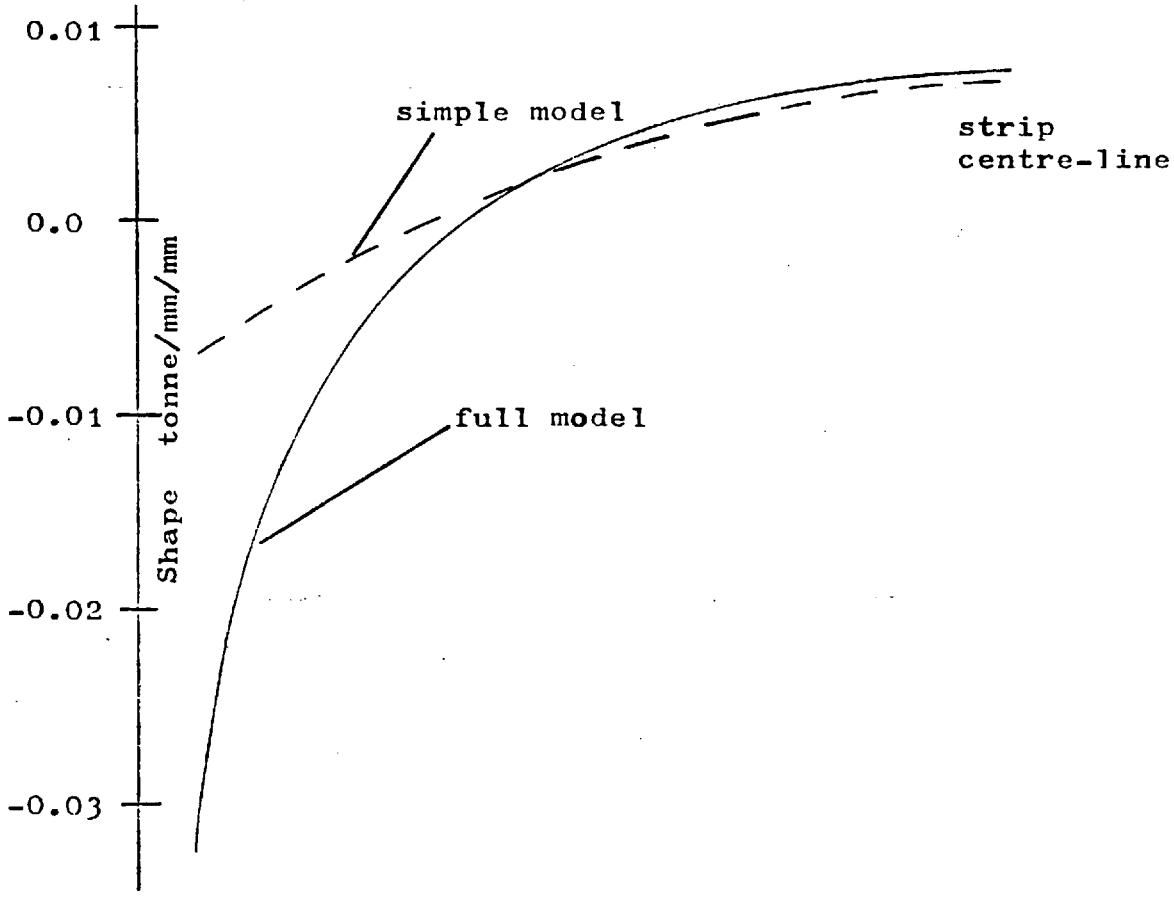

Figure 26b. Comparison of Simple and Full Model Results:Width=850,Jack Force=10 tonnes.

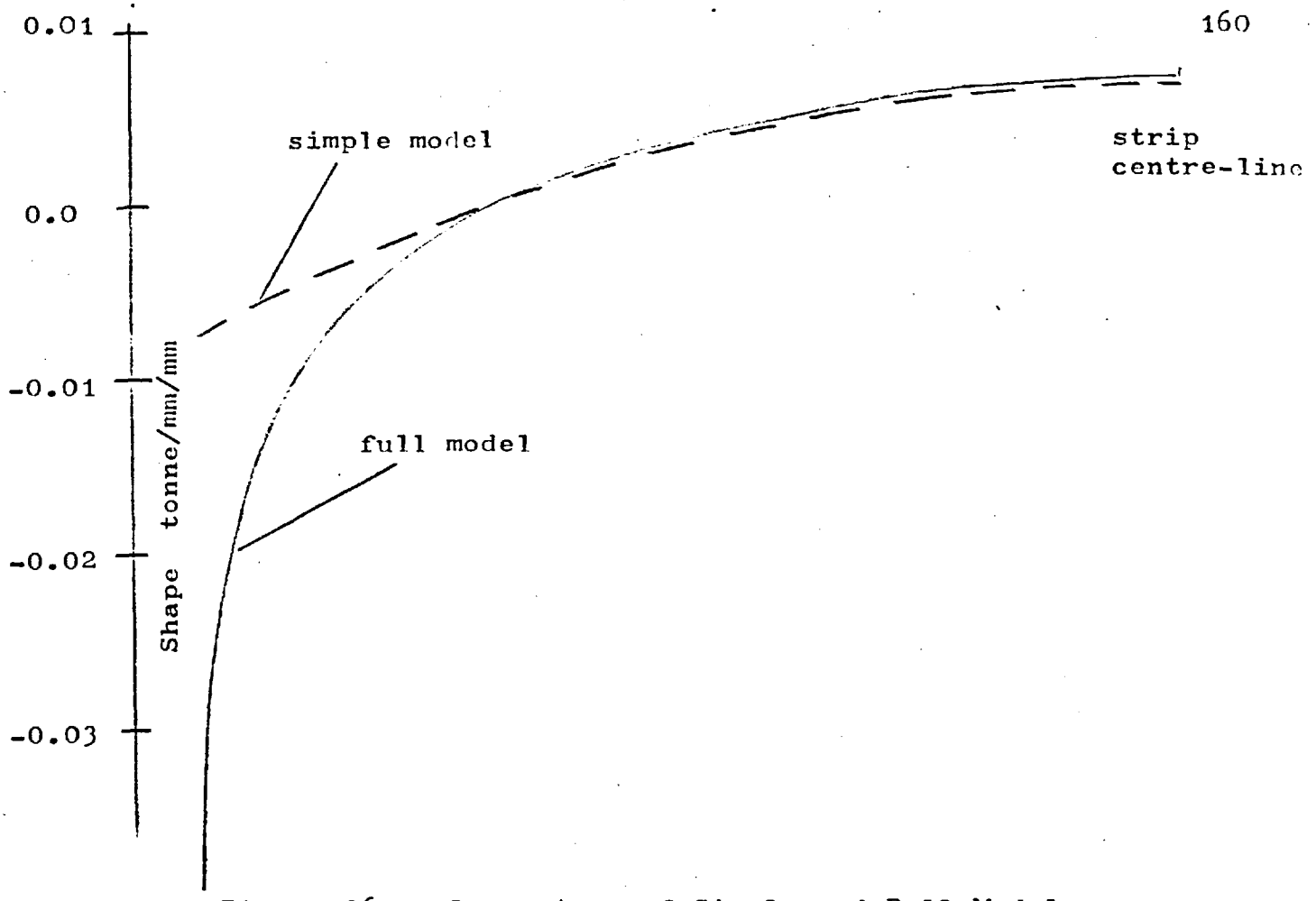

Figure 26c. Comparison of Simple and Full Model Results:Width=1150mm,Jack Force=10 tonnes.

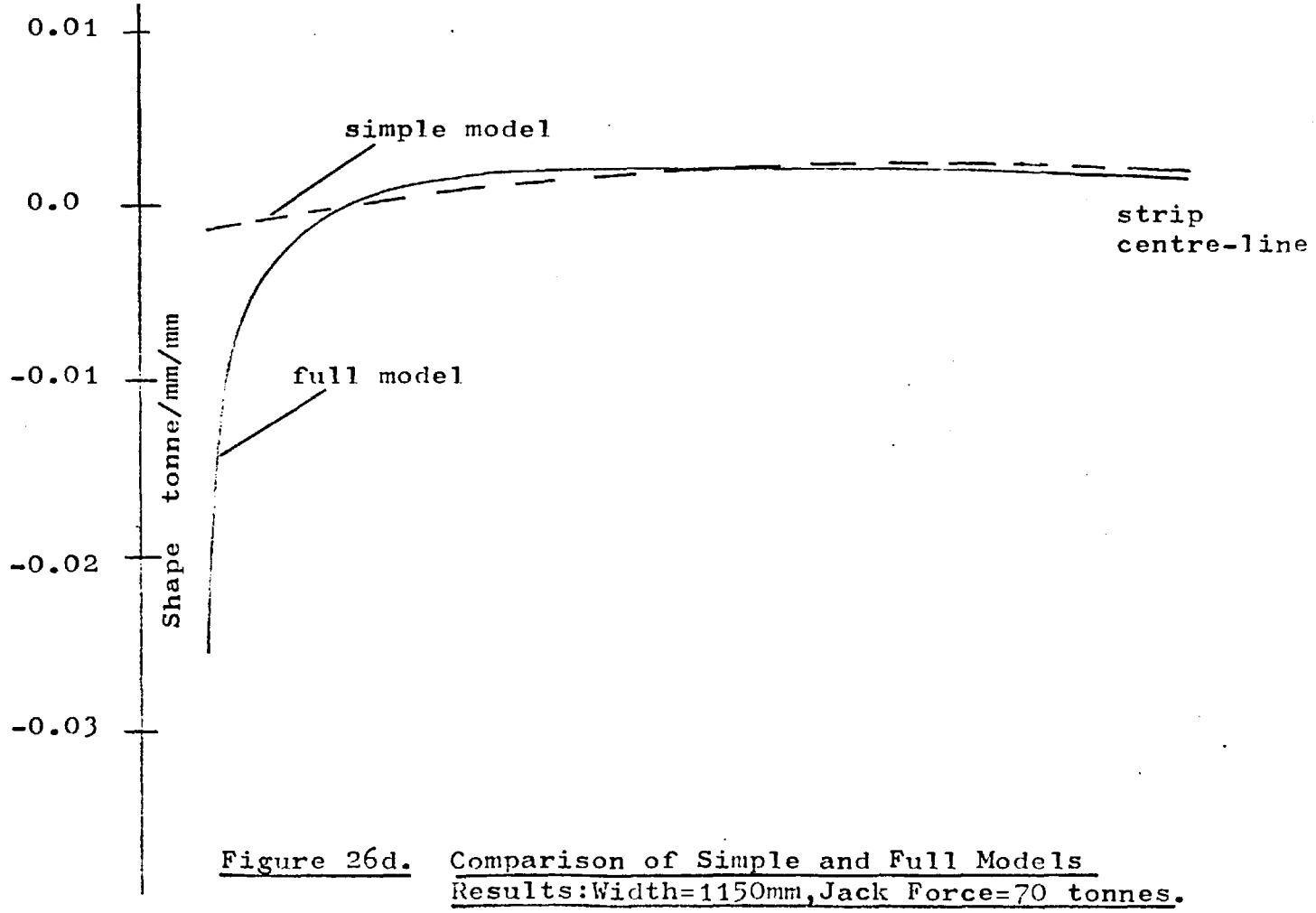

Figure 26d. Comparison of Simple and Full Models Results:Width=1150mm,Jack Force=70 tonnes.

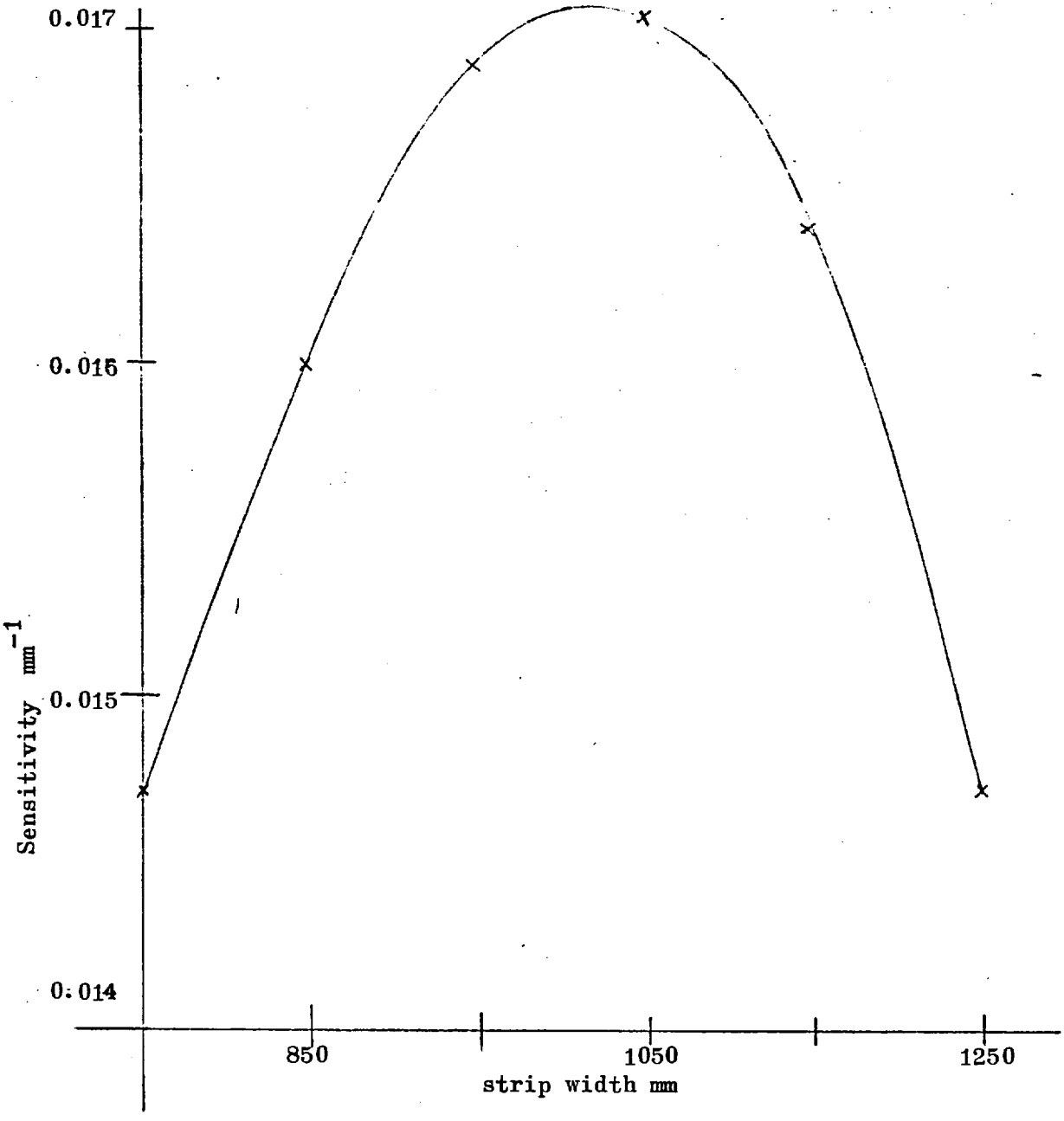

Figure 27. Graph of Sensitivity of Shape to Roll Force against Strip Width.

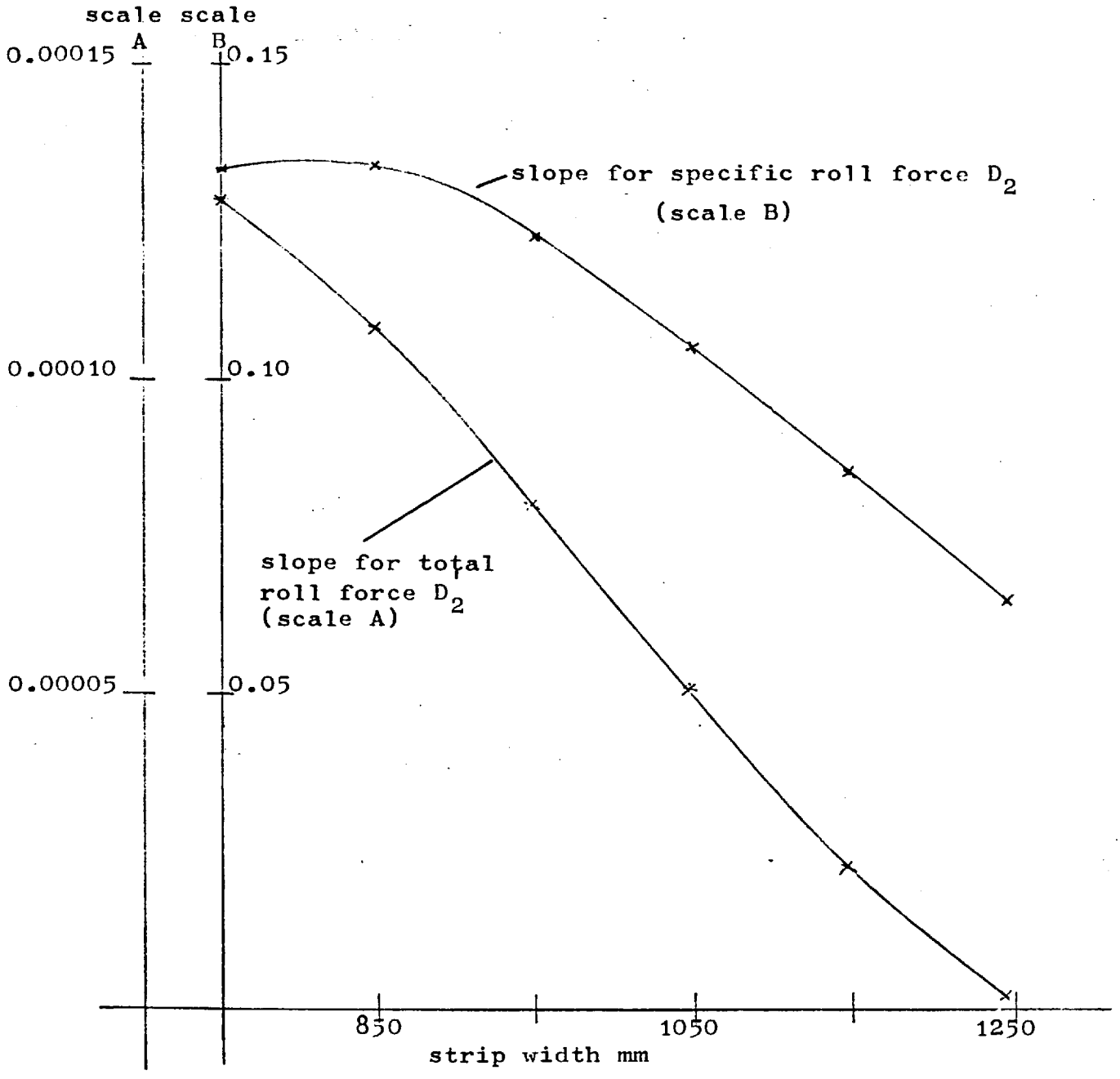

Figure 28. Graph of Slope D_2 against Strip Width.

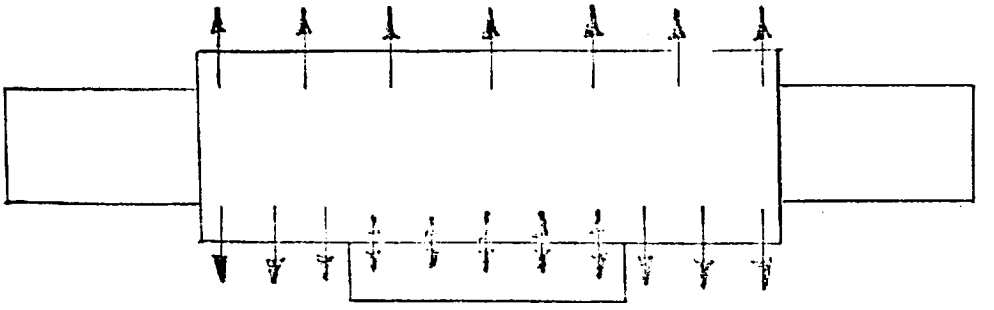

Figure 29. Heat Flow into and out of a Work Roll.

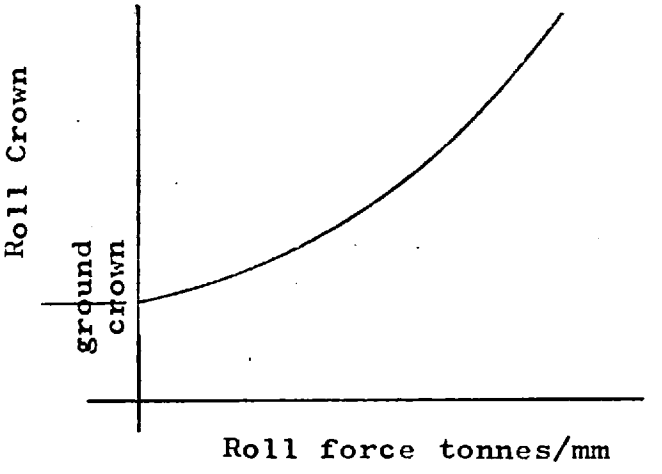

Figure 30. Graph of Roll Crown against Roll Force.

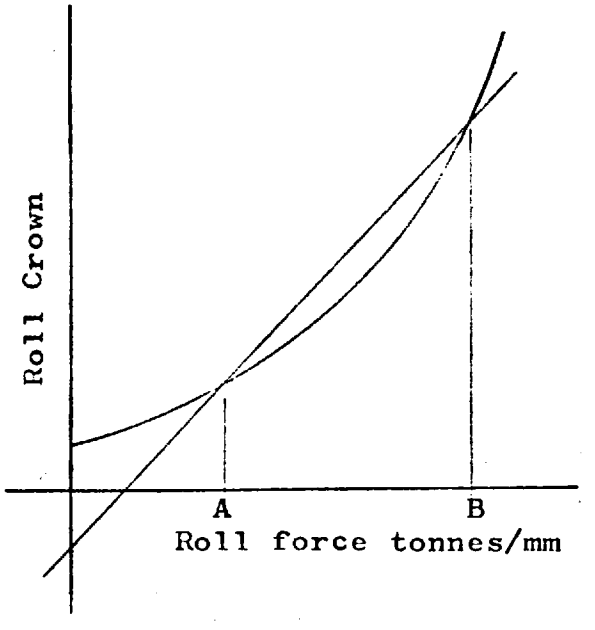

Figure 31. Scheduling Diagram.

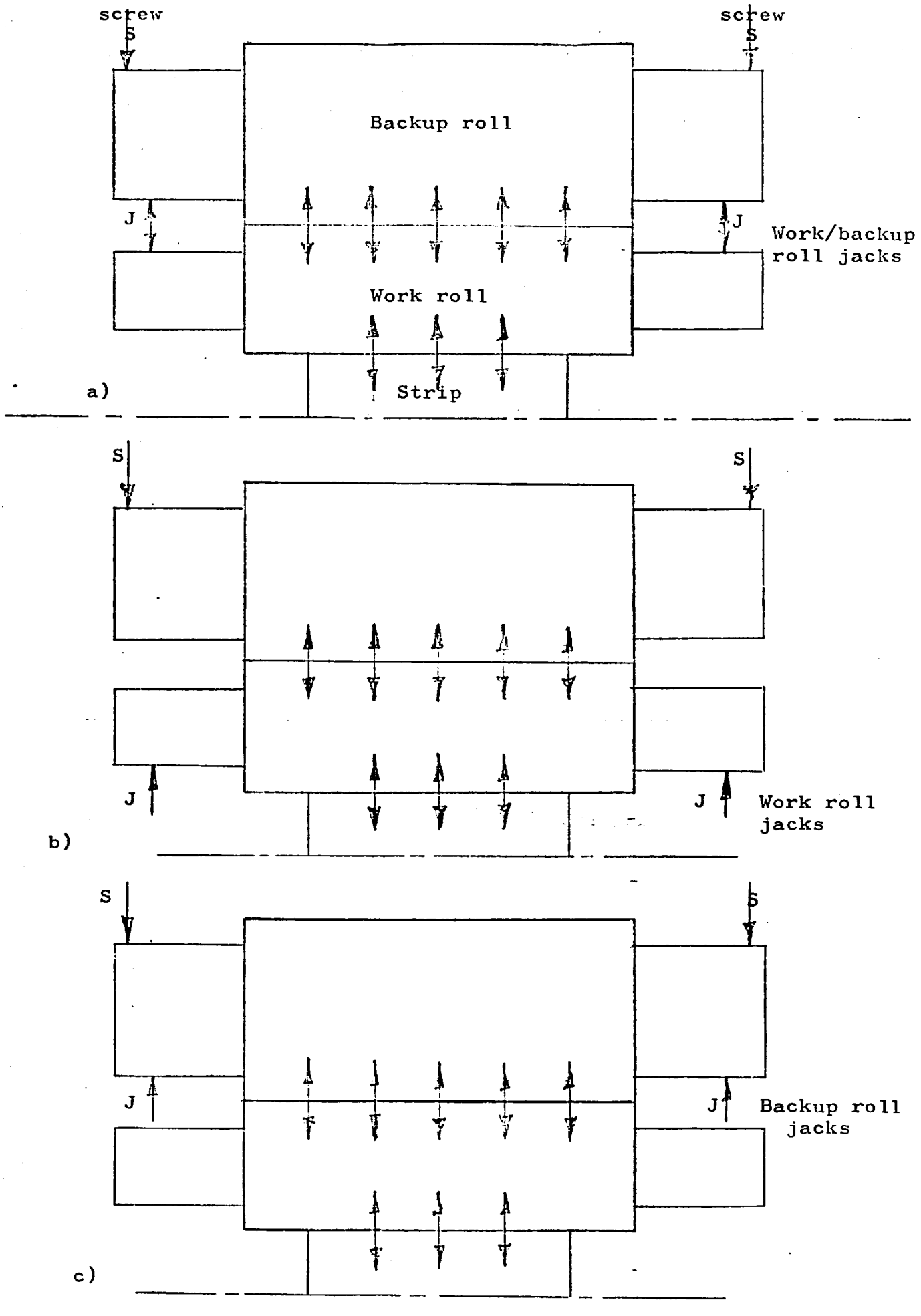

Figure 32. Roll Bending Jack Configuration.

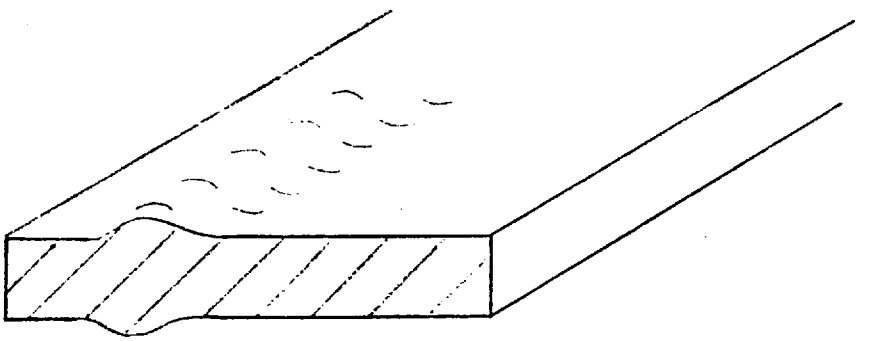

Figure 33. Cross Section of Strip.

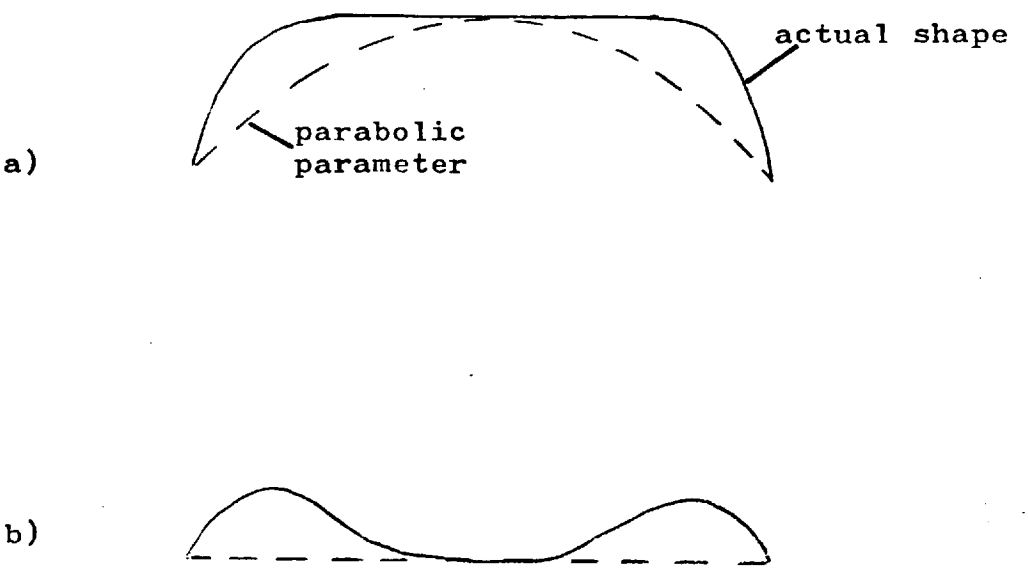

Figure 34. Effect of Incorrect Parameter Fitting.

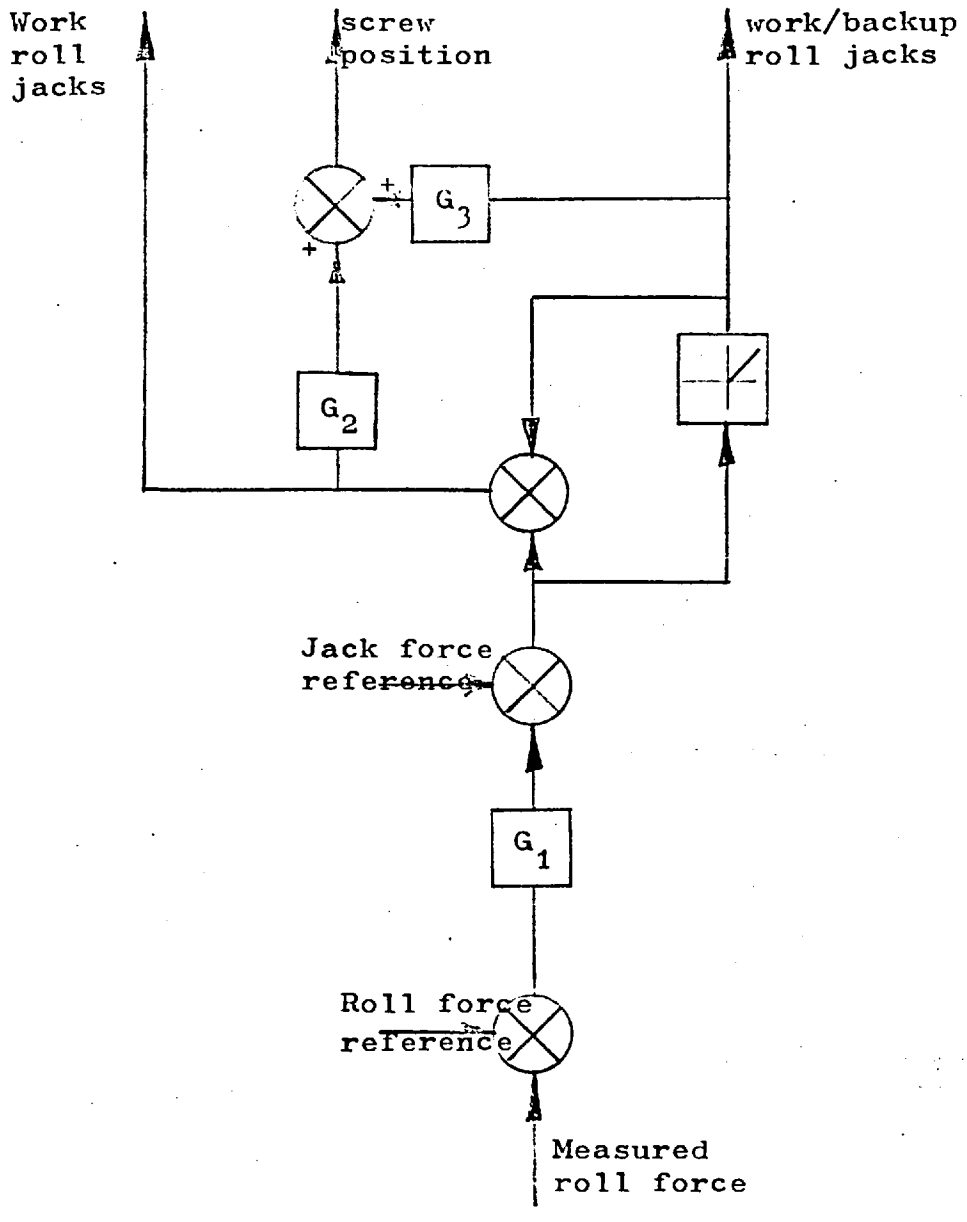

Figure 35. Open Loop Shape Control.

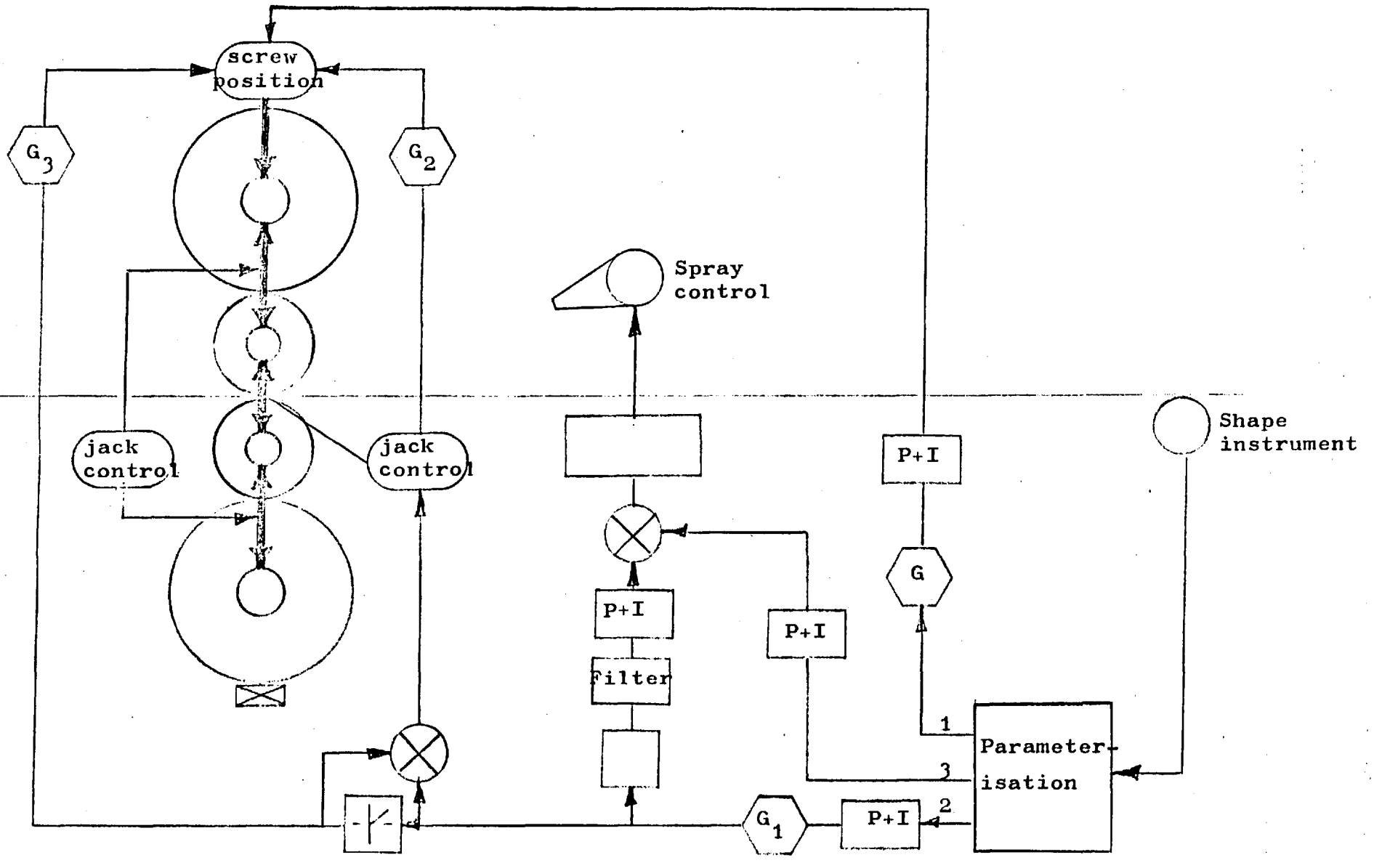

Figure 36. Feedback Shape Control.

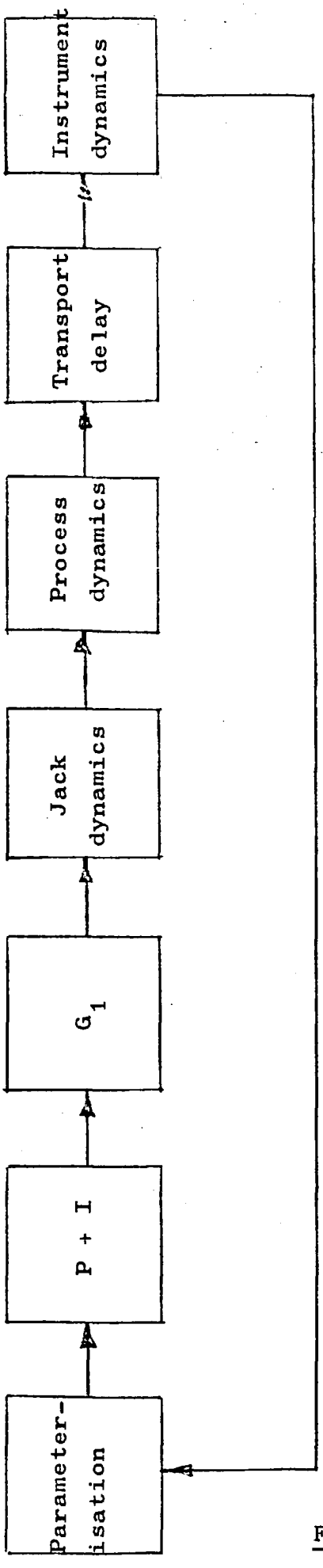

Figure 37. Roll Bending Jack Control Loop.

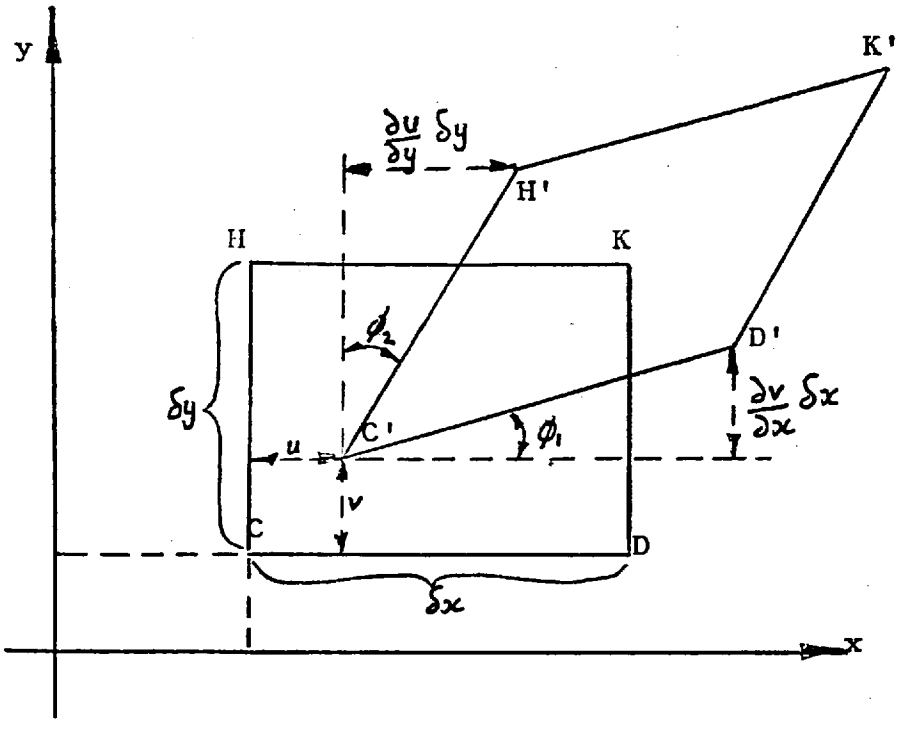

Figure 38. Strain in Two Dimensions.

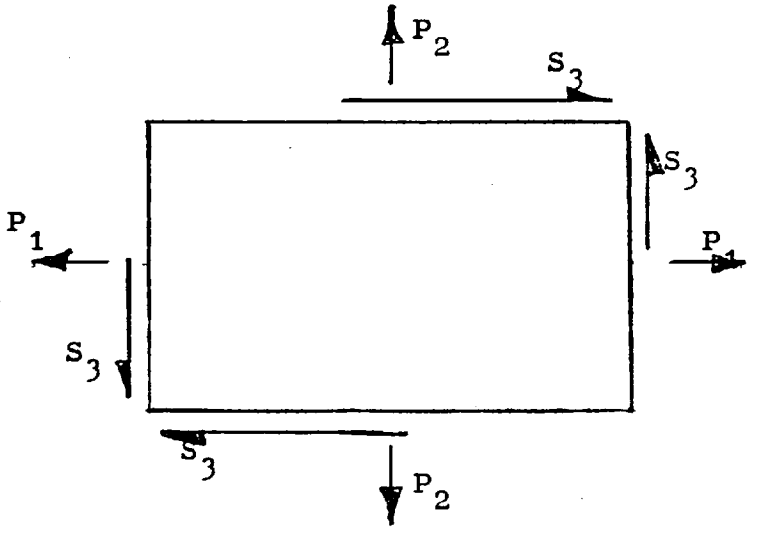

Figure 39. Rectangular Block Under Tensional and Shear Stresses.

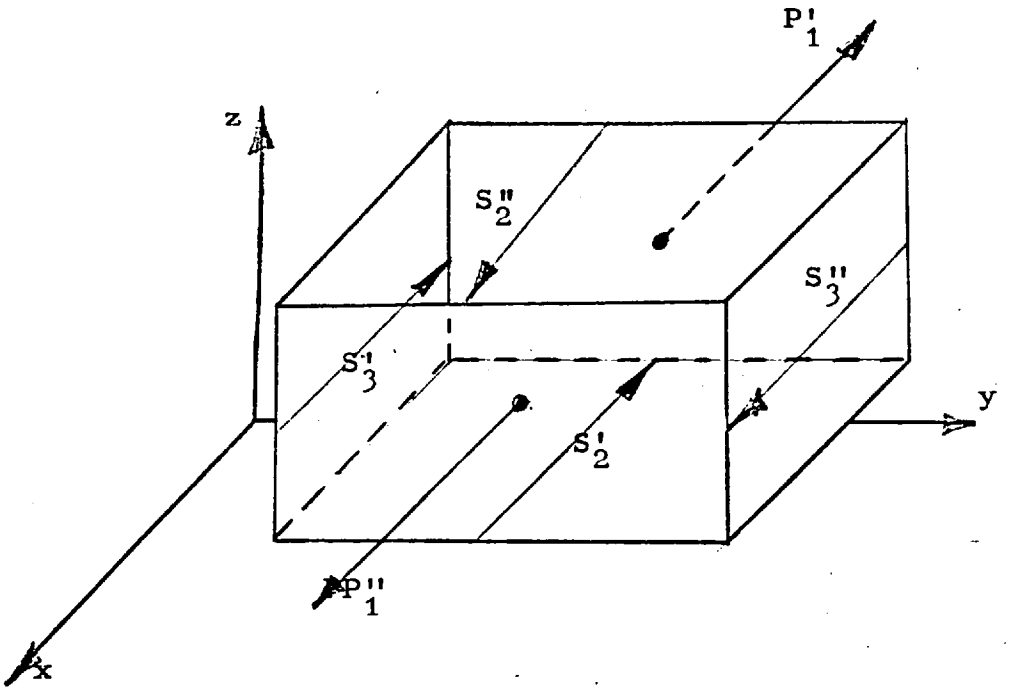

Figure 40. Relation Between Stresses and External Forces.

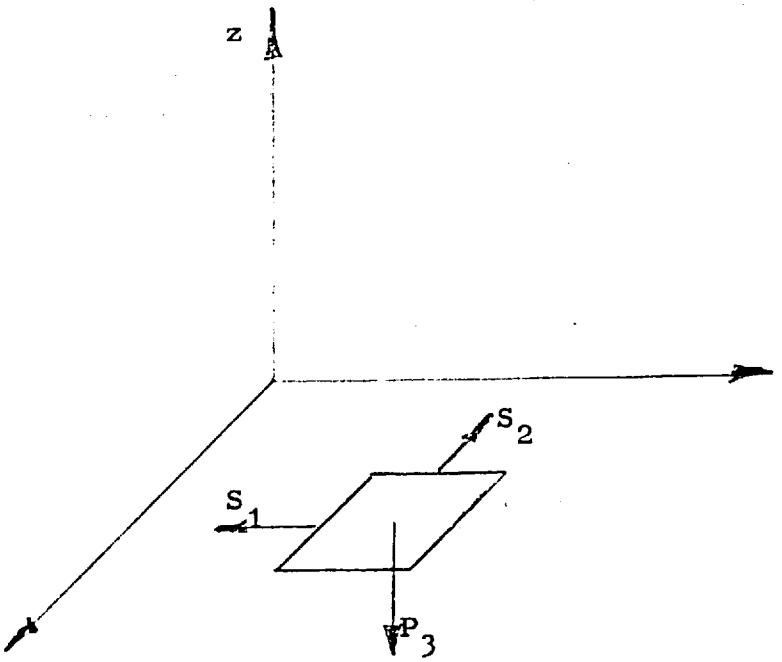

Figure 41. Concentrated Normal Force on the Surface of a Semi-Infinite Solid.

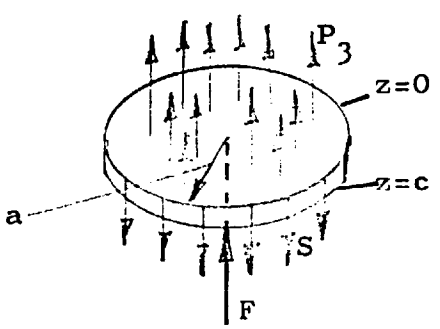

Figure 42. Small Cylindrical Portion of a Solid.

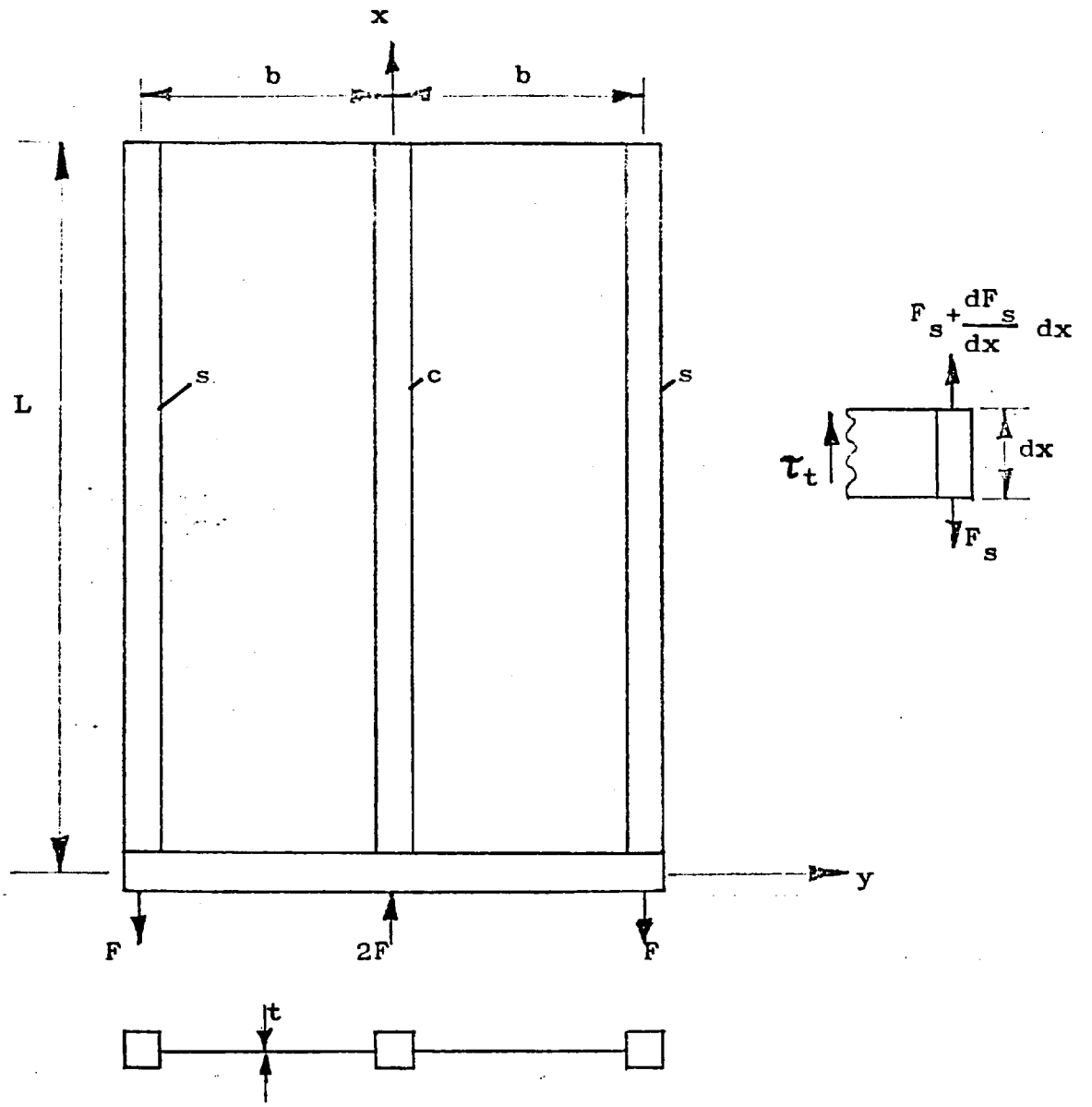

Figure 43. Simple Structural Model for Investigating St.Venants Principle.